LBL-3868
UC-11
TID-4500-R63

Sliding Response of Rigid Bodies to Earthquake Motions

M. Aslam
W. G. Godden
and
D. T. Scalise

September 1975

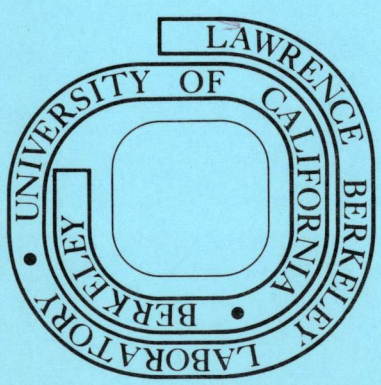

LBL-3868

LBL-3868

SLIDING RESPONSE OF RIGID BODIES TO EARTHQUAKE MOTIONS

A Report of an Analytical and Experimental Study
of the Sliding Response of Rigid Blocks Under
Simultaneous Horizontal and Vertical Earthquake Accelerations

by

M. Aslam
Associate Development Engineer
Department of Civil Engineering
University of California, Berkeley

W. G. Godden
Professor of Civil Engineering
University of California, Berkeley

and

D. T. Scalise
Mechanical Engineering Department and
Energy and Environment Division
Lawrence Berkeley Laboratory, University of California

September 1975

TABLE OF CONTENTS

LIST OF SYMBOLS

AH	Amplitude of sinusoidal horizontal acceleration in g's.
AV	Amplitude of sinusoidal vertical acceleration in g's.
B	Width of the block
b	B/2
F	Frequency of motion
g	Acceleration of gravity
H	Height of the block
h	H/2
K	Spring stiffness
M	Mass of the block
P	Horizontal force
s	Relative displacement of block (horizontal)
$\dot{s}$	ds/dt
$\ddot{s}$	d^2s/dt^2
t	time
T	Natural period of vibration
u	Horizontal ground displacement
$\dot{u}$	du/dt
$\ddot{u}$	d^2u/dt^2
v	Vertical ground displacement
$\dot{v}$	dv/dt
$\ddot{v}$	d^2v/dt^2
W	Weight of the block
x	Absolute horizontal displacement of the block
$\dot{x}$	dx/dt
$\ddot{x}$	d^2x/dt^2

Δt	Time increment
μ	Dynamic coefficient of friction
μ_s	Static coefficient of friction
ω	Angular frequency ($2\pi F$)

ABSTRACT

This report is on a fundamental study of the sliding response of massive concrete blocks to earthquake ground motions, including the effect of vertical accelerations/decelerations on the friction forces. This particular problem occurs when large concrete blocks are used as radiation shields in nuclear particle accelerator installations in seismic areas. The results of this study can also help in understanding the response of other rigid bodies (as approximated by some electrical/mechanical equipment) which are not anchored to the ground.

A separate report will address the rocking-mode response of concrete blocks.

Based upon the simple theory of friction and equations of motion, a computer program BLOKSLD was written to predict the sliding motion of a rigid block under the effect of simultaneous horizontal and vertical earthquake accelerations. The accuracy of computer-predicted results was checked against the experimental data and a satisfactory agreement (10 percent) was found.

Tests were conducted with concrete blocks on a newly constructed 20 x 20 ft. shaking table which can reproduce independent horizontal and vertical displacement components. Tests were made for both sinusoidal and actual earthquake ground motions. Various materials were tried between the concrete block and the shaking table to reduce the coefficient of friction and to study the suitability of such materials for this purpose. Input table accelerations and the relative displacements between table and block were recorded for comparison with computer results.

Using the computer program BLOKSLD, the sliding response of a rigid block with varying dynamic coefficient of friction was studied for various strong motion earthquake records, including the San Fernando Earthquake of 1971 (Pacoima Dam Record) and four artificial earthquake accelerograms. The Pacoima Dam Record with its unusually high accelerations gave the highest relative displacements between the block and ground. A relative velocity response spectrum with Coulomb damping for Pacoima Dam Record was also produced for comparison with the response spectra having viscous damping.

KEYWORDS

Radiation shielding systems, Shielding blocks, Sliding of rigid blocks, Friction, Relative displacement, Sliding response, Earthquake response, Response spectra, Rocking.

SUMMARY AND CONCLUSIONS

1. Response Modes

Systems comprised of solid blocks (such as radiation shielding or heavy electrical/mechanical equipment approximating rigid bodies) can be designed to respond to earthquakes by: (a) sliding within predetermined limits, (b) rocking (without overturning), or (c) moving integrally with the ground. For heavy masses, costs for support structure are least where sliding can be tolerated and greatest where no movement can be permitted relative to the ground. The structural engineer must choose which of the three types (a, b, or c) of support structure will meet the system and cost requirements.

For rigid bodies which are not firmly anchored to the ground, the two response modes to earthquakes are (a) sliding or (b) rocking. This report provides information and aids (e.g., computer program BLOKSLD) to help the reader determine the dynamic response (including the effect of vertical accelerations/decelerations on the friction forces) of solid blocks for those cases where sliding can be tolerated.

A separate report is being prepared for the rocking-mode of response.

2. Boundary between Sliding - and Rocking-Modes

The boundary between the sliding - and rocking-modes of solid blocks depends on μ_s, the static coefficient of friction between the block and the floor, and on H/B, the height-to-width ratio of the block. For an unrestrained block with perfectly plane interface with the floor, an earthquake can induce (a) sliding if $H/B < \mu_s$ or (b) rocking if $H/B > \mu_s$. If the interface surfaces are not plane, rocking can start at lower H/B ratios.

3. Computer Program BLOKSLD

BLOKSLD gives the instantaneous,maximum, and residual displacements (relative to the ground) and accelerations of an unrestrained block responding in the sliding-mode to simultaneous vertical and horizontal earthquake accelerations as a function of the dynamic coefficient of friction between the block and the floor.

BLOKSLD has been developed as a result of the present investigation. Computer and test results on the relative displacement of a block were found to agree within 10 percent. The acceleration time-histories in both the vertical and horizontal planes of any real or postulated earthquake can be used as input data to the BLOKSLD program.

BLOKSLD will become available from the Earthquake Engineering Research Center of the University of California at Berkeley.

4. Results using BLOKSLD

Some results on the sliding responses of blocks to earthquakes are given in Section 3 of this report.

In general, higher relative displacements were observed under those earthquake accelerograms which had higher ground accelerations. San Fernando Earthquake 1971 (Pacoima Dam Record) gave the highest relative displacement and were of the order of 20 in., 10 in. and 5 in. for μ (dynamic friction coefficient) values of 0.10, 0.20 and 0.30 respectively. This seems to represent an upper limit and the probability of relative displacements of this magnitude in most earthquakes may be considered rather low, because of the unusually high accelerations recorded at Pacoima Dam (the maximum acceleration recorded at Pacoima Dam was 1.25 g as compared with 0.32 g for the El Centro Earthquake of 1940). Maximum relative displacement of the block under the El Centro Earthquake for a μ value of 0.1 was less than two inches.

5. Design Suggestions for Cases where Movement of Blocks Relative to Floor can be Tolerated

5.1 Sliding systems: If some relative movement of the radiation shielding blocks with respect to the floor can be tolerated during an earthquake, a sliding shielding system would probably be the safest and most economical to design.

The designer must select the appropriate design parameters (friction coefficient, block height/width ratio, design basis earthquake); check to ascertain that the sliding-mode of response applies (see subsection 2 above); and use the computer program BLOKSLD to determine the instantaneous, maximum, and residual displacements of the block relative to the floor. Any equipment connections between the sliding system and and the floor should provide suitable allowance (e.g., flexible joints) for the relative displacement.

The use of linear springs as a means of reducing maximum relative displacement is not effective as it makes the system a single degree resonator and thus may not be worth all the extra cost entailed. They can however be quite effective in reducing the residual relative displacements. If a linear spring is used, the natural period of the system should be long and the effect of spring force on possible overturning must be studied because the use of a spring may introduce the possibility of rocking. The effect of a linear spring may be determined with the computer program BLOKSLD.

A radiation shielding system with more than one block, if designed to allow sliding movements during an earthquake, should be designed so that the whole system slides as a single unit. This is necessary to avoid any relative movements between the blocks that could result in impact damage. This could be achieved, for example, by placing

two continuous steel plates between the floor and the block system in order to restrict the sliding to the steel-to-steel interface. In such a solution the controlled coefficient of friction at the base of the stack (i.e., between the two steel plates in this case) must be lower than at all other horizontal surfaces. The coefficient of friction could be reduced by using graphite or some other lubricant between the steel plates depending upon the value desired. It should be noted that shielding systems with large H/B ratios could possibly be made to respond in the sliding-mode rather than the rocking-mode by this procedure (see Subsection 2). But in such a design any convexity of the sliding surfaces must be avoided to prevent the possibility of premature rocking.

5.2 Rocking systems: If the aspect ratio of the block is such that sliding cannot be easily ensured or if sliding of the blocks cannot be permitted for some other reason, the system should be designed for zero relative movement or possibly for controlled rocking without overturning. This may be achieved by suitably anchoring the blocks to the floor, making sure that the floor can withstand the large dynamic anchorage forces.

A forthcoming report will deal with design parameters for rocking systems and will include a computer program for determining dynamic rocking response.

5.3 Rigid systems: It should be noted that large shielding block systems with anchorages that permit no relative movement will transmit to the floor or foundation the full inertia forces induced in masses by the earthquake. If the floor or foundation is not sufficiently strong, these rigid anchorages can be less safe, as well as more costly, than the designs discussed above for sliding or rocking systems.

SECTION 1

INTRODUCTION

This investigation was undertaken to determine the seismic response of large free-standing concrete blocks. Such blocks, stacked in various configurations, are used to provide radiation shielding in particle accelerator laboratories. While the investigation is directed to large concrete blocks, any massive equipment presents a similar problem to the structural engineer. In the present state of the art, there is a lack of fundamental data and detailed analysis for selecting practical alternative solutions to the basic seismic problem for supporting massive equipment. Alternative approaches to the solution are as follows:

1) To design foundations or floor structure of sufficient strength to prevent any relative motion between the support and the block system. The problems here relate to cost and the adequacy of the foundation to withstand the resulting forces. In cases where the foundation strength is in question, any attempt to prevent relative motion may aggravate the earthquake damage and safety hazard.

2) To provide a safer or lower cost design which uses some decoupling of the earthquake motions from the block system. The problem here is that a better understanding of the nature of the seismic response is needed to furnish a rational basis for such designs.

It is hoped that the present investigation will indicate solutions to the immediate problem of shielding blocks as well as contribute to the state of the art for seismic safety of massive equipment in general.

At the Lawrence Berkeley Laboratory and other such laboratories, massive shielding blocks are often stacked as much as 20 feet high and 15

feet deep to shield high energy physics experiments. Some of these blocks are provided with a vertical keying system that prevents relative horizontal movement between them, but does not prevent rocking. While rocking of the blocks and their possible overturning would be extremely destructive in an earthquake, a reasonable amount of sliding between the blocks and the floor might be tolerated as being the least destructive means of accommodating earthquake forces. This raises the questions of (1) how much sliding displacement of a rigid block--or of a system of such blocks--could be expected in an earthquake, and (2) how can the sliding-mode response be made to dominate the more hazardous rocking-mode by selecting proper design parameters. Little work has been reported on these questions and it here becomes the subject of this study. The separate problem of rocking motion is presently under study and will be the subject of a later report.

To ensure sliding motion instead of other motions in response to ground accelerations, it is necessary to know and perhaps to modify the coefficient of friction between the bottom block and the floor. The precise modeling of existing structures for experimental testing is irrelevant as far as pure sliding is concerned, because blocks of differing size and material density will have the same motions under a given acceleration if their coefficients of friction are the same. To form a basic understanding of sliding motion, preliminary tests were made with a small scale block on a small scale shaker table. Tests were done with simultaneous horizontal and vertical ground motion and a constant horizontal force applied to the block.

A mathematical model based on these tests was written into a computer program (BLOKSLD) using direct forward integration to predict the sliding response of a rigid block subjected to simultaneous horizontal

and vertical ground motions. This program also included the effect of a horizontal spring-force, which might be one means of keeping the displacement of the block within prescribed limits. The sliding response of a block to sinusoidal horizontal acceleration and a constant horizontal force was also studied on the computer with a curve-fitting trial and error solution, but in comparison with the forward integration procedure, the trial and error approach lacked generality.

Using these computer programs, parametric studies were made for sinusoidal ground motions, varying the amplitude and frequency of the ground motion as well as the coefficient of friction. These theoretical studies are described in Section 2 of this report.

Large scale model tests were then made and the results compared with the theoretical results given in Section 2; these large scale tests are described in Section 3. The large scale test and predicted results generally agreed with $\pm$ 10 percent.

The dynamic response of blocks in a sliding mode was then studied under conditions simulating the maximum recorded motion measured during the San Fernando Earthquake of 1971, and four artificially generated earthquakes. After showing that the sliding response of a rigid block under earthquake conditions could be predicted successfully, the computer program described in Section 2 was used to make a parametric study from digitized earthquake records in order to find the likely upper bound of relative displacement. The effectiveness of a horizontal spring constraint applied to the block was also studied. These studies are described in Section 4.

SECTION 2

THEORETICAL STUDIES

2.1 Conditions for Sliding and Rocking

Whether rectangular block of height H and width B under given simultaneous horizontal and vertical ground accelerations will slide, rock, overturn, or remain standing depends on

(1) the static coefficient of friction μ_s between the block and the ground,

(2) the aspect ratio of the block (B/H), and

(3) the magnitude and form of the ground motion. The vertical component of ground motion is an important factor in the response of the block. Downward vertical acceleration will reduce the effective weight of the block, thus reducing the frictional force in sliding or the restoring moment in rocking.

Consider a rigid block with height H and width B subjected to a horizontal ground acceleration $\ddot{u}$ and a vertical ground acceleration $\ddot{v}$ as shown in Fig. 2-1(a). The block will slide as soon as the horizontal inertial force ($M\ddot{u}$) exceeds the effective frictional force ($\mu_s W_e$). Suppose the block is at the threshold of sliding, then

$$M\ddot{u} = \mu_s W_e$$

where

M = mass of the block

W_e = $W(1 + \ddot{v}/g)$ = effective weight of the block

W = weight of the block

g = acceleration due to gravity.

Therefore

$$M\ddot{u} = \mu_s W(1 + \ddot{v}/g)$$

$$\ddot{u} = \mu_s W(1 + \ddot{v}/g)/M$$

$$\ddot{u} = \mu_s g(1 + \ddot{v}/g)$$

Thus,

$$\ddot{u} > \mu_s g(1 + \ddot{v}/g). \qquad (1)$$

is the condition necessary for sliding to start (positive $\ddot{v}$ is taken in the upward direction).

Now, suppose that sliding is prevented, and the block is on the verge of rocking, which will happen when the moment of horizontal inertial force about the left edge of the block is equal to the restoring moment (see Fig. 2-1(b), i.e.,

$$M\ddot{u}(H/2) = W(1 + \ddot{v}/g)(B/2)$$

$$\ddot{u} = (B/H)(W/M)(1 + \ddot{v}/g)$$

$$\ddot{u} = (B/H)g(1 + \ddot{v}/g)$$

Thus

$$\ddot{u} > (B/H)g(1 + \ddot{v}/g) \qquad (2)$$

is the condition necessary for rocking to start. Comparing conditions (1) and (2), it is obvious that for $\ddot{u} > \mu_s\, g\, (1 + \ddot{v}/g)$, a block will

slide if $\mu_s < B/H$ and

rock if $\mu_s > B/H$.

It can be noted from Conditions (1) and (2) that the block will slide or rock at a smaller value of horizontal acceleration $\ddot{u}$ if the vertical acceleration $\ddot{v}$ is negative (i.e., in the downward direction).

2.2 Assumptions for Mathematical Model for Sliding of a Block

The mathematical model used to compute the response of a block in the sliding mode was based on the following assumptions:

(1) Block Motion

The motion of the block consist of sliding without rocking. Theoretically this will occur if $\mu_s < B/H$ and $\ddot{u} > \mu_s g (1 + \ddot{v}/g)$ as proved in the previous sub-section. In practice it depends on the contact surfaces of the block and the ground being perfectly plane. If the contact surfaces are not plane, pure sliding may not occur, even if the condition $\mu_s < B/H$ is satisfied, and a combination of sliding and rocking can be expected.

(2) Friction Coefficient

The dynamic coefficient of friction is assumed to be equal to the static coefficient and is taken as a simple constant. If this were true, the acceleration-time response of a sliding block under a horizontal sinusoidal ground acceleration will be of the rectangular form shown in Fig. 2-2(a) (provided the amplitude of the ground acceleration is high enough compared with the value $\mu_s g$ so that the block does not reattach). In this case, the acceleration of the block will be μg in both directions. The accuracy of this assumption can be noted in Fig. 2-3 which shows two typical oscilloscope traces of a block sliding due to sinusoidal ground motion. It can be seen that although the assumption cannot be strictly true, the actual traces in Fig. 2-3 are close to the idealization of Fig. 2-2. The assumption is obviously better for those materials where the difference between the dynamic and static coefficients of friction is relatively small and is more significant in some situations than in others. In Fig. 2-3 the assumption holds better in the lower trace than in the upper trace, where there is a sharp drop in the

acceleration of the block after the block reverses its acceleration. The block changes the direction of its acceleration when the direction of relative velocity of the block changes with respect to the ground. During the changing of the sign of the relative velocities, the block and the ground must momentarily assume the same velocity. Thus the block momentarily reattaches to the ground, and at this moment the coefficient of friction changes from dynamic to static, then resumes its dynamic value as the block accelerates in the new direction.

If the shape of the coefficient of friction curve as it changes from static to dynamic value is known experimentally, it can be easily incorporated in a computer program for exact solution if desired. The coefficient of friction curve can be determined from the traces shown in Fig. 2-3. But for this study, the assumption of the dynamic and static coefficients being the same was followed and found satisfactory. The errors caused by this assumption would be insignificant compared for example, with the uncertainties associated with the value of μ and the prediction of future earthquake intensities.

(3) Change of Acceleration

It is assumed that the direction of acceleration changes instantaneously as shown in Fig. 2-2(a) at point 1 and 2. In the actual physical system the change of the direction of acceleration takes a finite but short time as can be seen in Fig. 2-3 but the assumption of instantaneous change is sufficient for practical purposes.

(4) Level Ground

The ground is taken as horizontal so that the weight of the block always acts normal to the ground surface. This applies even when the ground has a vertical component of acceleration.

2.3 Basic Concepts About Sliding and Computational Procedure

There are three important factors in understanding the sliding behavior of a block under any form of ground excitation. These are:

(1) how does sliding start?

(2) when does the acceleration of the block change direction? and

(3) what controls the reattachment of the block to the ground?

Consider a block subjected to the horizontal ground acceleration $\ddot{u}$ as shown in Fig. 2-4(a). The condition for sliding to start is $|\ddot{u}| > \mu g\ (1 + \ddot{v}/g)$ as shown in Section 2.1. Since the vertical ground acceleration $\ddot{v}$ is equal to zero, the block will slide relative to the ground at time t_1 as soon as $\ddot{u} > \mu g$ as shown in Fig. 2-4(a). When the block is sliding, the only external force acting on the block is the frictional force which is equal to μW if there is no vertical acceleration.

Let $\ddot{x}$ be the acceleration of the block, then

$$M\ddot{x} = \mu W\ [\text{sign}\ (\dot{s})] \tag{3}$$

where $\dot{s} = \dot{u} - \dot{x}$ = the relative velocity of the block with respect to the ground, $\ddot{x} = \mu W/M = + \mu g$ from t_1 to t_3 in Fig. 2-4(a).

It should be noted that in the absence of a vertical component of ground acceleration, $\ddot{x}$ remains constant and does not change sign regardless of the horizontal ground acceleration from time t_1 to t_3, as shown in Fig. 2-4(a), although the ground changes acceleration at t_2. The reason for this will be clear by looking at the velocities of the block and ground in Fig. 2-4(b) which were obtained by integrating the acceleration curves of Fig. 2-4(a). It will be seen from the velocity diagram that from t_1 to t_3 the velocity of the ground is higher than

the block velocity and thus the sign of s(i.e., $\dot{u} - \dot{x}$) remains positive and therefore $\ddot{x}$ does not change its sign. At time t_3, the velocity of the block and that of the ground become equal and the block reattaches to the ground momentarily. At this point, if $|\ddot{u}| < \mu g$ the block will remain attached to the ground, and if $|\ddot{u}| > \mu g$, the block will slide again.

It can be seen that in Fig. 2-4(a) the latter condition controls so the block will slide again with respect to the ground. As we pass time t_3, the sign of the relative velocity $\dot{s}$ changes from positive to negative (Fig. 2-3(b)) and therefore the direction of the frictional force on the block also changes from positive to negative. Therefore the acceleration of the block as given by Eq. (3) will be

$$\ddot{x} = - \mu g$$

The block will again slide with the constant acceleration until the two velocities again become the same and the relative velocity $\dot{s}$ goes to zero at time t_4 as shown in Fig. 2-4(b). At this point the block attaches to the ground, and since $|\ddot{u}| < \mu g$ the block remains attached after that point. When the block is attached to the ground, then

$$\ddot{x} = \ddot{u}$$

$$\dot{x} = \dot{u}, \text{ and}$$

$$\dot{s} = 0$$

To get the absolute displacements of the ground and the block, the velocity curves of Fig. 2-4(b) can be integrated as shown in Fig. 2-4(c). The difference of the ground displacement (u) and the block displacement (x) will give the relative displacement (s), which in most cases is of prime interest. It is obvious that if one is only interested in the

relative displacement s, it could be obtained directly by integrating $\dot{s}$, which might save some computer time. In this study however, we did not do this.

The maximum relative displacement in Fig. 2-4(c) occurs at time t_3. The relative displacement after t_4 remains constant as after that the block does not slide.

It should be noted that the acceleration of a sliding block $\ddot{x} = \pm \mu g$ as given by Eq. (3) is only dependent upon the coefficient of friction μ and the acceleration of gravity g, and is independent of the weight of the block or its dimensions. The same will hold true if the ground also has vertical acceleration ($\ddot{v}$) accompanying the horizontal acceleration, the only difference being that the acceleration of the sliding block is given by $\ddot{x} = \pm \mu g\ (1 + \ddot{v}/g)$.

The sliding response of a block under sinusoidal horizontal acceleration is shown by a typical plot in Fig. 2-5. Acceleration, velocity, and displacement of the block and ground have been superimposed in Fig. 2-5 and the solution was carried out using the numerical integration procedure described in Section 2-6, and the results were plotted by Calcomp plotter. The horizontal ground acceleration amplitude and frequency are 0.75 g and 5 Hz respectively, vertical ground acceleration is equal to zero, and $\mu = 0.3$. It is assumed that the block is initially attached to the ground. It can be seen in Fig. 2-5 that the solution reaches a steady state after about two cycles and the block acceleration and velocity responses are rectangular and triangular respectively. It is interesting to note that if the amplitude of the ground motion is increased beyond 0.75 g, the steady state response of the block will not change; the only difference will be in the transient section during the first few cycles.

Figure 2-6 shows another case in which amplitude of the ground acceleration AH is decreased to 0.5 g. Here the block reattaches to the ground in each cycle and the block reaches a steady state response after the first half cycle. Once the block reaches its steady state response under harmonic horizontal ground acceleration, it vibrates by sliding about a neutral point.

2.4 Block Under Horizontal and Vertical Ground Accelerations

Initiation of sliding under horizontal ($\ddot{u}$) and vertical ($\ddot{v}$) ground accelerations will be governed by condition (1), i.e. $|\ddot{u}| > \mu g\,(1 + \ddot{v}/g)$. (positive $\ddot{v}$ is upward). When the block is sliding relative to the ground, the absolute acceleration $\ddot{x}$ of the block is given by the expression

$$\ddot{x} = \mu g\,(1 + \ddot{v}/g) \cdot [\text{sign}\,(\dot{s})]. \qquad (4)$$

Whether the block will reattach to the ground as the relative velocity of the block and the ground changes sign will depend upon whether $|\ddot{u}|$ is greater than or less than $\mu g\,(1 + \ddot{v}/g)$ at the time when $\dot{s} = 0$. If $|\ddot{u}| < \mu g\,(1 + \ddot{v}/g)$ at $\dot{s} = 0$, the block will reattach. When the block is attached to the ground then $\ddot{x} = \ddot{u}$. It can be noted that $\ddot{x}$ is not a function of the weight (W) or dimensions of the block.

Note that Eq. (4) will not be applicable when $\ddot{v}$ in the downward direction exceeds 1 g. In this case the block will separate from the ground and therefore $\ddot{x} = 0$. Because such high vertical accelerations are extremely unlikely in an earthquake, this provision was not made in the computer program.

Typical Calcomp plots showing the theoretical sliding response of a block when subjected to sinusoidal in-phase horizontal and vertical

accelerations are shown in Figs. 2-7 through 2-11. The block is assumed to be attached to the ground initially. From these plots it can be seen that after a few cycles, the block reaches a steady state response and the average velocity of the block relative to the ground over any cycle becomes constant. (It is this steady state average velocity that is compared with the similar experimental results in Section 3). The number of cycles required before the block reaches the steady state condition depends upon the relative magnitudes of the ground accelerations and the coefficient of friction. In Fig. 2-7 it takes about two cycles, while in Figs. 2-8 and 2-9 it takes about three and five cycles respectively. In Figs. 2-10 and 2-11, the block reaches the steady state condition within one cycle because here the ground accelerations are such as compared with the coefficient of friction that the block reattaches to the ground in each cycle. After the steady state condition is reached, the displacement curve of the block can be approximated by a straight line, the slope of which will give a constant average velocity. This method is used in the experimental studies described in Section 3 to determine the average velocity for comparison with the computer results.

2.5 Horizontal and Vertical Accelerations with a Horizontal Force

In addition to ground accelerations, the block was subjected to a horizontal force P which in general may be variable. A constant horizontal force was applied to the block and again a comparison was made between the test and computer results. Later a linear spring was added to the block, making it a single degree of freedom system. In the latter case the horizontal force $P = Ks$ where k is the spring stiffness, and s is the relative horizontal displacement of the block.

Suppose a positive (positive here means to the right) horizontal force P is acting on the block shown in Fig. 2-4(d) in addition to the frictional force. If $\ddot{u}$ is positive, the block will slide when

$$|\ddot{u} - P/M| > \mu g(1 + \ddot{v}/g)$$

Reattachement of the block with the ground at the moment when the relative velocity $\dot{s}$ becomes zero, will again be governed by the conditions described above in this Article.

During sliding the acceleration of the block ($\ddot{x}$) will be given by

$$\ddot{x} = \mu g(1 + \ddot{v}/g) \{\text{sign of } \dot{s}\} + P/M$$

Figs. 2-12 and 2-13 are typical examples of the sliding motion of a block under a sinusoidal horizontal ground acceleration and a constant unidirectional horizontal force. The sine and cosine waves in these figures represent the ground motion. The block is assumed to be attached to the ground at the beginning of ground motion and assumes a steady state response after a small number of cycles. In the steady state condition the block assumes a constant average velocity over any cycle. This can be seen from the fact that displacement of the block in Figs. 2-12 and 2-13 can be approximated by a straight line during the steady state response. It is this constant average velocity under steady state condition which has been compared in Section 3 with test results.

The fact that a block under a sinusoidal horizontal acceleration and a constant force attains a constant velocity under steady state response means that the area under the acceleration diagram must be zero in each cycle. Using this fact, the steady state response of a block

under the above conditions can be easily calculated on the computer using the Curve Fitting Method described in Section 2.7.

2.6 Integration Procedure Used in the Computer Program BLOKSLD

Based upon the assumptions outlined in Section 2.2, a general computer program was written which could read digitized acceleration records to analyze the response of the block under earthquake ground motions. In general, the acceleration may not be given at equal intervals of time, and the vertical acceleration values may not be given at the same points in time as those of the horizontal acceleration for the same earthquake record. The acceleration points were usually spaced at intervals ranging from 0.01 to 0.025 sec. Each time interval was further subdivided into an equal number of parts, assuming a linear distribution of acceleration between any two given consecutive points for better accuracy. Usually, a time interval of 0.002 sec. was used for integration. The exact vertical acceleration was determined at each time step by interpolation techniques as the given vertical acceleration points in time did not always coincide with the given horizontal points in time.

A straight line distribution over time interval Δt was assumed for numerical integration and a time interval was used such that further reduction in Δt did not improve the solution. If $\ddot{u}_i$ and $\ddot{x}_i$ are respectively the ground and block accelerations at any step i then $\dot{u}_{i+1}$, $\dot{x}_{i+1}$, u_{i+1} and x_{i+1} at the step $i+1$ were calculated by the following equations

$$\dot{u}_{i+1} = \dot{u}_i + (\ddot{u}_i + \ddot{u}_{i+1})\,\Delta t/2 \tag{4}$$

$$\dot{x}_{i+1} = \dot{x}_i + (\ddot{x}_i + \ddot{x}_{i+1})\,\Delta t/2 \tag{5}$$

$$u_{i+1} = u_i + (\dot{u}_i + \dot{u}_{i+1})\,\Delta t/2 \tag{6}$$

$$x_{i+1} = x_i + (\dot{x}_i + \dot{x}_{i+1})\,\Delta t/2 \tag{7}$$

then

$$s_{i+1} = u_{i+1} - x_{i+1} \tag{8}$$

Each quantity on the right hand side in Eqs. (4) through (8) is known except for $\ddot{x}_{i+1}$, which will not be known exactly if there is any spring force acting on the block. Such a spring force is dependent upon s_{i+1} and thus is unknown, i.e.,

$$\ddot{x}_{i+1} = \mu g(1 + \ddot{v}_{i+1}/g) \{\text{sign } \dot{s}_{i+1}\} + Ks_{i+1}/M \tag{9}$$

If $K = 0$ in Eq. (9) then $\ddot{x}_{i+1}$ can be determined provided the sign of $\dot{s}_{i+1}$ is known. The sign of $\dot{s}_{i+1}$ is unknown too, but in general will be the same as that of $\dot{s}_i$ except at a few steps where $\dot{s}$ changes sign. Taking constant acceleration distribution at those few steps does not affect the solution.

However, it was found that if the spring force is present and the step size is not small enough compared with the period of vibration, the solution can easily become unstable with constant acceleration method. To minimize such errors for a given Δt, the solution of Eqs. (5), (7), and (8) was iterated in each step. During the first iteration $\ddot{x}_i$ was assumed constant over the interval. At the end of the j^{th} iteration, $\ddot{x}_{i+1}$ was calculated for $(j+1)^{th}$ iteration using Eq. (9) until

$$|(\ddot{x}_{i+1})_{j+1} - (\ddot{x}_{i+1})_j| < \delta$$

where δ is a very small prescribed value depending upon the accuracy required. Usually two or three iterations were enough to get the desired accuracy.

Figure 2-14 is a typical example showing the response of a freely sliding block subjected to San Fernando Earthquake 1971 (Pacoima

Dam Record S16°E). Coefficient of friction μ between the block and the ground is taken as 0.05. From top to bottom are the Calcomp plots of horizontal accelerations, vertical accelerations (in g), horizontal velocities (in./sec) and horizontal displacements (in.). In each case the response of the block and the ground are superimposed. More detailed studies of the sliding response of blocks under various earthquakes is presented in Section 4.

2.7 'Curve Fitting Method' of Solution

A 'Curve Fitting Method' was found to be very efficient in finding the steady state motion of a block under horizontal sinusoidal ground acceleration and a constant horizontal force P. It should be emphasized that the method is limited in scope and cannot be extended to the general case of ground motion. It is also assumed that the amplitude of ground motion is high enough so that the block does not reattach to the ground.

Consider the acceleration and velocity diagrams shown in Fig. 2-15. As pointed out in Section 2.5, under steady state conditions, the area under the $\ddot{x}$ curve must be equal to zero, and therefore the shaded areas in Fig. 2-15(b) must be equal, i.e.,

$$\ddot{x}1 \times T1 = \ddot{x}2 \times T2 \tag{10}$$

also

$$T = T1 + T2 \quad \text{(see Fig. 2-15(b))} \tag{11}$$

where T is the period of ground vibration

$$\ddot{x}1 = -\mu g + P/M; \quad \ddot{x}2 = +\mu g + P/M$$

Now from Eqs. (10) and (11), T1 and T2 can be calculated. Knowing T1, T2, $\ddot{x}1$ and $\ddot{x}2$, the shape of the block velocity diagram is automatically known as shown in Fig. 2-15(a). Between points a and b, the slope of $\dot{x} = \ddot{x}1$ and between b and c, the slope of $\dot{x} = \ddot{x}2$. The shape of the ground velocity is also known. Now the $\dot{x}$ curve abc can be moved up and down over the $\dot{u}$ curve and a position can be found by trial and error such that the relative velocity $\dot{s}$ at the change points a, b and c is zero. Note that there is only one such unique position of $\dot{x}$ relative to $\dot{u}$, and any other position such as the dotted position of $\dot{x}$ in Fig. 2-15(a) will not satisfy the condition of $\dot{s}$ equal to zero at the change points a, b and c. This unique position of $\dot{x}$ relative to $\dot{u}$ was determined by trial and error solution with a simple algorithm on the computer. Once this unique position is known on the velocity diagram, then the average velocity $\dot{s}_{ave}$ of the block under horizontal ground acceleration and a constant force will be given by the expression

$$\dot{s}_{ave} = [(v_a + v_b)T1 + (v_b + v_c)T2]/T$$

where v_a, v_b and v_c are the velocities at a, b and c.

A comparison of the steady state average block velocity computed by integration method and by curve fitting method is given in Table 2-1; for the case of $\mu = 0.2$, $P/W = 0.0429$, and frequency of vibration = 20 hz. The amplitude of the motion was varied. The reason for the small differences is that the solution by the integration method carries some effect of the initial transient response, as the solution was carried up to only 10 cycles.

2.8 Parametric Studies of a Sliding Block Under Sinusoidal Ground Motion

The variation of the steady state average block velocity $\dot{s}_{ave}$ under sinusoidal ground acceleration was studied to see the trends in

velocity variation with changes in frequency F and amplitude of ground motion, coefficient of friction, and horizontal force P. These parametric studies are briefly described below and show some interesting results.

(1) Variation of Velocity with Ground Motion Frequency:

Figure 2-16 shows the variation of steady state average velocity of the block with change in frequency of horizontal and vertical ground motions for a coefficient of friction equal to 0.2. The values plotted in Fig. 2-16 are also tabulated in Table 2-3. The acceleration of ground motion are sinusoidal and the amplitudes of horizontal and vertical accelerations are kept constant at 0.5 g. It can be seen from Table 2-3 that average velocity relationship with frequency can be represented by the following equation.

$$\frac{F_m}{F_n} = \frac{(\dot{s}_{ave})_n}{(\dot{s}_{ave})_m}$$

where

$(\dot{s}_{ave})_n$ = velocity corresponding to the frequency F_n

$(\dot{s}_{ave})_m$ = velocity corresponding to the frequency F_m

(2) Variation of Block Velocity with μ and Amplitude of Motion:

Figure 2-17 shows the variation of average block velocity with coefficient of friction μ and the amplitude of vibration of the ground. The plotted values are also given in Table 2-2. Frequency of the sinusoidal horizontal and vertical accelerations was kept constant at 5 Hz. μ was varied from 0.1 to 0.3, and the amplitudes of horizontal and vertical accelerations were varied between 0.25 g and 0.75 g.

Some interesting observations can be made from Fig. 2-17. It will be seen in this figure that for a given set of horizontal and

vertical values of the ground motion there is a unique value of μ at which maximum velocity will occur, e.g., at a horizontal ground acceleration $\ddot{u} = 0.25\ g\ (\sin \omega t)$, the maximum velocity of the block occurs when $\mu = 0.1$, while for $\ddot{u} = 0.5\ g\ (\sin \omega t)$ the maximum velocity occurs for $\mu = 0.2$ and not for $\mu = 0.1$ as one might expect. Similarly for $\ddot{u} = 0.75\ g\ (\sin \omega t)$ the maximum velocity occurs at $\mu = 0.3$.

It can also be noted in Fig. 2-17 that the steady state average velocity of the block for $\mu = 0.1$ increases as the amplitude of $\ddot{u}$ is increased from 0.25 g to 0.50 g and then decreases again at an amplitude of 0.75 g for a given value of vertical acceleration. Similar trends should be expected for $\mu = 0.2$ or $\mu = 0.3$ if horizontal amplitudes are further increased.

The above trends were also verified by the test results.

(3) Variation of Block Velocity with Horizontal Acceleration and Horizontal Force:

Figure 2-18 shows the variation of steady state block velocity under a constant horizontal force P and varying amplitude of sinusoidal horizontal ground acceleration. Frequency of ground motion was 20 Hz, coefficient of friction 0.2, and horizontal force/weight ratio (P/W) was 0.0429. The plotted values are also given in Table 2-1. The block will assume a steady state velocity in the direction of the applied force when the amplitude of $\ddot{u}$ exceeds the quantity $(\mu - P/W)g$. It can be seen in Fig. 2-18 that the velocity curve is almost a straight line except the small initial portion when the amplitude of acceleration is relatively close to μg. Note that $\ddot{v}$ is zero.

(4) Variation of Block Velocity with μ and Horizontal Force:

Variation of steady state block velocity with variation in coefficient of friction μ and horizontal force P is shown in Fig. 2-19.

Frequency and amplitude of horizontal ground vibration were 20 Hz. and 1 g respectively. μ was varied from 0.2 to 0.6 and the ratio P/W from 0.0429 to 0.128.

TABLE 2-1 VARIATION OF BLOCK VELOCITY WITH HORIZONTAL GROUND ACCELERATION AND A FORCE (F=20Hz., P/w=.0430, μ=0.2)

AMPLITUDE OF ACCELERATION (g)	AVERAGE BLOCK VELOCITY (INCHES/SECOND)	
	INTEGRATION METHOD	CURVE FITTING METHOD
0.50	0.40	0.393
0.75	0.70	0.691
1.00	0.96	0.964
1.25	1.23	1.230
1.50	1.50	1.490
1.75	1.76	1.750
2.00	2.02	2.010
2.25	2.27	2.270

TABLE 2-2 VARIATION OF BLOCK VELOCITY WITH COEFFICIENT OF FRICTION AND AMPLITUDE OF SINUSOIDAL HORIZONTAL AND VERTICAL ACCELERATIONS. (F=5Hz)

AMPLITUDE OF HORIZONTAL ACCELERATION (g)	COEFFICIENT OF FRICTION	AVERAGE VELOCITY (INCHES/SECOND) FOR VERTICAL AMPLITUDES OF ACCELERATION (g)		
		0.25	0.50	0.75
0.25	0.1	0.521	1.015	1.453
	0.2	0.316	0.624	0.990
	0.3	0.017	0.232	0.616
0.50	0.1	0.612	1.243	1.896
	0.2	1.041	2.030	2.907
	0.3	0.950	1.823	2.532
0.75	0.1	0.451	1.094	1.733
	0.2	1.184	2.419	3.629
	0.3	1.562	3.044	4.361

TABLE 2-3 AVERAGE VELOCITY OF BLOCK VS. FREQUENCY OF SINUSOIDAL GROUND MOTION ($\mu = 0.2$), $\ddot{u} = 0.5g.Sin\omega t$, $\ddot{v} = 0.5g.Sin\omega t$)

FREQUENCY (H_Z)	AVERAGE BLOCK VELOCITY (INCHES/SECOND)
5	2.030
10	1.015
15	0.677
20	0.507
25	0.406
30	0.338

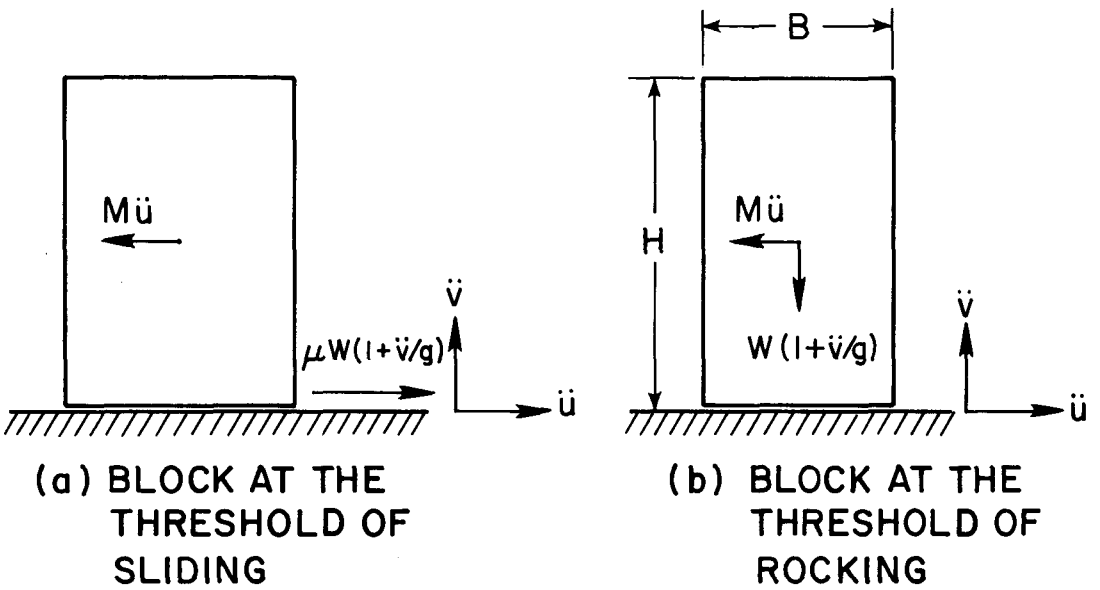

FIG. 2-1 RIGID BLOCK WITH SIMULTANEOUS HORIZONTAL AND VERTICAL GROUND ACCELERATIONS.

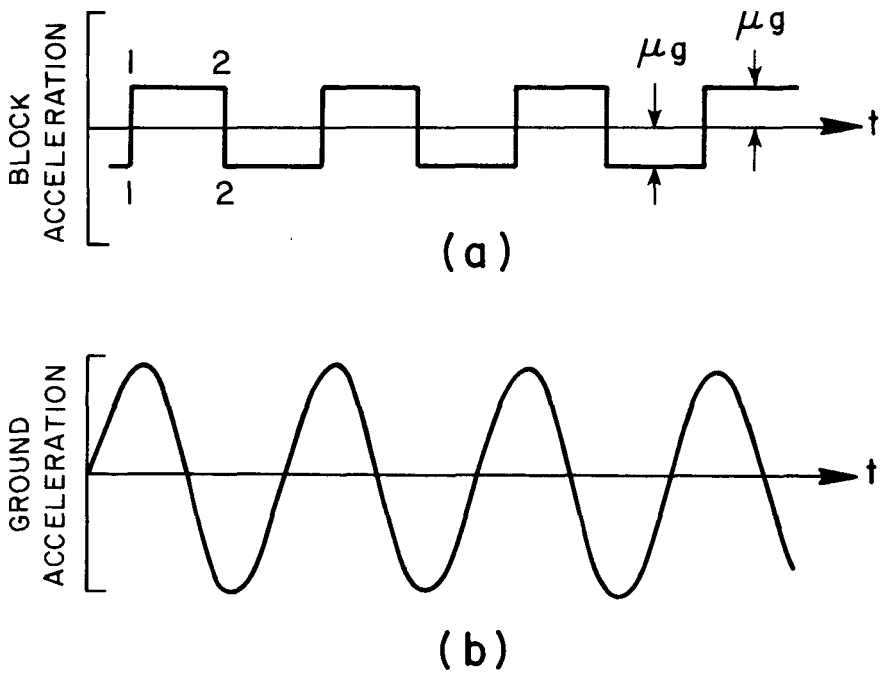

FIG. 2-2. IDEALIZATION OF BLOCK ACCELERATION AND COEFFICIENT OF FRICTION (COMPARE WITH FIG. 2-3).

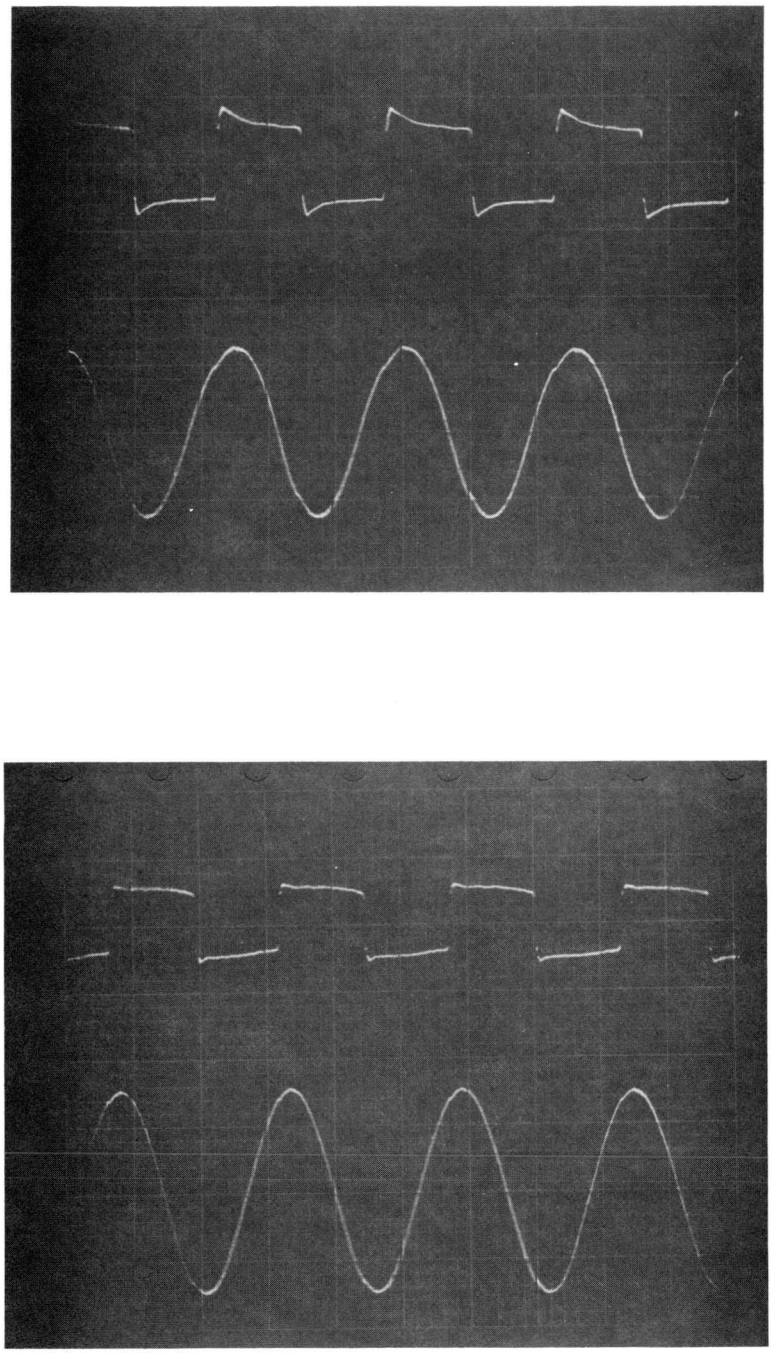

FIG. 2-3. OSCILLOSCOPE TRACES OF BLOCK ACCELERATION (UPPER CURVES) AND GROUND ACCELERATION (LOWER CURVES) FOR PLASTIC BLOCKS WITH TWO DIFFERENT SURFACE FINISHES. (FREQ = 10 Hz, SCALE: 1 cm = 0.4 g.)

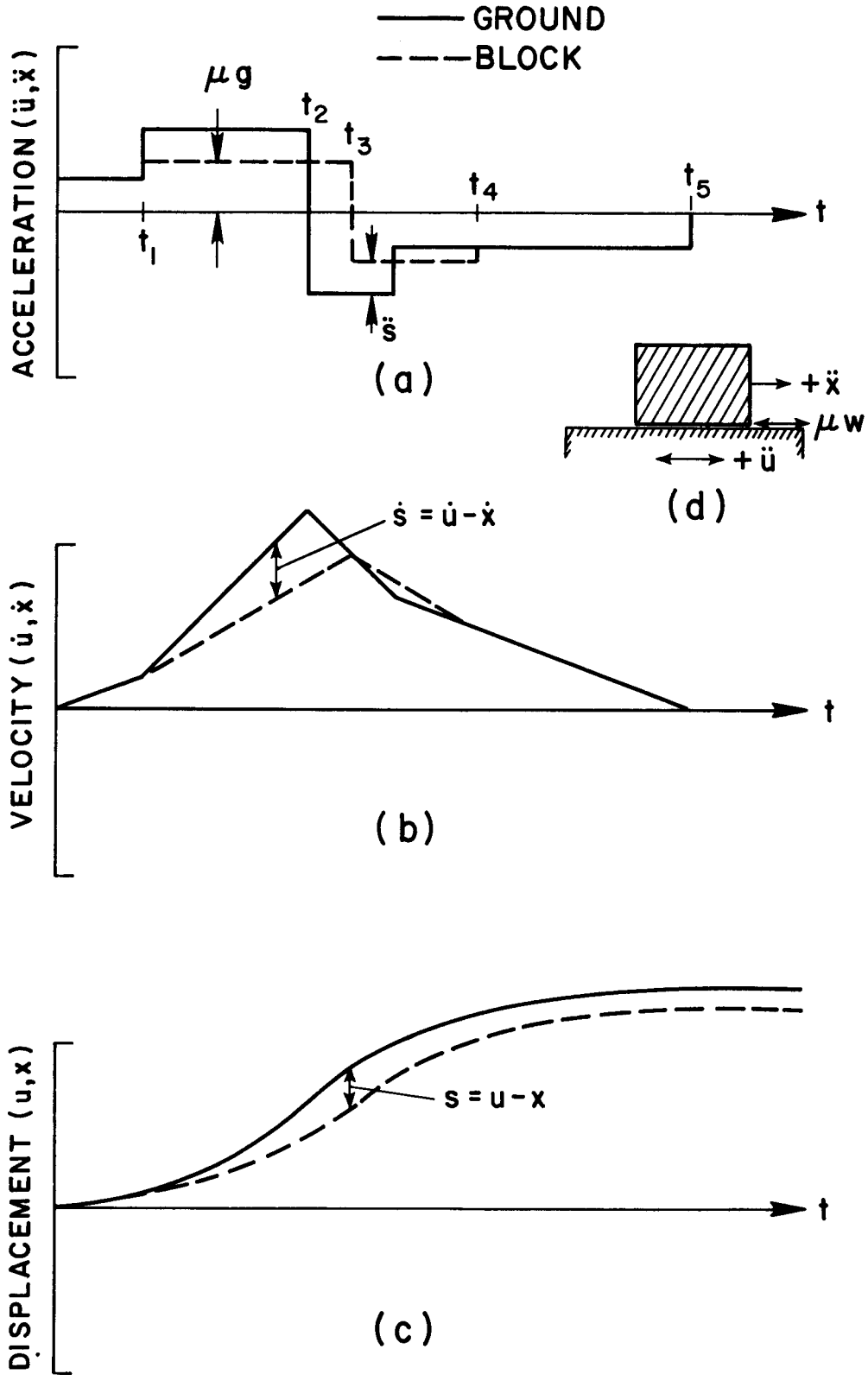

FIG. 2-4. SLIDING OF A BLOCK UNDER HORIZONTAL GROUND ACCELERATION.

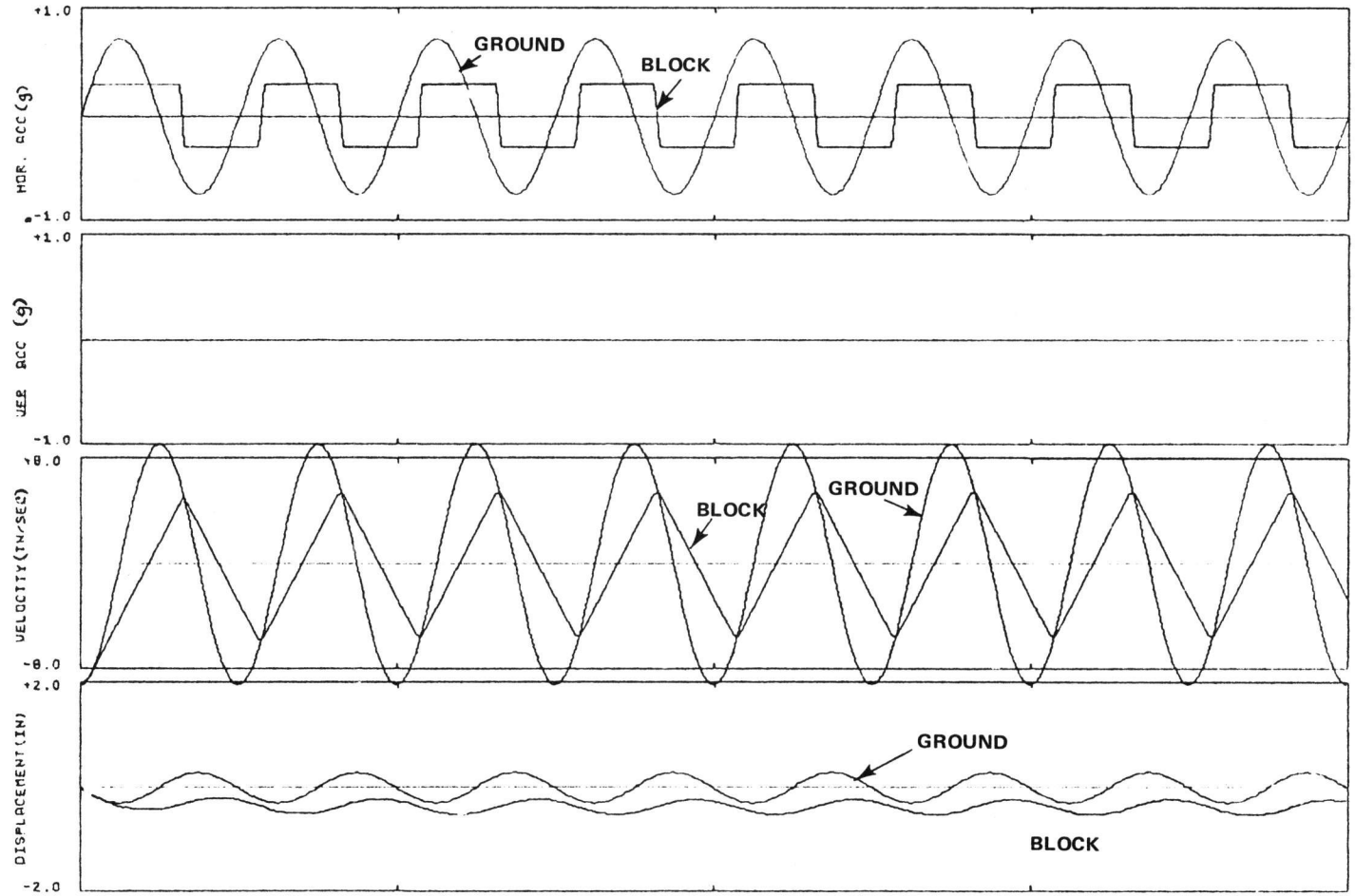

FIG. 2-5. MOTION OF A BLOCK DUE TO SINUSOIDAL HORIZONTAL(AH) AND VERTIC AL(AV) GROUND ACCELERATIONS, FREQUENCY=5HZ, μ=.30, AH=.75, AV=.00

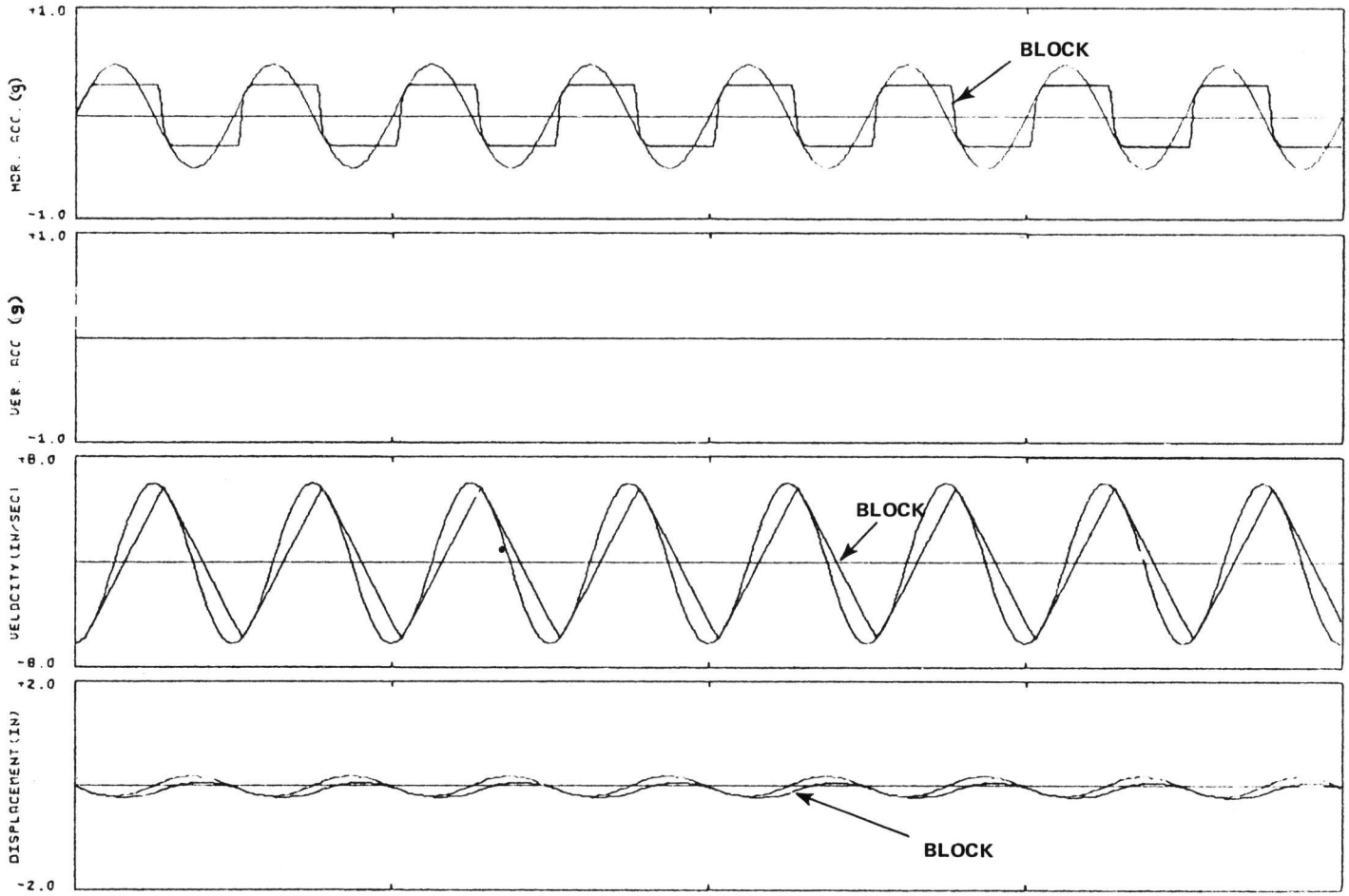

FIG. 2-6. MOTION OF A BLOCK DUE TO SINUSOIDAL HORIZONTAL(AH) AND VERTIC AL(AV) GROUND ACCELERATIONS, FREQUENCY=5HZ, μ=.30, AH=.50, AV=.00

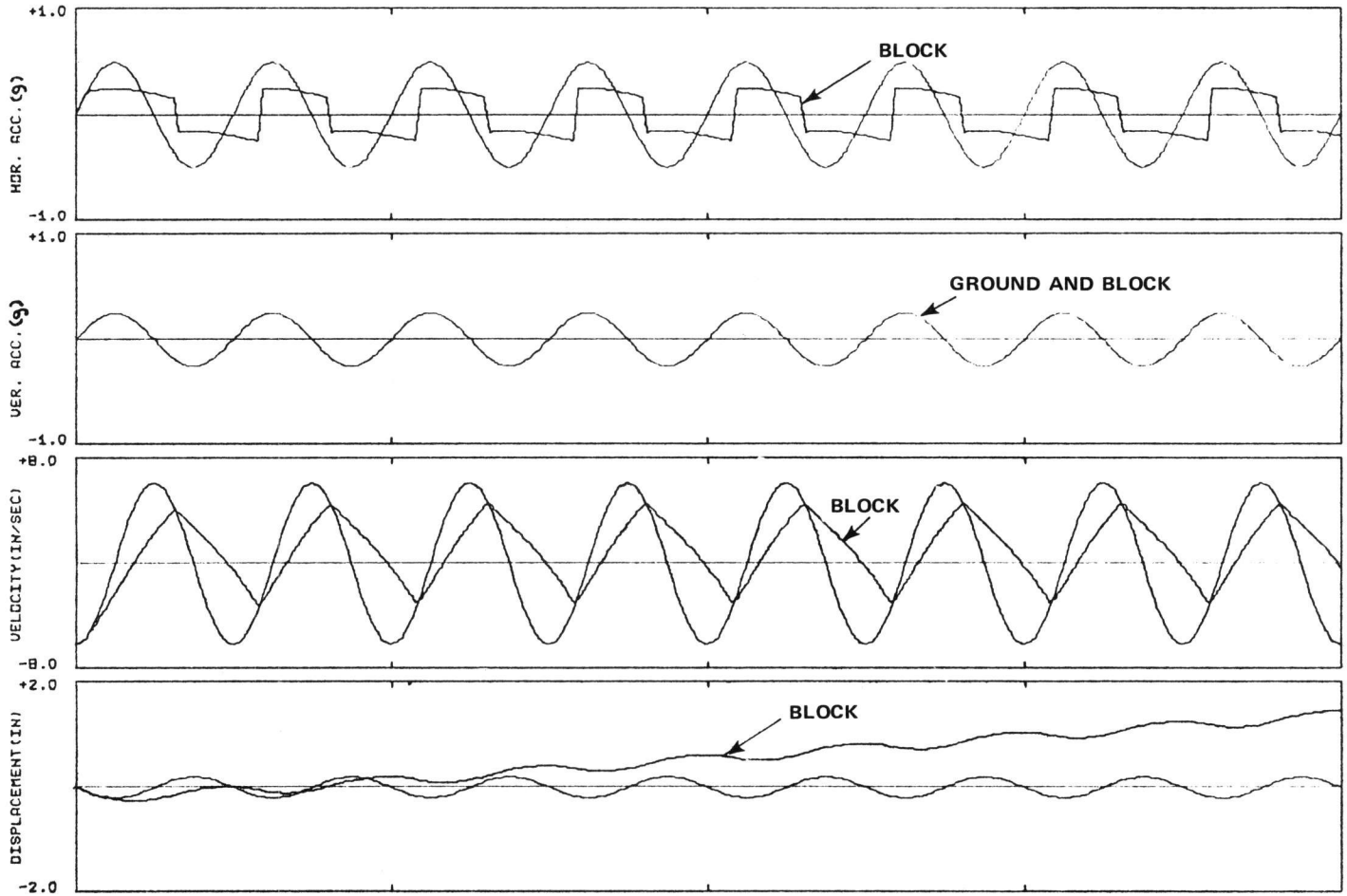

FIG. 2-7. MOTION OF A BLOCK DUE TO SINUSOIDAL HORIZONTAL(AH) AND VERTIC AL(AV) GROUND ACCELERATIONS, FREQUENCY=5HZ, μ=.20, AH=.50, AV=.25

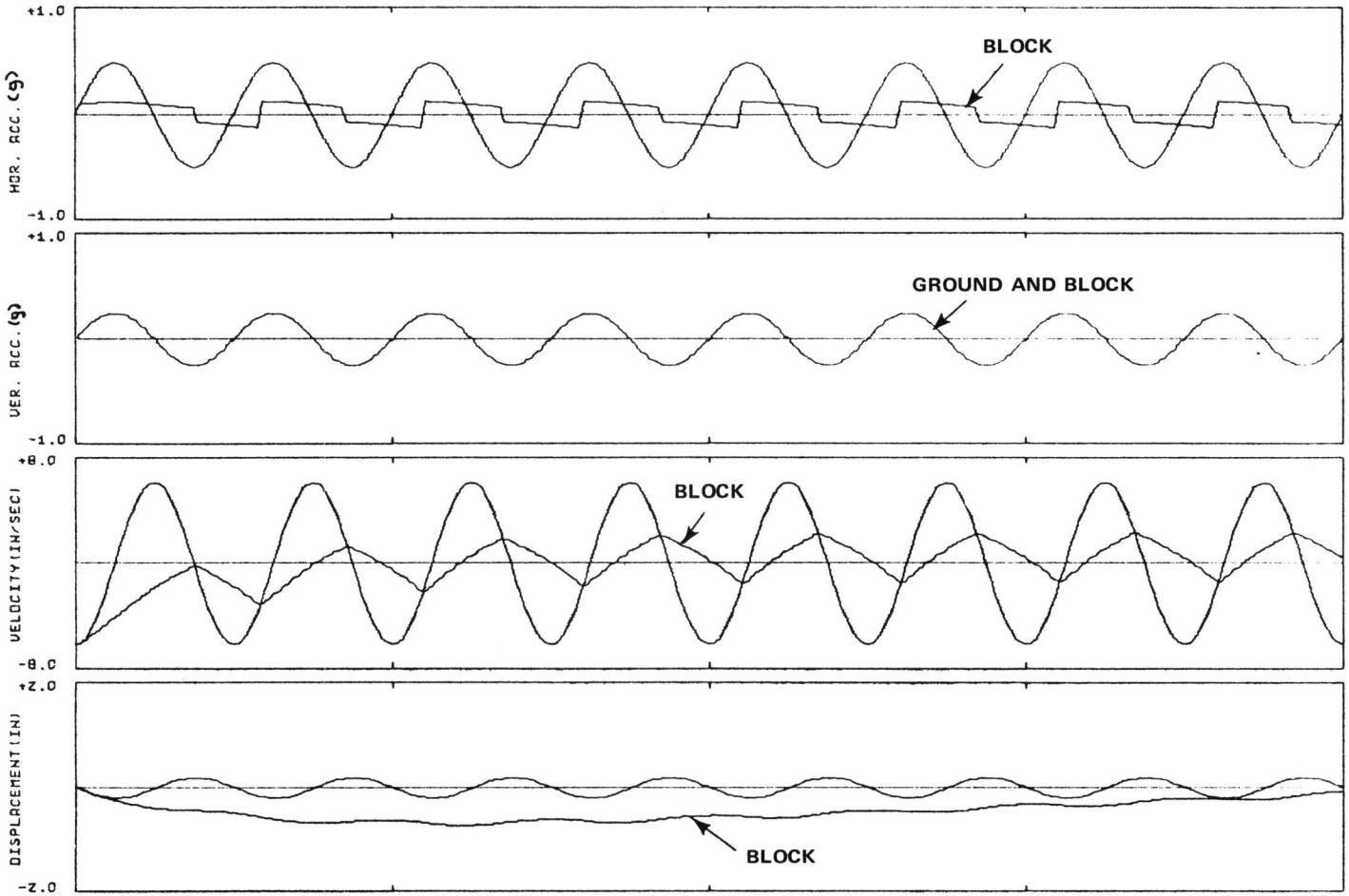

FIG. 2-8. MOTION OF A BLOCK DUE TO SINUSOIDAL HORIZONTAL(AH) AND VERTIC AL(AV) GROUND ACCELERATIONS, FREQUENCY=5HZ, μ=.10, AH=.50, AV=.25

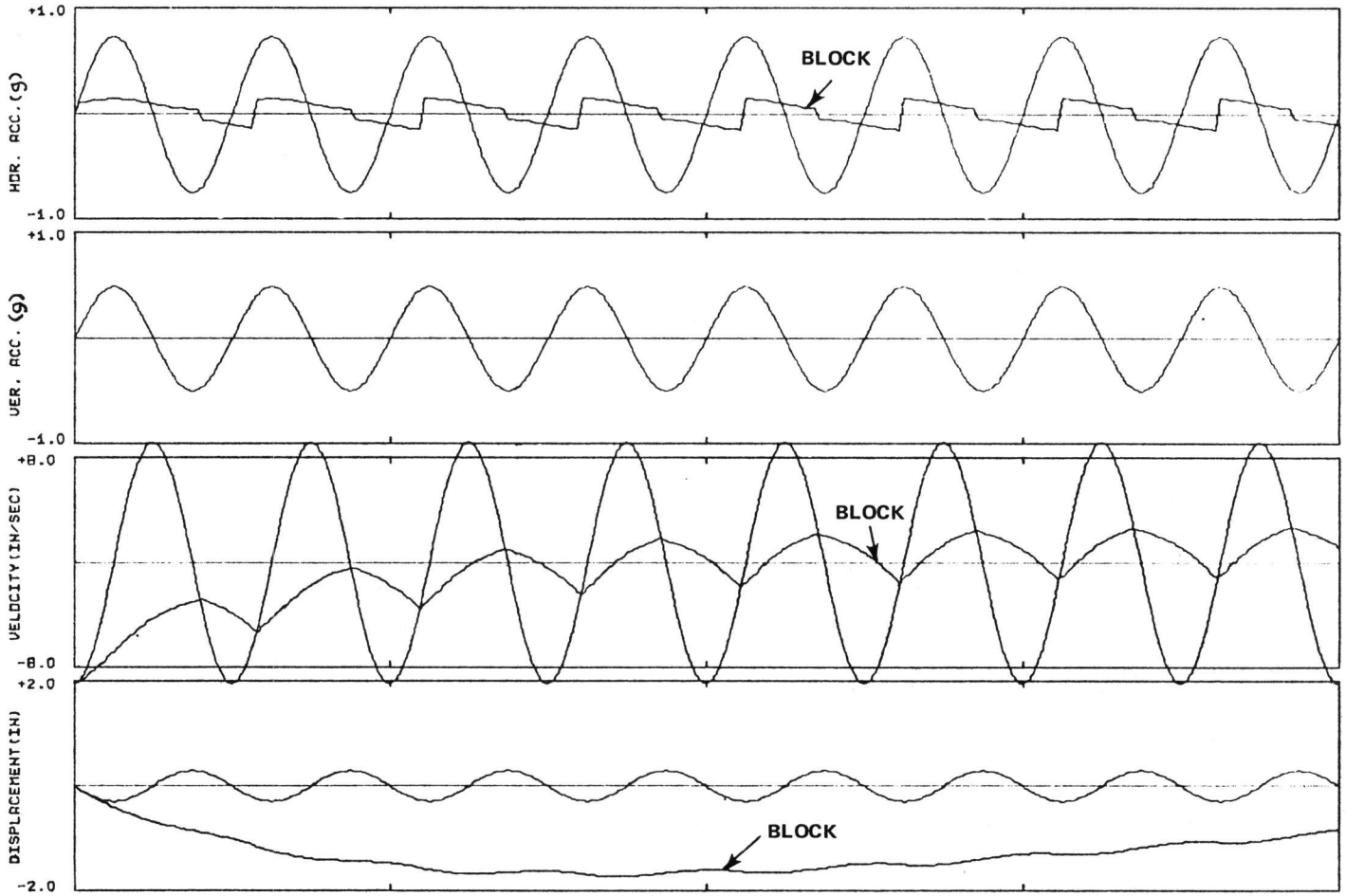

FIG. 2-9. MOTION OF A BLOCK DUE TO SINUSOIDAL HORIZONTAL(AH) AND VERTIC AL(AV) GROUND ACCELERATIONS, FREQUENCY=5HZ, μ=.10, AH=.75, AV=.50

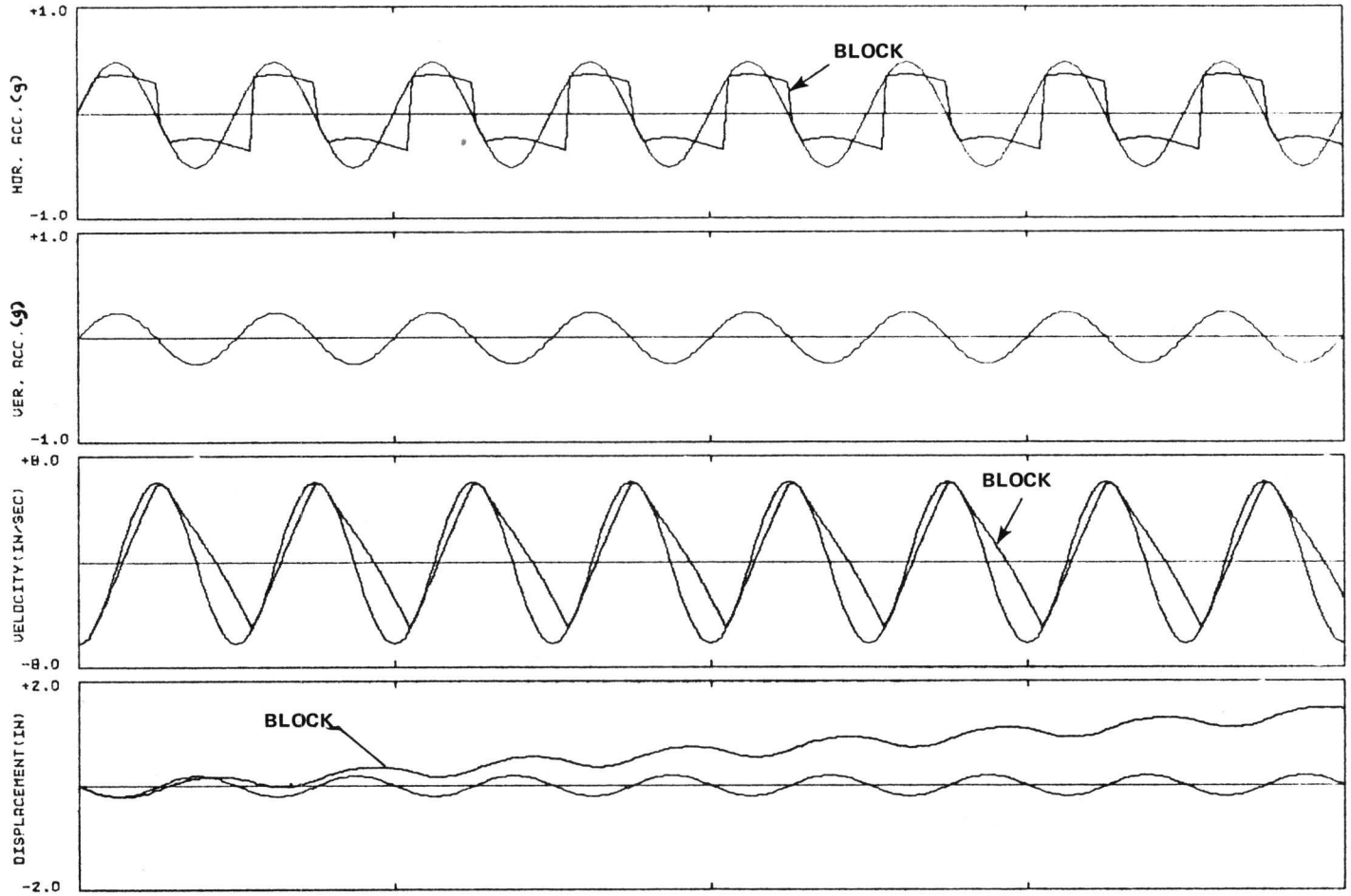

FIG. 2-10. MOTION OF A BLOCK DUE TO SINUSOIDAL HORIZONTAL(AH) AND VERTIC AL(AV) GROUND ACCELERATIONS, FREQUENCY=5HZ, μ=.30, AH=.50, AV=.25

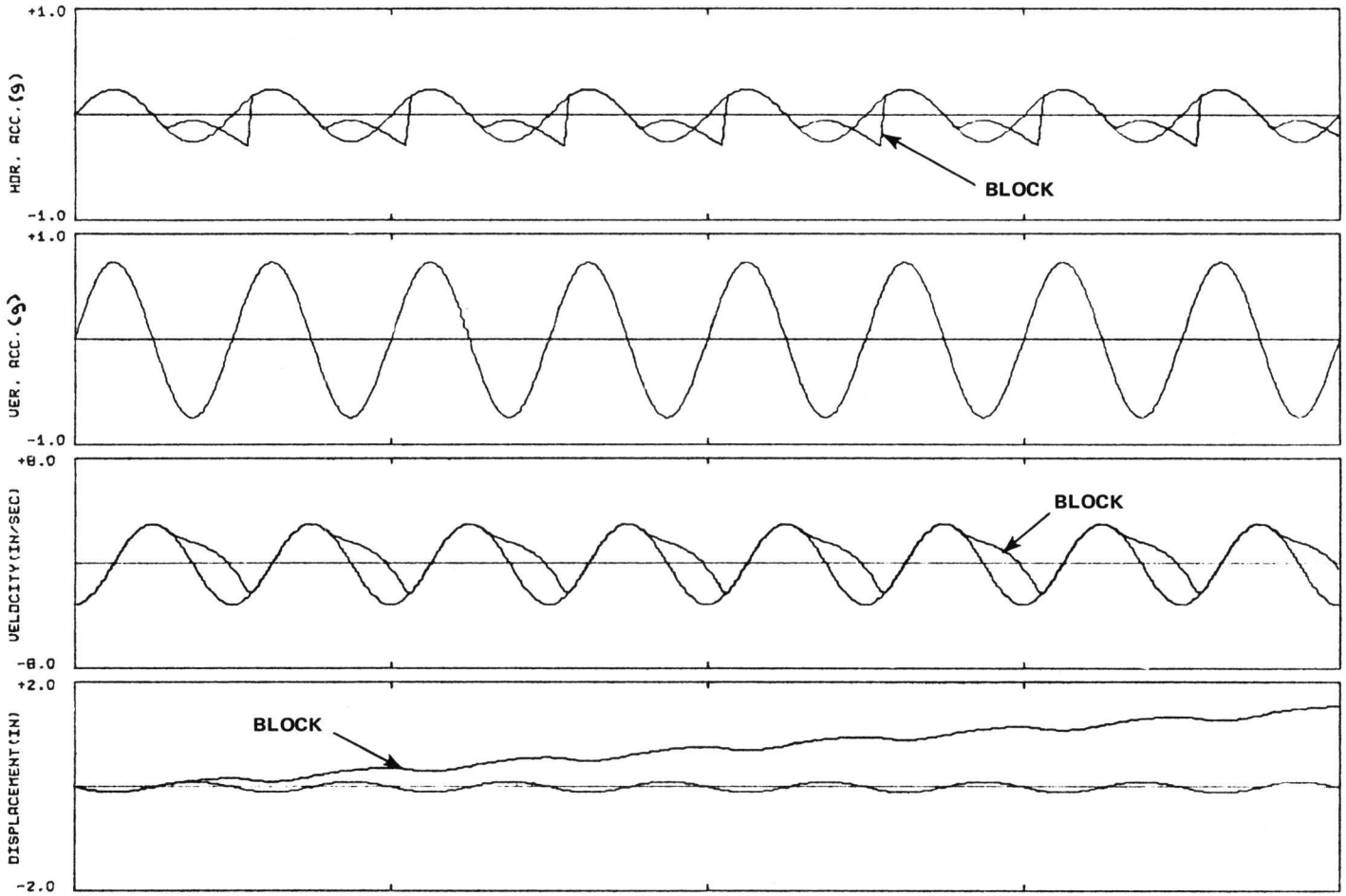

FIG. 2-11. MOTION OF A BLOCK DUE TO SINUSOIDAL HORIZONTAL(AH) AND VERTICAL(AV) GROUND ACCELERATIONS, FREQUENCY=5HZ, μ=.20, AH=.25, AV=.75

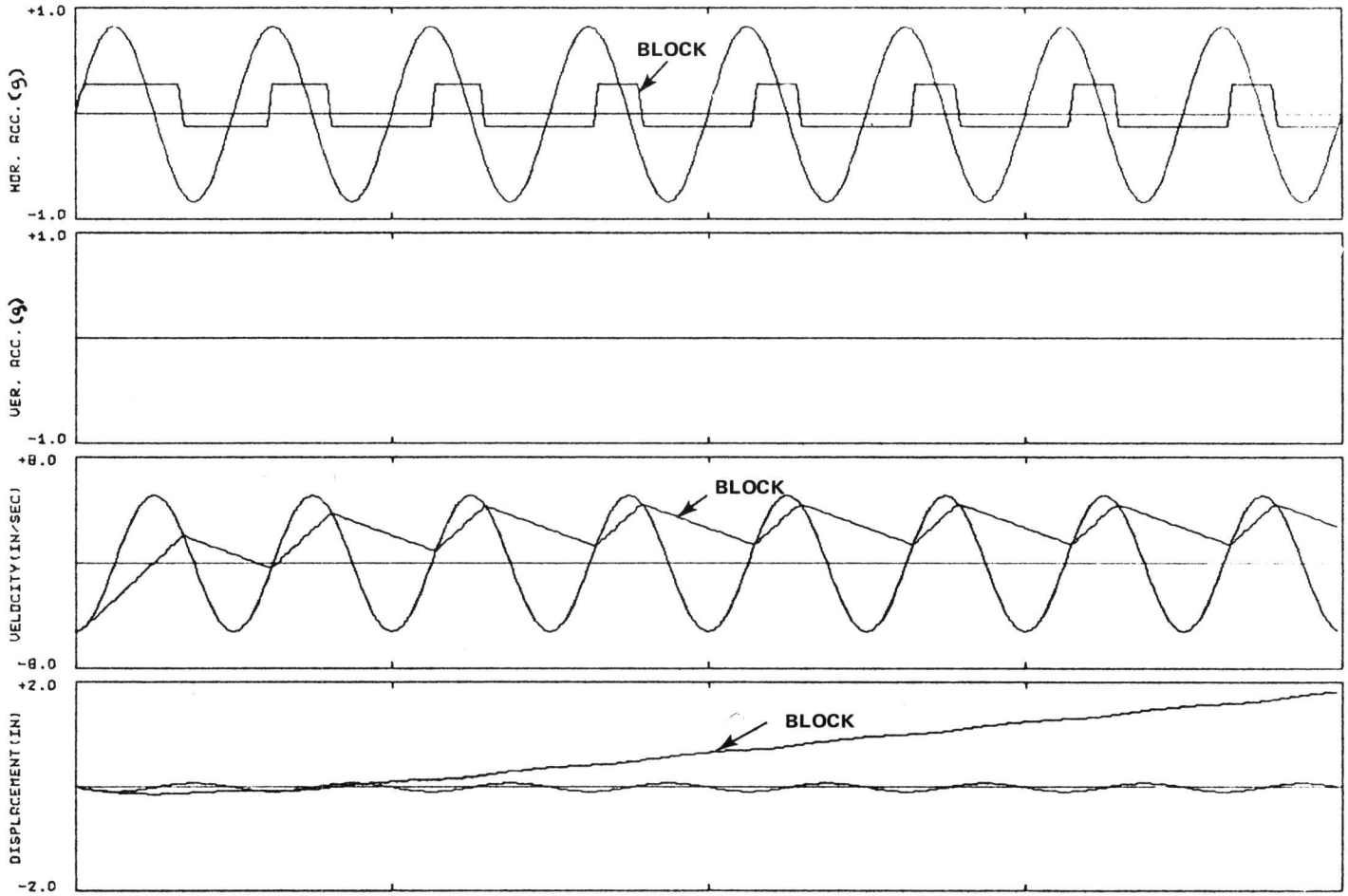

FIG. 2-12. MOTION OF A BLOCK DUE TO SINUSOIDAL HORIZONTAL GROUND ACCELERATION AND A FORCE(P),FREQUENCY=10HZ.,P/W=.086,μ=.20,AH=.84G

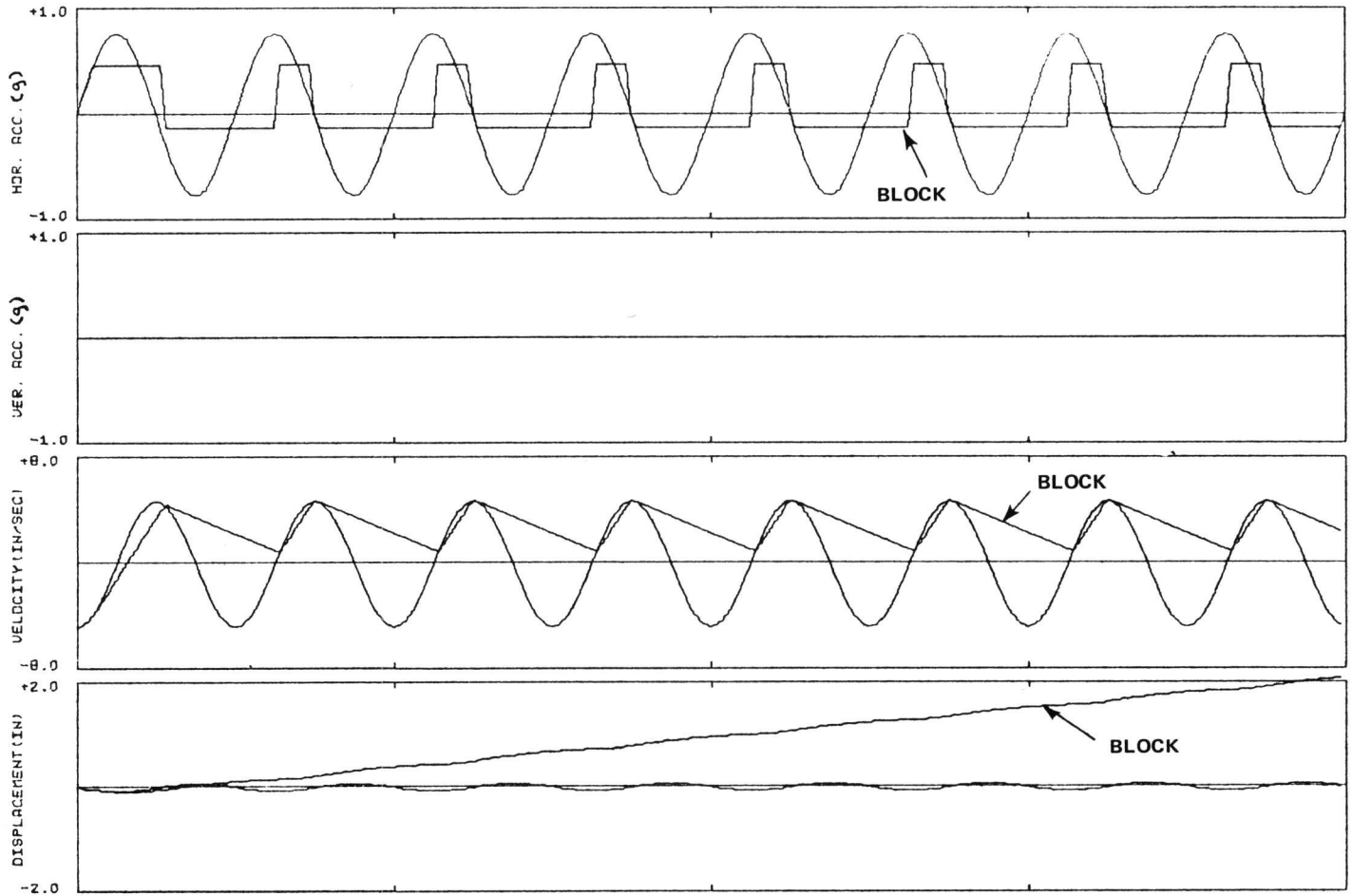

FIG. 2-13. MOTION OF A BLOCK DUE TO SINUSOIDAL HORIZONTAL GROUND ACCELERATION AND A FORCE(P),FREQUENCY=10HZ.,P/W=.168,μ=.30,AH=.77G

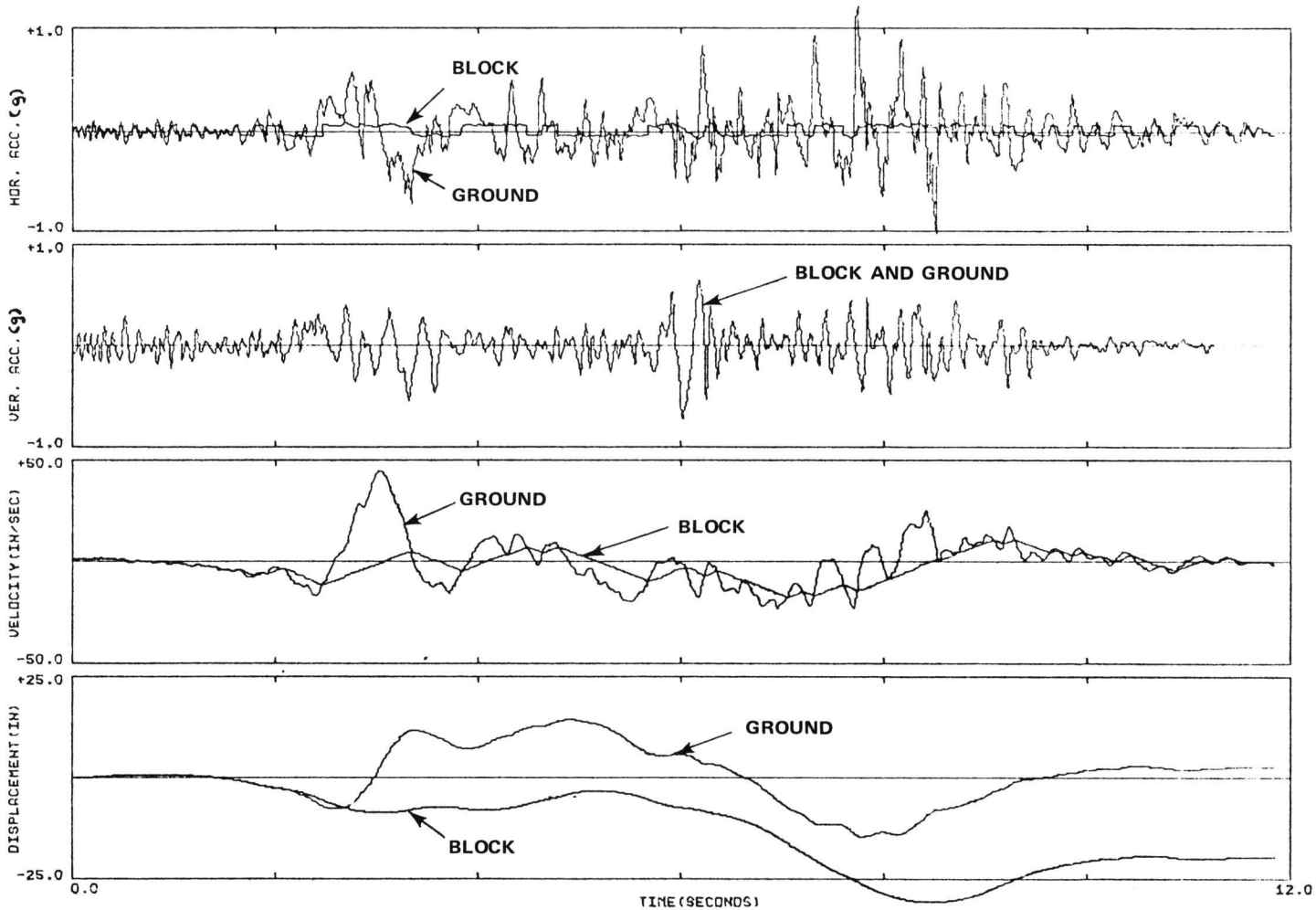

FIG. 2-14. MOTION OF A SHIELDING BLOCK SUBJECTED TO SAN-FERNANDO EARTHQUAKE 1971(PACOIMA DAM RECORD S16E)U=.05,K=.000W/IN

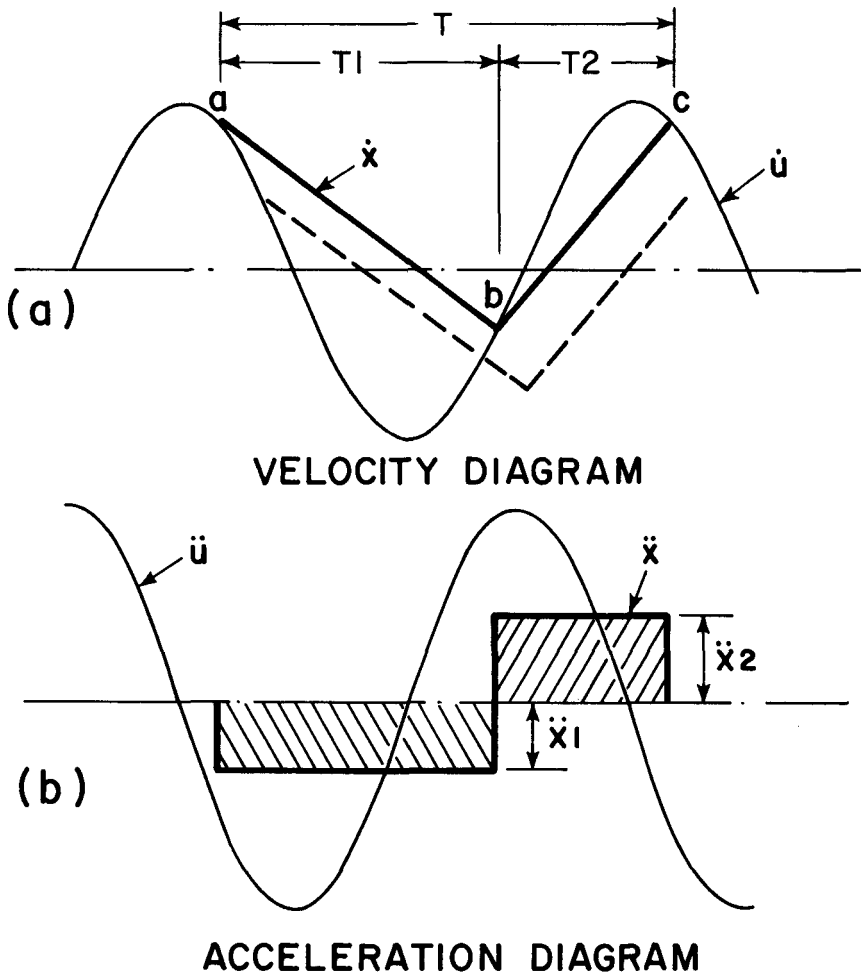

FIG. 2-15. CURVE FITTING METHOD OF SOLUTION.

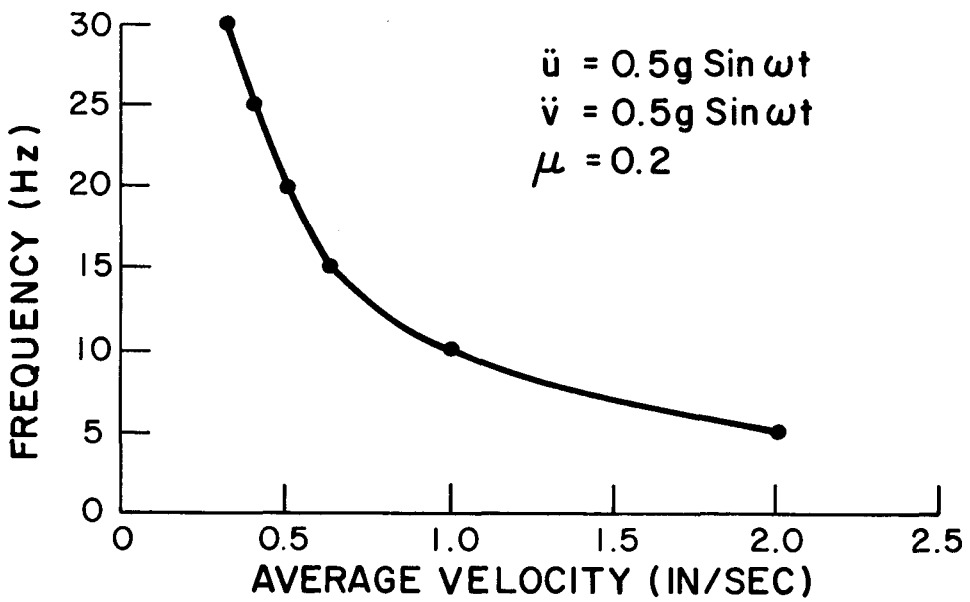

FIG. 2-16. AVERAGE VELOCITY OF BLOCK VS FREQUENCY OF SINUSOIDAL GROUND MOTION.

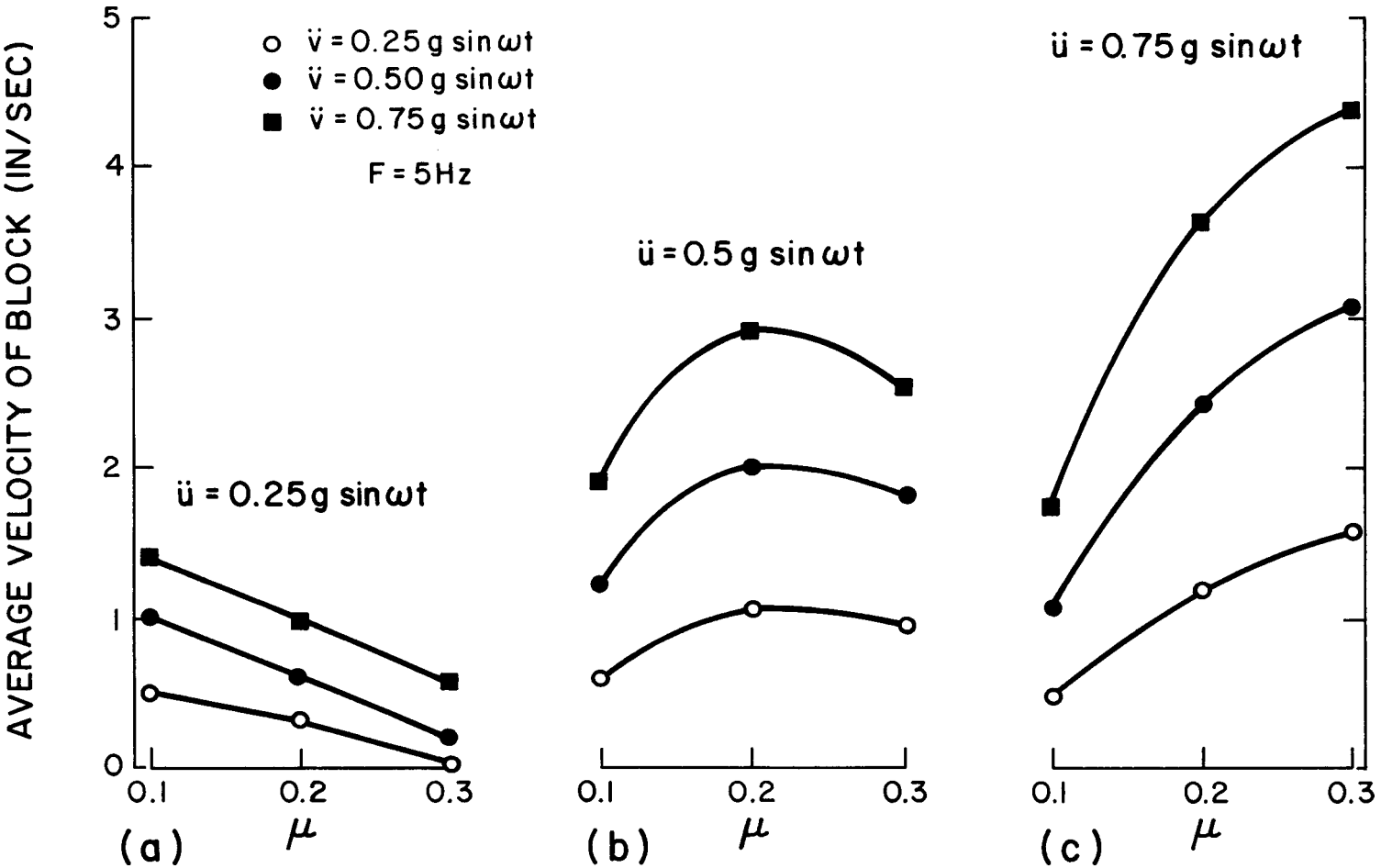

FIG. 2-17. VARIATION OF BLOCK VELOCITY WITH COEFFICIENT OF FRICTION AND AMPLITUDE OF SINUSOIDAL HORIZONTAL AND VERTICAL ACCELERATIONS.

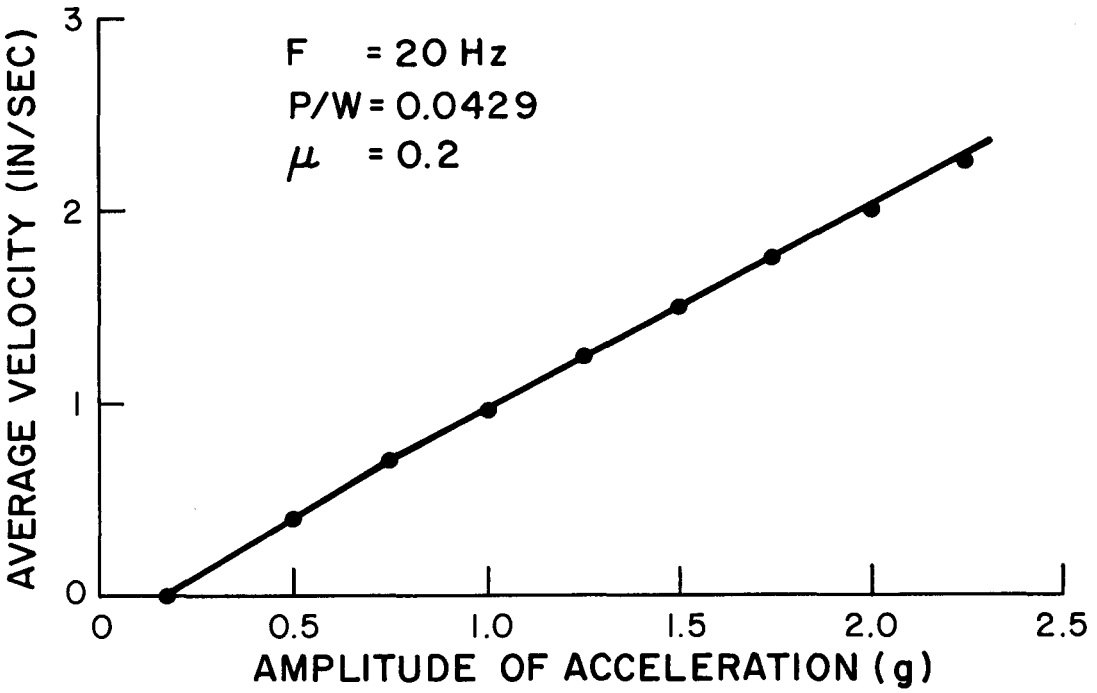

FIG. 2-18. VARIATION OF BLOCK VELOCITY WITH HORIZONTAL ACCELERATION AND A CONSTANT FORCE.

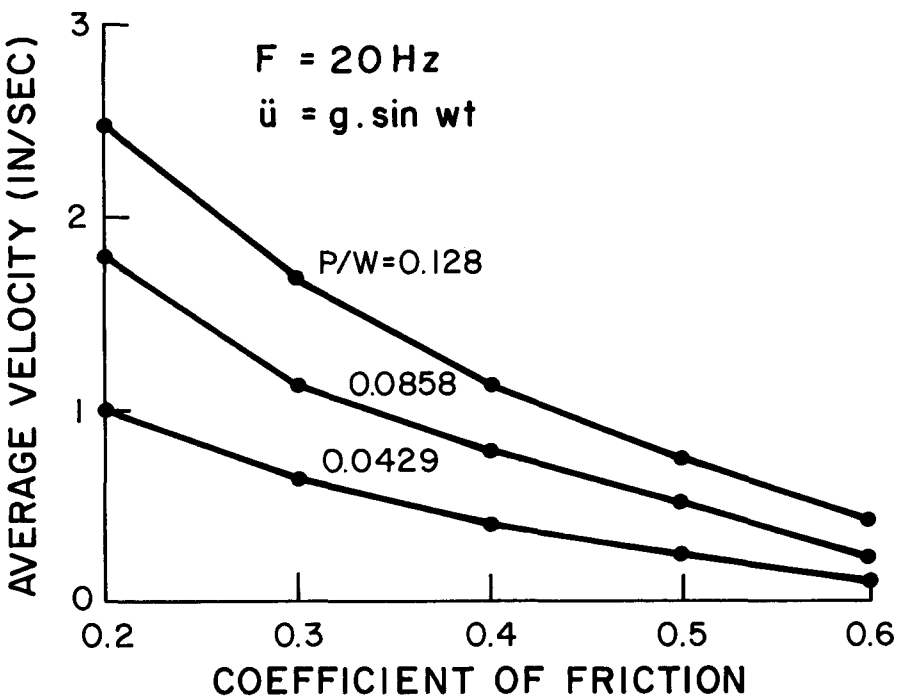

FIG. 2-19. VARIATION OF BLOCK VELOCITY WITH COEFFICIENT OF FRICTION AND HORIZONTAL FORCE.

SECTION 3

EXPERIMENTAL STUDIES AND COMPARISON WITH THEORETICAL RESULTS

3.1 General

Tests were conducted with concrete blocks on a 20 ft x 20 ft shaking table. The basic purpose of these experimental studies was to verify the mathematical model described in Section 2. The shaking table at the time of initial testing was still in the developmental stage and only sinusoidal type accelerations could be given in one horizontal and vertical direction. Tests were conducted either under sinusoidal horizontal acceleration and a constant horizontal force or sinusoidal horizontal and vertical accelerations together. Steady state average block velocity was measured and the comparison is given in Section 3.8. Later, when it was possible to put earthquake motions into the shaking table, tests were made on the sliding response of a block subjected to simulation of the San Fernando Earthquake (Pacoima Dam Record 1971). Time history of relative displacement of the block with respect to the shaking table was measured and the test results are compared with theory in Section 3.8. Based upon the testing experience, the suitability of various materials for reducing the coefficient of friction is discussed briefly in Section 3.9.

3.2 Shaking Table and Associated Systems

The shaking table, which can simulate an earthquake motion, is located at the University of California Richmond Field Station. It has plan dimensions of 20 ft x 20 ft, with one horizontal and the vertical degrees of freedom. It may be used to subject structures weighing up to 100 kips to motion of about twice the intensity of the N-S component of El Centro (1940) earthquake.

The shaking table is constructed with a combination of reinforced and prestressed concrete. Structurally, it may be considered as a 1-ft thick 20-ft square plate, stiffened by heavy central transverse ribs that are 1-ft wide and extend 1 ft 9 in. below the bottom surface of the table. Figure 3-1 shows the table being lowered in place during construction. The hydraulic actuators that drive the table horizontally are attached to the table by means of one of the transverse ribs. The vertical actuators are attached to the table by means of prestressing rods. The table weighs 100 kips.

The shaking table is driven horizontally by three 50-kip hydraulic actuators and vertically by four 25-kip hydraulic actuators as shown in Fig. 3-2. The actuators have swivel joints at both ends so that they can rotate about the foundation swivel joints as the table moves. The horizontal and vertical actuators are 10 ft 6 in. and 8 ft 8 in. long respectively and are located in a pit beneath the table. Figure 3-2 shows the pit before the table was mounted in place. The horizontal and vertical actuators are equipped with 200 gpm and 90 gpm servo-values respectively. The horizontal actuators are limited to displacements of $\pm$ 5 in. and vertical actuators are limited to displacements of $\pm$ 2 in. The flow rate of the servo-valves limits the maximum velocities in the horizontal and vertical directions to 25 in/sec and 15 in/sec respectively.

When the table is in operation, the air within the pit and beneath the shaking table is pressurized so that the total dead weight of the table and the test structure is balanced by the difference in air pressure between the air in the pit and the air above the table. The 1-ft gap between the table and the interior foundation walls is sealed by a 24-in. wide strip of vinyl covered nylon fabric. The fabric, in its inflated position, can be seen in Fig. 3-3. Because the dead weight is

balanced by air pressure, the four vertical actuators can accelerate the table up to a maximum of 1 g vertically. The three horizontal actuators can accelerate the table up to about 1.5 g horizontally. Oil, at an operating pressure of 3000 psi, is supplied to the actuators by four 80-gpm variable volume pumps, each of which is driven by a 120 HP electric motor. The actuator forces are reacted by a massive reinforced concrete foundation in the form of an open box with outside and inside dimensions of 32 x 32 x 15 ft and 22 x 22 x 10 ft respectively. The foundation weighs 1580 kips.

The electronic control system for the shaking table (see Fig. 3-4) was supplied by MTS Systems Corporation, Minneapolis, Minnesota, and is based on controlling five degrees of freedom of the shaking table. The sixth degree of freedom, translation perpendicular to the direction of the horizontal translational degree of freedom, is controlled by a sliding mechanism. Transducers are installed in each actuator to measure displacements and forces. From the displacement signals, feedback signals representing the average horizontal and vertical displacement, the pitch, roll and yaw (or twist) are derived on the assumption that the table is a rigid body. Corresponding force signals are also derived that are used to supplement the primary displacement feedback signals. Normally the pitch, roll and yaw command signals are zero, and the horizontal and vertical command signals represent translational displacement time histories of an earthquake record.

Associated with the table is a data acquisition and processing system which is based on a NOVA 1200 mini-computer operating in conjunction with a Diablo 31 moving head magnetic disc unit. The data acquisition and processing system is used for three main purposes: (1) generation of command signals in the form of displacement time histories,

(2) acquisition of data from up to 128 transducers that monitor the behavior of the test structure and shaking table during a test, and (3) processing of test data.

The shaking table command signals must be in the form of displacement time histories and the NOVA computer is used to derive this from the acceleration records. The original acceleration time histories may be fed to the computer by means of the teletype keyboard or the teletype paper tape reader. The time histories of the required earthquake are checked to see if the maximum values of acceleration, velocity or displacement will exceed the limits on the shaking table motion. After satisfactory displacement time histories are available for both the horizontal and vertical command signals, they are fed via a digital-to-analog converter to an analog tape recorder. The signals are stored there until they are required for a test, and at that time are fed to the MTS Control Console.

During a test the mini-computer is dedicated to the collection of data. Analog signals originating in accelerometers, LVDT's, etc. are fed to amplifiers, multiplexers, and an analog to digital converter housed in the Neff System 620. It is possible to sample up to 128 analog channels at a rate of 100 samples per second per channel. The sampled data is stored initially on the disc, and if permanent storage is desired, the data is transferred to the nine-track Wang digital magnetic tape recorder. The computer is also used to process test data stored on the disc or on the magnetic tape recorder, as well as to plot the complete time history of the signal of any channel on the Versatec printer/plotter.

However, during the initial stages of testing the data acquisition system was not in full operative stage, and therefore most of the data were obtained through the oscilloscope, oscillograph and x-y plotter,

which was quite adequate for sinusoidal ground motions. The data acquisition system was used for earthquake tests as described later.

3.3 Model and Equipment Design

It was shown in Sections 2.3 and 2.4 that the acceleration of a sliding block under ground acceleration is only a function of coefficient of friction μ between the block and the ground. When μ is independent of contact area and normal pressure it is evident that any two blocks with the same value of μ will have similar sliding response regardless of the block size and the density of the block material.

Because of the above factors, it was unnecessary to model the radiation shielding blocks and the tests were made on a 3 x 2 x 1 ft. reinforced concrete block weighing 935 lb and shown in Fig. 3-5. The block was provided with two shackles, one at the top and the other at one side (see Fig. 3-5). The top shackle was used for lifting and moving the block and the side shackle was intended to apply a constant horizontal force by means of a rope as shown in Figs. 3-5 and 3-6. Special care was taken to make the lower surface of the block as plane as possible so that pure sliding could be ensured without any rocking. The horizontal acceleration of the shaking table was always along the 3-ft dimension of the block, giving the block a B/H ratio of 3.0, which is much greater than μ, thus eliminating any possibility of rocking.

(1) Protective Slab:

A 6 ft x 6 ft x 6 in. protective slab was hydrostoned and prestressed to the shaking table as shown in Fig. 3-5. Four 1-in. diameter steel rods were used for prestressing the slab to the table at four corners of the slab. The weight of this reinforced concrete slab resting on nine 3-in. legs was 3500 lb. A prestressing force of about

5000 lb. in each prestressing rod gave enough frictional force against any relative movement of the slab with respect to the shaking table. The protective slab was designed and used for two purposes: (1) to eliminate any damage to the shaking table, and (2) to give a plane surface for sliding, because the surface of the shaking table was not plane enough to produce conditions for pure sliding.

(2) Transducer Stand:

A 13-in. high transducer stand was constructed out of 1/2-in. thick aluminum plates. The plates were welded together to form a stiff stand to avoid any resonance and this was fastened tightly to the slab by a 1-in. steel rod at one end and by means of two Phillip's bolts at the other end as shown in Fig. 3-7. The transducer could be moved up and down in two slots as shown in Fig. 3-7. The transducer was spring loaded and the flexible string of the transducer was attached to a hook on the block to measure any relative movement between the block and the slab.

(3) Frame for Horizontal Force:

An A-type frame, 3 x 4 ft at the base and 5 ft high was constructed out of 2 x 2 x 3/16 in. steel angles except those two members which support the two adjustable pulleys as shown in Fig. 3-6. These members that supported the pulleys were made out of 3 x 2 x 3/16 in. structural tubing. Each pulley could be adjusted by means of two nuts each at the top and bottom side of the channel members. The lower pulley had to be adjustable so that rope could be made horizontal. A constant horizontal force to the block was applied by means of a rope and weights passing over the two pulleys as shown in Fig. 3-6. The maximum horizontal force applied in these tests was about 210 lb, and the frame was fastened

appropriately to the floor to avoid overturning or sliding of the frame.

3.4 Instrumentation

An accelerometer was used to measure the horizontal block acceleration. The accelerometer is shown attached to the block in Fig. 3-7 and was connected to the oscilloscope and oscillograph through a charge amplifier, as shown in Figs. 3-6 and 3-8. Signals of the horizontal and vertical accelerations of the shaking table were measured by means of accelerometers attached to the table and connected to the oscilloscope and oscillograph for measurement purposes. The accelerometers were also connected to the data acquisition system for digitizing the data.

The displacement of the block relative to the shaking table was measured with a position transducer mounted on the aluminum frame as shown in Fig. 3-7. The transducer translates a mechanical movement into a linear voltage dc signal by using an infinite resolution slide wire which provides a nonlinearity of less than $\pm$ 0.1%. The output of the transducer was 31 mV/V of excitation voltage/inch. The output signal of the transducer was connected to an x-y plotter as shown in Fig. 3-8 and a continuous plot of the relative displacement of the block was obtained as a function of time under any table motion. The same plot was used to determine the average steady state velocity of the block under sinusoidal ground accelerations which was then compared with the computer results in Section 3.8.

3.5 Determination of Dynamic Coefficient of Friction

The dynamic coefficient of friction of the block was determined by sliding the block on the shaking table. The procedure for this experiment was the same as shown in Fig. 3-6 except that no horizontal force was applied, and the vertical acceleration of the shaking table

was also kept at zero. A sinusoidal horizontal input was given to the shaking table and the amplitude of the acceleration was increased slowly. As shown in Section 2, the block will slide as soon as the amplitude of the ground (shaking table) acceleration $\ddot{u}$ is greater than μg. After sliding occurs, the shape of the block acceleration $\ddot{x}$ will change from sinusoidal to rectangular as shown in typical oscilloscope traces of Fig. 2-3.

It should be noted that the amplitude of the shaking table acceleration was taken to a value high enough to make sure that the block did not reattach to the shaking table at the time when relative velocity of the block with respect to the table changed sign. This was possible to judge by observing the oscilloscope signal. It may also be noted that increasing the amplitude of the shaking table beyond that shown in Fig. 2-3 does not effect the wave form of the block acceleration $\ddot{x}$, because $\ddot{x}$ under the sliding situation with no vertical table motion has to be equal to μg.

The calibration of the accelerometer was done before starting the experiment and thus it was possible to read the value of μ directly from the traces similar to those shown in Fig. 2-3.

Table 3-1 shows the dynamic coefficient of friction values for various materials which were used in this study. It will be seen that there is a wide variation in the value of μ for concrete. The concrete blocks that were taken for testing directly from the radiation shielding systems of the Lawrence Berkeley Laboratory had a μ value close to 0.6, while the concrete block that was constructed especially for testing had a μ value of 0.3 which subsequently reduced to 0.2. The reason for the low initial value for the test block was its smoother finish and higher ratio of cement; and the further reduction in the value of μ

from 0.3 to 0.2 was caused by sliding which made the contact surfaces very smooth and glassy. Difficulty was also encountered in working with teflon. Because of the rubbing action during sliding, teflon produced an electrostatic charge which attracted dust particles from the atmosphere, making the surfaces dirty and thus increasing the effective value of μ rather rapidly.

The effect of the frequency of vibration of ground motion on the value of coefficient of friction was also studied on a concrete block and the results are plotted in Fig. 3-9. The value of μ did not show any significant dependence on frequency within the frequency test range. These tests were made under sinusoidal ground motions.

An attempt was made to study the effect of variation of contact area on the coefficient of friction for a given weight for the concrete blocks. These tests, however, proved to be inconclusive because of a large variation in the value of μ for concrete from one surface to another. The independence of friction coefficient from the area of contact was assumed to be accurate enough for this study.

3.6 Testing Procedure for Sinusoidal Ground Accelerations

As pointed out earlier, during the initial part of these studies the shaking table was still under development and only sinusoidal ground acceleration inputs could be applied. Two types of tests were conducted in this part of the program. The first consisted of the sliding response of the block under a horizontal ground acceleration with a constant horizontal force acting on the block. The second phase was concerned with the sliding of a rigid block under simultaneous horizontal and vertical ground accelerations. The coefficient of friction, the horizontal force (P), and the amplitude of ground vibration

were varied to get the test data over a wide range for comparison with the theoretical results.

Different materials were used between the concrete block and the shaking table to vary the coefficient of friction and to study the suitability of these materials for use under radiation shielding blocks. The materials tried included plywood, masonite and teflon. In the latter part of the testing program, under the actual earthquake-type ground accelerations, formica sheets were used with graphite (Section 3.7). In each case two sheets of these materials varying in thickness from 1/16 in. to 1/4 in. were placed between the block and the shaking table. The problems associated with the use of these materials are described briefly in Section 3.9. The testing procedures were as follows:

(1) Block Under Horizontal Acceleration and A Horizontal Force:

The test set up for this experiment is shown in Fig. 3-6. The concrete block was placed on the protective slab with two sheets of plywood between the slab and the block. The horizontal force was applied through a nylon rope. This rope had enough longitudinal flexibility to eliminate any significant transmission of cyclic accelerations to the applied dead weight, and thus the horizontal force could be taken as a constant.

The amplitude of the sinusoidal horizontal acceleration of the shaking table was slowly increased to the required value and the block was kept from sliding during this process by placing a temporary stop between the block and the transducer stand. As soon as the amplitude of the acceleration reached the required level, the stop was removed to release the block. The block then started moving in the direction of the applied force provided the sum of the inertial force plus the applied horizontal force P exceeded the frictional force.

The relative displacement of the block with respect to the table was recorded on an x-y recorder as a function of time. Two such typical plots are shown in Fig. 3-10(a). It will be seen from these plots that apart from the variation in local slope of the displacement-time curve in each cycle of the ground motion, the overall slope of the displacement curve is constant, indicating that the block had an overall constant velocity. This average velocity was determined for each test from these plots and the values are given in Table 3-2 for comparison with the theoretical results.

A continuous trace of the horizontal accelerations of the shaking table and the concrete block was taken on an oscillograph. The oscillograph trace was used to measure the amplitude of the table acceleration and the coefficient of friction. As explained in Section 2.7 and Fig. 2-15, the acceleration of the block in the direction of the force $\ddot{x}_1 = \mu g + P/W$ and in the other direction $\ddot{x}_2 = \mu g - P/W$. Therefore $\ddot{x}_1 + \ddot{x}_2 = 2\mu g$.

Knowing $\ddot{x}_1$ and $\ddot{x}_2$ from these oscillograph traces, μ was determined for each test. As a check, an oscilloscope trace was also taken for each test. A typical oscilloscope trace is shown in Fig. 3-11. The oscillograph trace was also used for graphical comparison with the theoretical results. A trace of a part of a typical oscillograph trace is shown in Fig. 3-12 in comparison with the predicted curves.

The frequency of vibration of the horizontal acceleration in this series of tests was 5 Hz. The results of these tests are given in Table 3-2 in the form of average block velocity along with other important measured parameters. These included the amplitude of horizontal acceleration, the ratio of the horizontal force to the weight of the block (P/W), and the coefficient of friction. This information was used

to predict theoretically the average velocity of the block. These values are compared in Table 3-2.

(2) Block Under Horizontal and Vertical Accelerations:

The procedure for determining the sliding response of the block under simultaneously applied horizontal and vertical accelerations was the same as shown in Fig. 3-6 except that no horizontal force was applied to the block.

At the start of a test with each new material between the block and the protective slab, the coefficient of friction was measured by subjecting the block to sinusoidal horizontal acceleration only as explained in Section 3.5. The same was repeated to determine the value of μ at the end of testing and the average of the two was used in computer analysis to predict the response theoretically.

For each test as before, the block was constrained, and the vertical acceleration of the shaking table was brought up to the required amplitude. Then the amplitude of horizontal acceleration of the table was increased to the intended level. For the sake of simplicity, horizontal and vertical accelerations were applied in phase with each other. As soon as the acceleration levels of the table were up to the desired level, the block was allowed to move, and it assumed a constant average steady state velocity as before.

Displacement vs time was recorded on the x-y plotter. Two such typical plots are shown in Fig. 3-10(b). An oscilloscope trace of the horizontal and vertical accelerations of the table, as well as the horizontal acceleration of the block was taken for each test. A record was also taken by oscillograph. These traces were used to determine the exact table accelerations. A part of an oscillograph trace of the

accelerations is shown in Fig. 3-13 for comparison purposes with the theoretically predicted curves.

The measured experimental data on the average velocity of the block determined from plots such as shown in Fig. 3-10(b) and the corresponding values of horizontal and vertical accelerations of the shaking table, frequency of the table vibration and coefficient of friction are presented in Table 3-3. The data on the shaking table accelerations, frequency, and coefficient of friction were then used to predict the velocity of the block by using the computer program BLOKSLD. The theoretical values are also given in Table 3-3 for comparison.

3.7 Testing Procedure for Earthquake Ground Excitations

During the latter part of this investigation, it was possible to simulate horizontal and vertical earthquake ground motions on the shaking table facility. Thus, it was decided to study experimentally the sliding response of a block for earthquake motions so as to check the accuracy of the computer program named BLOKSLD.

The test set-up of the block was the same as shown in Fig. 3-6 except that in this case no horizontal force was applied. Full use of the data acquisition system associated with the shaking table facility was made this time. The signals from measured horizontal and vertical accelerations and displacements of the table, horizontal block acceleration and the relative displacement of the block were all connected to an analog-to-digital converter to keep a digitized record. The details of the data acquisition system are described in Section 3.2.

The horizontal ground motion record selected was that recorded at Pacoima Dam (S74°W) during the San Fernando Earthquake of 1971. The reason for this selection was the high accelerations associated with

this record which would produce appreciable block sliding. The two peak accelerations on this record which exceeded 1 g were reduced to 1 g. Using this record, it was possible to keep the displacements of the shaking table well within the available $\pm$ 5 in. range and still be able to get about 80% intensity of the actual earthquake record in the horizontal direction. The vertical signal applied to the table was not, however, the signal actually recorded at Pacoima. The reason for this was that preliminary computer studies indicated that the actual vertical signal would have little influence on the block sliding response, and it was considered more important in a test aimed at validating theory to use a vertical component that would have a marked influence. For this reason the horizontal signal was also applied in-phase with the vertical direction because the computer data suggested that equal horizontal and vertical amplitudes would produce a block response almost twice that due to the horizontal component alone.

Two formica sheets, 1/8 in. thick were placed between the block and the shaking table to reduce the coefficient of friction. During the initial testing it was found that the formica crumbled and pulverized under shear stress concentration at a few points, the particles between the two sheets raising the coefficient of friction to 0.4. To overcome this problem, graphite was used between the formica sheets to reduce the friction coefficient μ. The use of graphite gave a value of μ between 0.09-0.12 depending upon the condition of the formica sheets, and the use of graphite, prevented the failure of the formica.

The selected earthquake acceleration record was punched on a paper tape for the input signal to the shaking table as explained in Section 3.2. Four tests were made in all. In each test the intensity of

horizontal acceleration was about 80% of the Pacoima Dam (S74°W) record while the intensity of the vertical acceleration was about 0%, 10%, 20% and 30% for the first, second, third, and fourth tests respectively.

The output horizontal and vertical accelerations and displacements of the shaking table, the horizontal block accelerations and the relative block displacement were recorded on an oscillograph as a function of time. The same data was also digitized with the help of analog-to-digital converter at a rate of 50 samples per second and was stored on disc. The digitized data was processed with the help of a mini-computer (NOVA 1200) to search for maximum and minimum values, which were printed out along with zero corrections required for each channel.

The oscillograph traces of accelerations and displacements of the shaking table, the horizontal acceleration of the block and the relative displacement of the block were plotted optically on a photographic paper (Visicorder paper) and were not suitable for reproduction. Therefore, the digitized data on the disc was plotted by an already existing program on the Versatec printer/plotter. This program could plot up to a maximum of four traces at a time. The horizontal and vertical displacements of the shaking table were not considered important. The quantities plotted for each test were the horizontal acceleration of the shaking table, horizontal acceleration of the block, vertical acceleration of the table, and the relative displacement of the block with respect to the table (Figs. 3-14 through 3-17). It can be noted in these plots that the actual earthquake acceleration record starts after about 2 to 3 seconds from the starting zero time. The reason for this was that the data acquisition system had to be started a few seconds earlier than the command signals of the shaking table so as not to lose any data.

Precise value of dynamic coefficient of friction was determined from the digitized record of horizontal acceleration of the block from Test No. 1 when the vertical acceleration of the table was zero. Under this condition the acceleration of block $\ddot{x} = \mu g$, provided the block is sliding. The digitized record kept on the disc was printed on the Versatec printer and an average value of μ was determined. The average value of dynamic friction of coefficient for graphite between two formica sheets was found to be 0.090 when the formica sheets were in a perfect condition. The value of static coefficient of friction at those points where the block would break loose from the shaking table and started sliding was found to be as high as 0.15. It should be remembered that it is the static coefficient of friction which should be used in determining the boundary between sliding and rocking of a block and not the dynamic value of friction coefficient as the static coefficient presents the more serious condition for rocking. At the end of testing, the first test was repeated to check if there was any change in the coefficient of friction as precise determination of μ was necessary to carry out the computer analysis.

The digitized record of horizontal as well as vertical acceleration records of the shaking table was punched on a paper tape on the teletypewriter directly from the magnetic disc for each test. These digitized acceleration records punched on the tape were used to carry out the theoretical prediction of the sliding response of the block for each test. The Calcomp plots of these computer results are given in Figs. 3-18 through 3-21 for comparison with experimental results.

3.8 Comparison of Test and Theoretical Results

A comparison of test and theoretical results is presented briefly in this section. The comparison was made for both sinusoidal

and earthquake-type ground motions and a good agreement was found between the test and predicted results. For sinusoidal ground motions, the comparison was made between the test and predicted steady state average block velocities, while in the case of earthquake ground motions the comparison was made between the test and predicted relative displacements. These comparisons for sinusoidal and earthquake motions were as follows:

(1) Block Under Sinusoidal Horizontal Acceleration and a Horizontal Force:

A comparison of steady state average test and theoretical block velocities under a sinusoidal horizontal acceleration and a horizontal constant force is given in Table 3-2. The horizontal force (P) in this table is given as a ratio of the weight (W) of the block. The results are given over a wide variation of acceleration amplitudes and P/W ratios, and the coefficient of friction was also varied. The frequency of vibration was 5 Hz. It will be seen in Table 3-2 that there is generally a good agreement between the test and theoretical results and the average difference between the two is within 8%.

Figure 3-12 shows a comparison of a typical test and theoretical result when the block was subjected to a sinusoidal horizontal acceleration of amplitude of 0.54 g and a P/W ratio of 0.058. The values of μ and frequency of vibration were 0.23 and 5 Hz respectively. Figure 3-12 shows a portion of steady state acceleration and displacements of the ground (shaking table) and the block, against time. The experimental plots in Figure 3-12 were taken from oscillograph traces and the theoretical curves were drawn from the Calcomp plots. It can be seen that there is good agreement between the test and predicted results on the block acceleration and the predicted displacements are about 10% higher than the test values.

(2) Block Under Sinusoidal Horizontal and Vertical Accelerations:

Comparison of steady state average test and theoretical block velocity under simultaneous sinusoidal horizontal and vertical ground excitations is given in Table 3-3. The agreement between the test and predicted values of the block velocity is generally satisfactory and the average difference between the two is within about 10%.

Figure 3-13 shows a comparison of the sliding response of a block when subjected to sinusoidal horizontal and vertical ground accelerations of amplitudes of 0.50 g and 0.45 g respectively. The values of μ and frequency of vibration were 0.20 and 5 Hz respectively. Figure 3-13 which shows a portion of the steady state accelerations and displacements of the ground and the block against time was taken from the experimental oscillograph traces and the theoretically predicted Calcomp plots in the same manner as Fig. 3-12. Figure 3-13 shows that the test and theoretical trends in the accelerations and displacements of the block are similar. Although the differences in the test and predicted values of acceleration are obvious, they do not seem to have a great effect on the displacements which are in good agreement. The differences in the test and predicted values of acceleration can be easily explained on the basis of the assumptions made in Section 2.2.

(3) Block Under Earthquake Ground Motions:

Table 3-4 shows the test and predicted values of maximum relative displacements of the block with respect to the ground (shaking table) when subjected to San Fernando Earthquake (Pacoima Dam Record S74°W) of 1971. The results of each test were plotted and are shown in Figs. 3-14 through 3-17. Corresponding theoretical results are shown in

Calcomp plots of Figs. 3-18 through 3-21. Testing and theoretical analysis was done for the horizontal and vertical ground accelerations detailed in Section 3.7.

It can be seen in Table 3-4 that the agreement between test and predicted values of maximum relative displacements is satisfactory. The maximum values occurred at the same time. The difference between the test and the predicted values varies from 5% to 10% when calculated on the basis of test results as shown in Table 3-4.

Comparison of Figs. 3-14, 3-15, 3-16, and 3-17 with Figs. 3-18, 3-19, 3-20, and 3-21 respectively shows an excellent agreement between the test and predicted relative displacements. In comparing these plots, it should be remembered that the experimental plots are unadjusted for zero corrections as explained in Section 3.7. The initial straight line portion should be considered to coincide with the zero line and the whole plot be shifted down accordingly. The trends in both cases follow each other very closely, and it is apparent that the assumption of static and dynamic coefficients of friction being the same does not have any appreciable effect on the sliding response of the block, possibly as sliding occurs in both directions.

It can also be seen by comparing the above mentioned figures that the test and predicted horizontal accelerations of the block agree closely in magnitudes and trends. The main difference occurs at the initiation of sliding where the coefficient of friction starts as its static value and falls very rapidly to the dynamic value as sliding continues (compare Figs. 3-14 and 3-18). It was found from the digitized record of horizontal block acceleration that it takes less than 0.04 seconds for the coefficient of friction to change from static value to dynamic value for the graphite.

3.9 Suitability of Various Materials for Reducing Coefficient of Friction

Various materials were tried between the concrete block and the shaking table to reduce the coefficient of friction. These materials included plywood, masonite, teflon, formica and graphite. Different problems were encountered with each and it was found that graphite was the best, easiest to use and most inexpensive compared with the other materials tried.

Masonite and formica failed under high shear stress concentrations, resulting in powdering which increased the coefficient of friction. High local shear stresses occurred because the block and table surfaces were not perfectly plane, despite the care taken in construction. Plywood did not fail under the comparatively smaller concrete block, but it could easily fail under the larger normal pressure of actual field conditions. Moreover, it had a higher coefficient of friction, making it undesirable.

Teflon sheets were satisfactory only when they were comparatively thick (3/8 in. or more), making them rather expensive for practical use. Thin sheets of teflon tended to break down, producing high coefficients of friction. Moreover teflon is highly electro static and attracts dust particles making it difficult to keep clean.

At this point it seems that the most appropriate means of decreasing the coefficient of friction between concrete shielding blocks and the floor where this is desired would be to use steel plates lubricated with graphite. Where shielding consists of a system of blocks, these should be connected in such a way that they slide as a single unit relative to the floor. Where there is a free-standing block stack and the coefficient of friction is being used to limit the susceptibility of rocking, great care should be taken to ensure that the lowest block rests

on the ground at its outer edges, as any lack of planeness which causes a local high spot on the floor within the contact surface of the block can lead to premature rocking of the stack.

TABLE 3-1 DYNAMIC COEFFICIENT OF FRICTION FOR VARIOUS MATERIALS

MATERIAL	DYNAMIC COEFFICIENT OF FRICTION
Concrete	0.18 - 0.60
Plywood	0.26 - 0.30
Teflon	0.10 - 0.15
Graphite	0.09 - 0.12

Note: The static coefficient of friction could be 20-50% higher than the values shown in this table.

TABLE 3-2. COMPARISON OF TEST AND THEORETICAL AVERAGE VELOCITY OF A BLOCK UNDER SINUSOIDAL HORIZONTAL ACCELERATION AND A HORIZONTAL FORCE (F = 5 Hz).

AMPLITUDE OF HORIZONTAL ACCELERATION (g's)	FORCE / WT. OF BLOCK (P/W)	COEFFICIENT OF FRICTION	AVERAGE VELOCITY OF BLOCK (INCHES/SECOND)		THEORY / TEST
			TEST	THEORY	
0.52	0.086	0.20	1.50	1.55	1.03
0.84	0.086	0.20	2.77	2.95	1.06
0.94	0.113	0.18	4.10	4.55	1.11
0.50	0.113	0.18	2.00	2.08	1.04
0.50	0.168	0.18	2.82	2.88	1.02
1.04	0.168	0.18	6.30	6.20	0.99
0.54	0.058	0.23	0.85	0.94	1.10
1.12	0.058	0.22	2.50	2.61	1.04
0.48	0.168	0.30	1.35	1.35	1.00
0.77	0.168	0.30	3.15	2.83	0.90
0.31	0.113	0.28	0.36	0.33	0.92
0.56	0.113	0.26	1.83	1.60	0.90
1.03	0.113	0.26	4.25	3.63	0.86
0.31	0.168	0.26	0.64	0.81	1.26
0.46	0.168	0.26	1.70	1.62	0.95
0.96	0.168	0.26	5.30	4.40	0.83
0.61	0.223	0.26	3.10	3.17	1.02
0.55	0.223	0.28	2.33	2.54	1.09
0.90	0.223	0.27	4.60	4.77	1.04

TABLE 3-3. COMPARISON OF TEST AND THEORETICAL VELOCITY OF BLOCK UNDER SINUSOIDAL HORIZONTAL AND VERTICAL GROUND ACCELERATIONS.

AMPLITUDE ON HORIZONTAL ACCELERATION (g)	AMPLITUDE ON VERTICAL ACCELERATION (g)	FREQUENCY (Hz)	COEFFI. OF FRICTION	AVERAGE VELOCITY OF BLOCK(INCHES/SECOND)		THEORY / TEST
				TEST	THEORY	
0.50	0.45	5	0.20	1.80	1.83	1.01
0.52	0.22	5	0.20	0.79	0.94	1.19
0.50	0.20	5	0.20	0.75	0.84	1.12
0.25	0.25	5	0.20	0.30	0.31	1.03
0.40	0.48	10	0.20	0.75	0.75	1.00
0.40	0.20	5	0.28	0.46	0.53	1.15
0.68	0.25	5	0.28	1.33	1.43	1.07
1.02	0.25	5	0.28	1.90	1.71	0.90
0.74	0.50	5	0.28	2.30	2.97	1.29
0.92	0.46	5	0.28	2.95	3.01	1.02
0.35	0.26	10	0.28	0.28	0.23	0.82

TABLE 3-4. COMPARISON OF TEST AND THEORETICALLY PREDICTED VALUES OF MAXIMUM RELATIVE DISPLACEMENT OF A RIGID BLOCK UNDER 80% INTENSITY OF PACOIMA DAM S74°W ACCELEROGRAM AND VARYING INTENSITIES OF VERTICAL ACCELEROGRAM (S74°W ACCELEROGRAM WAS ALSO USED FOR VERTICAL ACCELERATION)

% INTENSITY OF VERTICAL ACCELERATION (S74W USED)	MAXIMUM RELATIVE DISPLACEMENT OF BLOCK IN INCHES		THEORY/TEST
	TEST	THEORY	
0	6.10	5.47	0.90
10	6.80	6.34	0.93
20	7.24	6.86	0.95
30	8.06	7.43	0.92

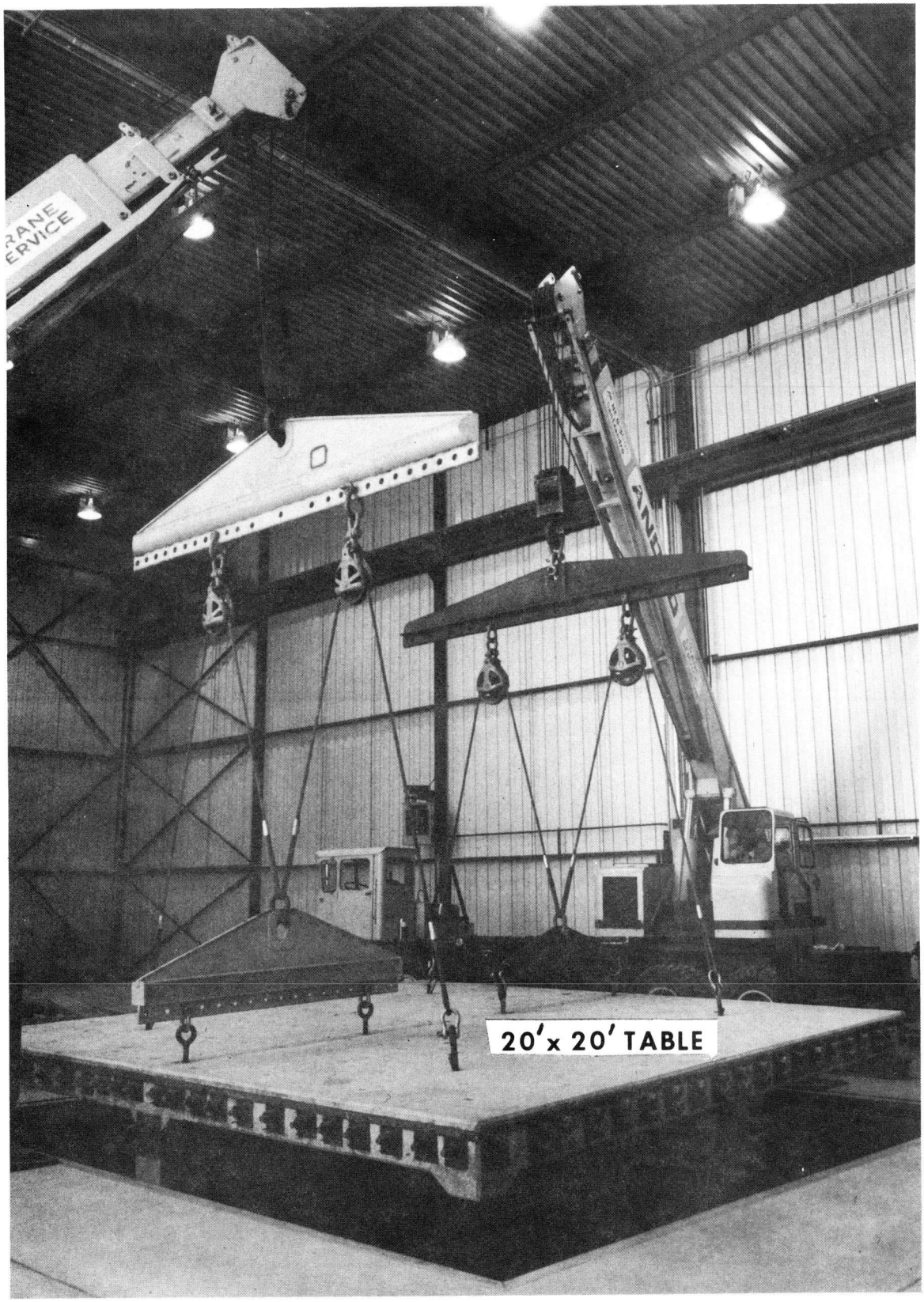

FIG. 3-1. 20 X 20 FOOT PRESTRESSED CONCRETE TABLE BEING LOWERED IN PLACE.

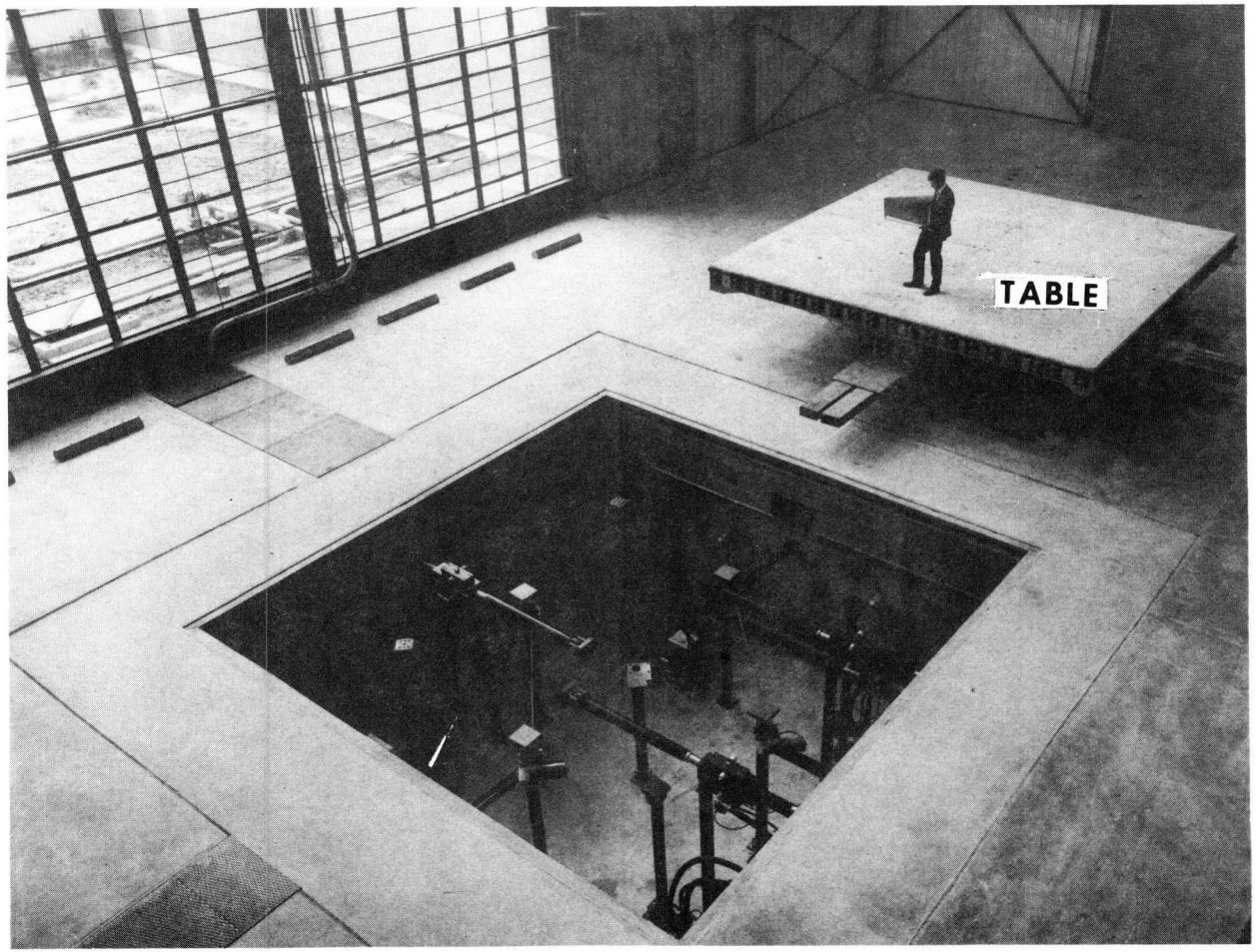

FIG. 3-2. HYDRAULIC ACTUATORS LOCATED IN PIT UNDER SHAKING TABLE.

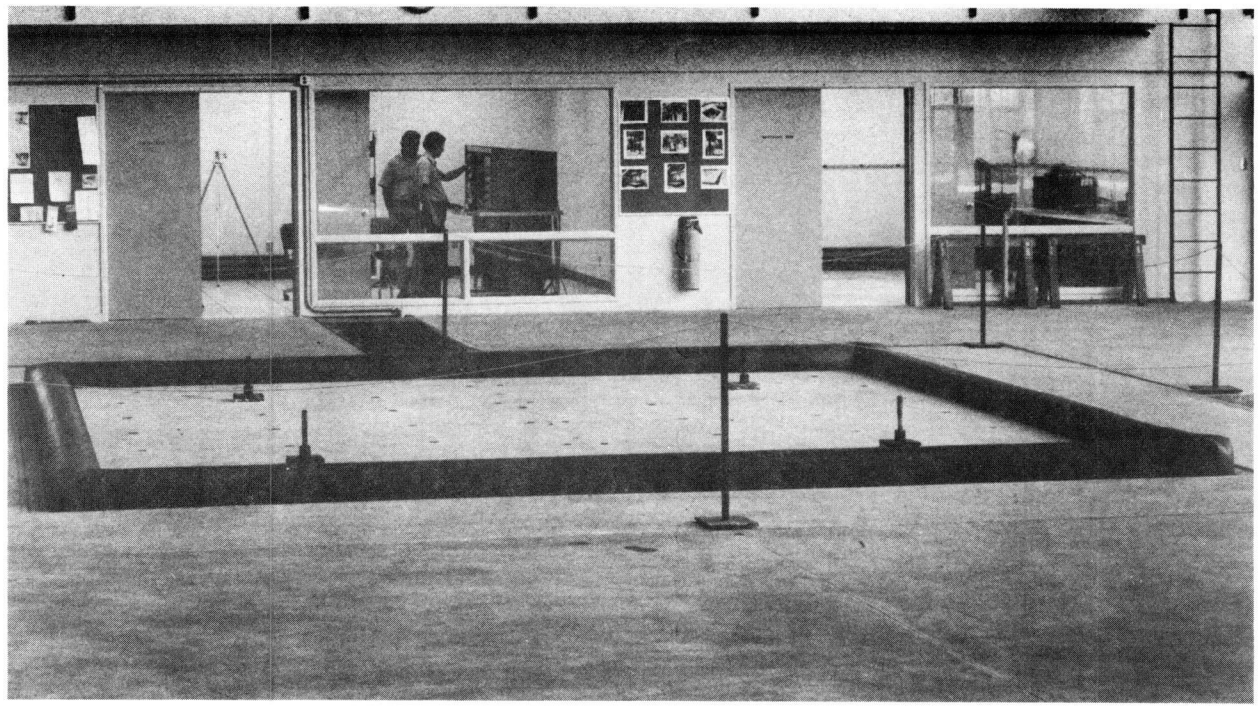

FIG. 3-3. OVERALL VIEW OF THE SHAKING TABLE SHOWING NYLON FABRIC IN INFLATED POSITION.

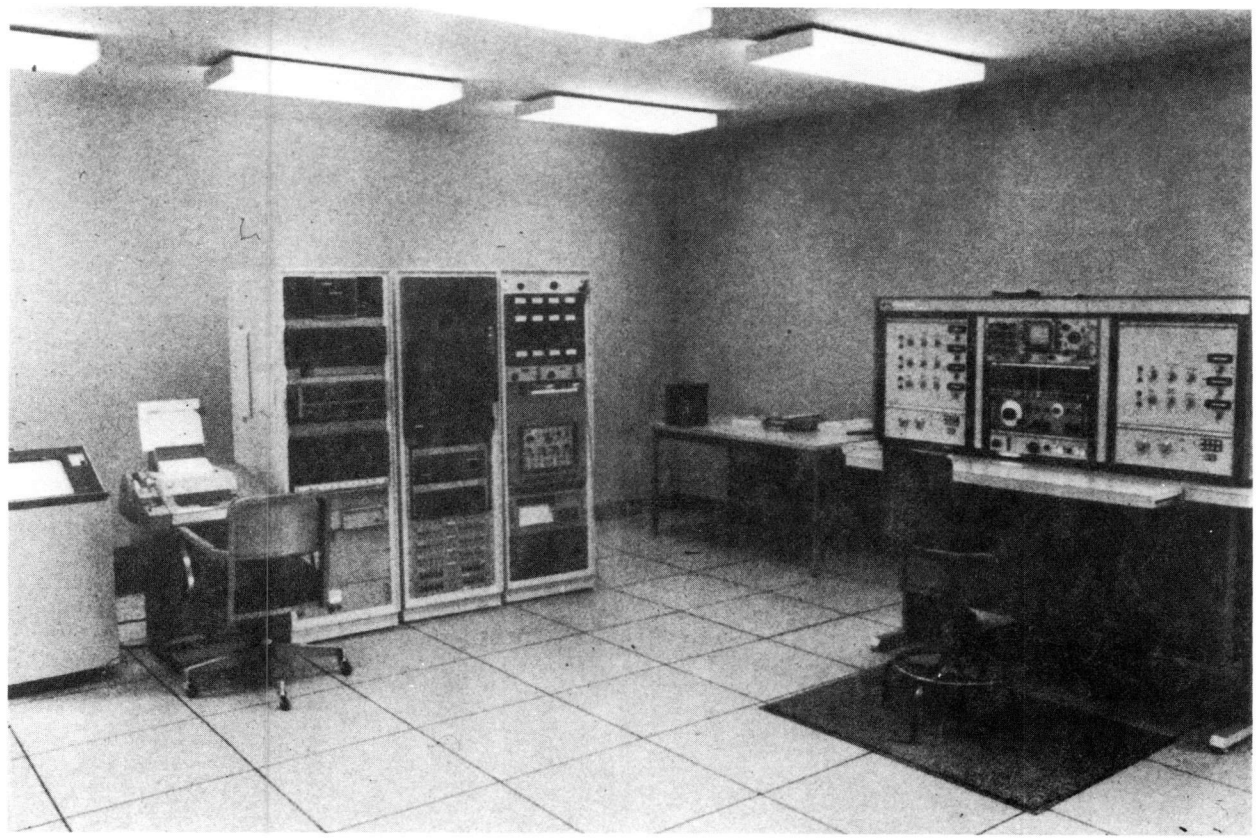

FIG. 3-4. ELECTRONIC CONTROL AND DATA ACQUISITION SYSTEM OF THE SHAKING TABLE.

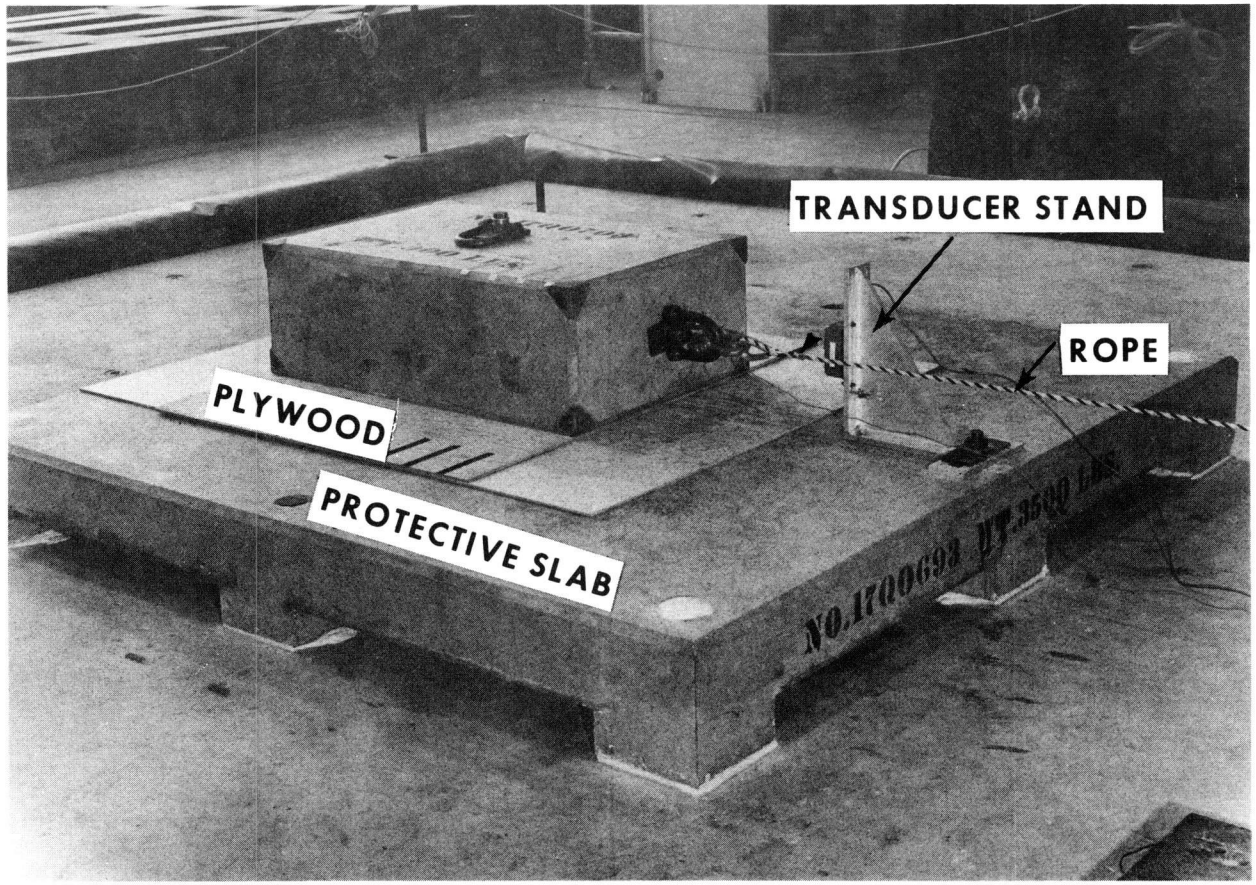

FIG. 3-5. CLOSE UP VIEW OF CONCRETE BLOCK AND PROTECTIVE SLAB WITH PLYWOOD SHEETS BETWEEN.

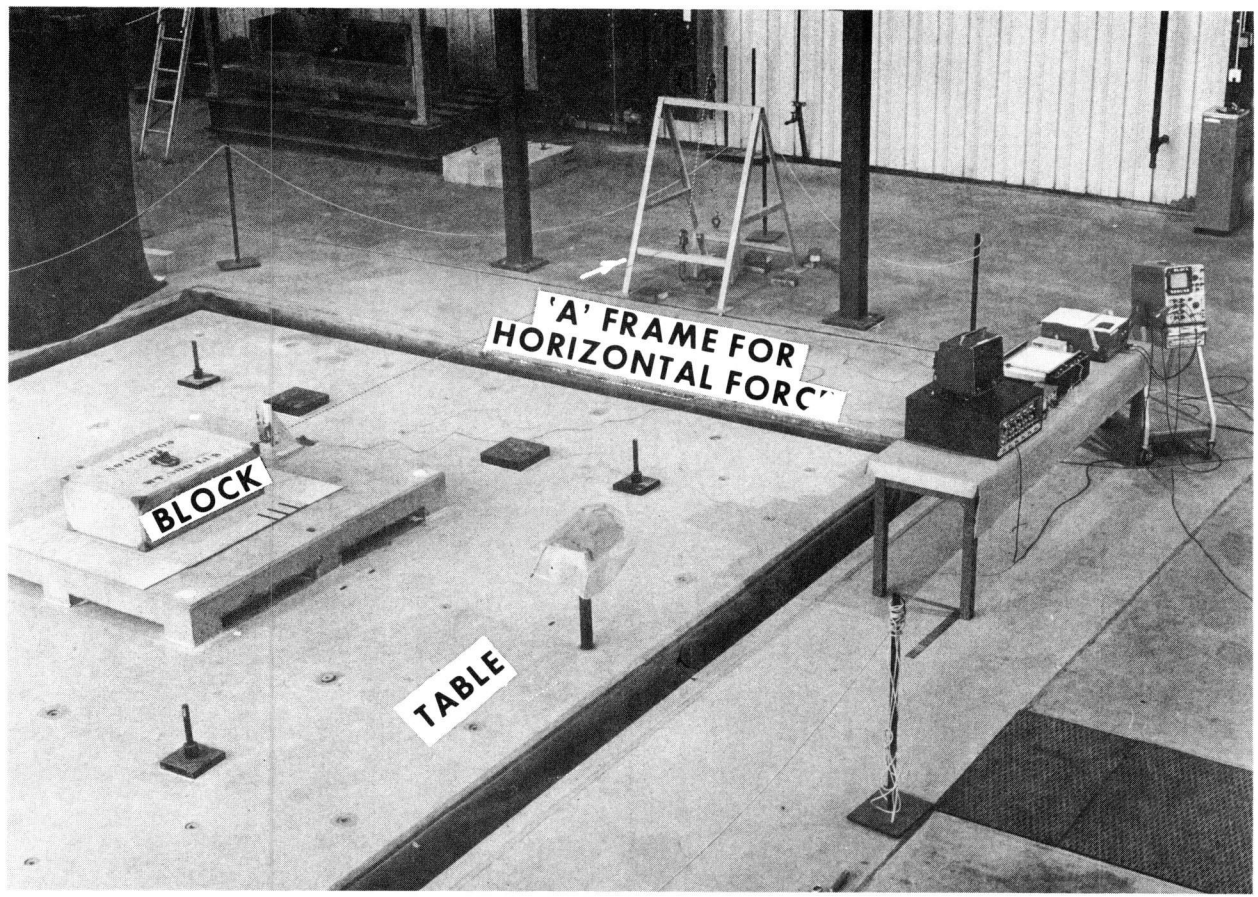

FIG. 3-6. OVERALL SET-UP SHOWING FRAME FOR HORIZONTAL FORCE AND OTHER EQUIPMENT.

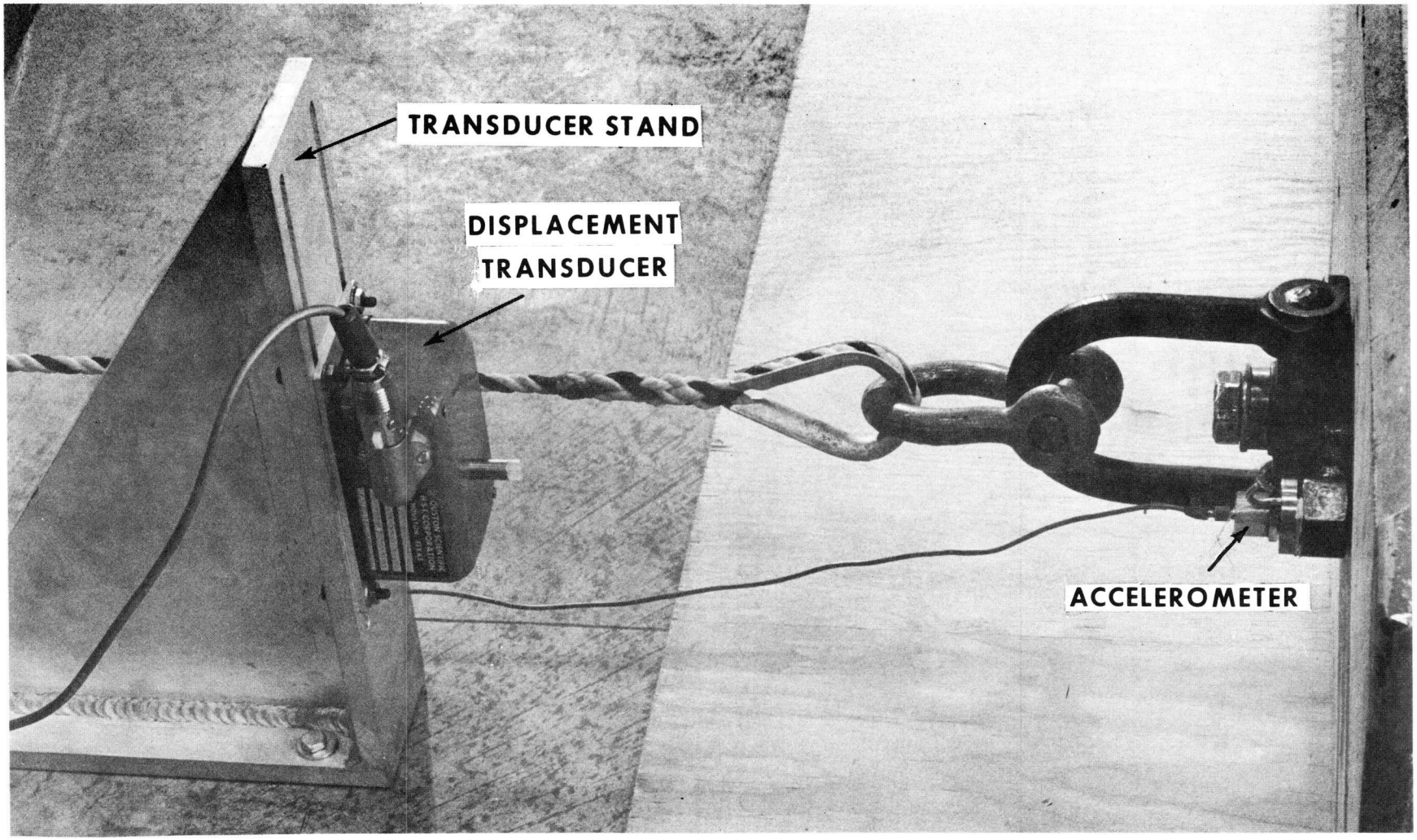

FIG. 3-7. CLOSE UP VIEW OF TRANSDUCER STAND AND ACCELEROMETER.

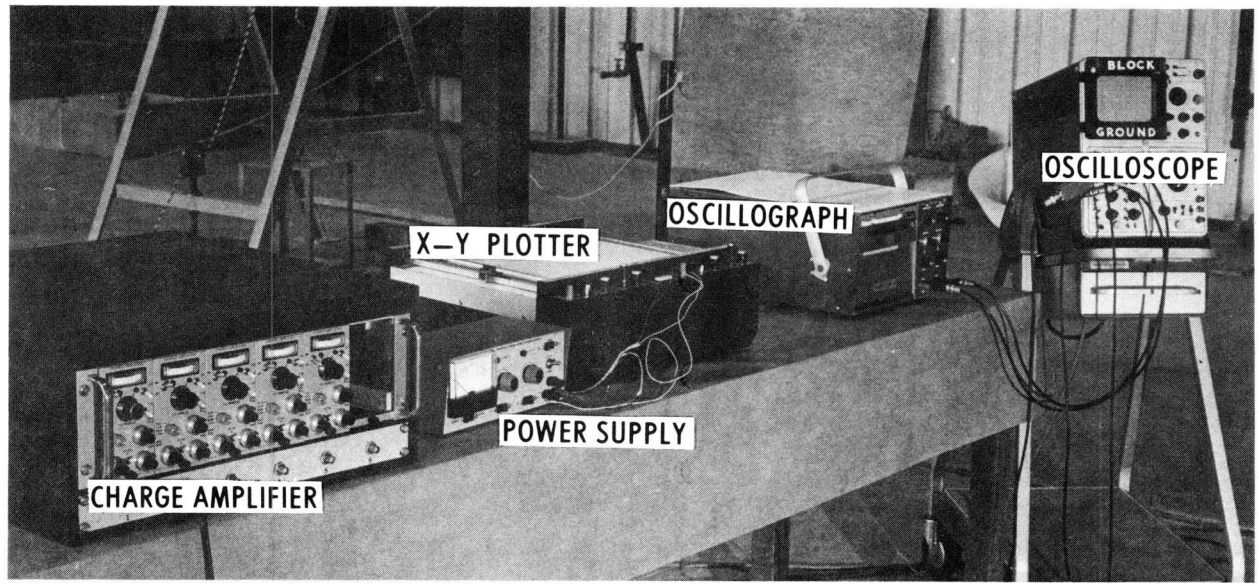

FIG. 3-8. CLOSE UP VIEW OF RECORDING EQUIPMENT.

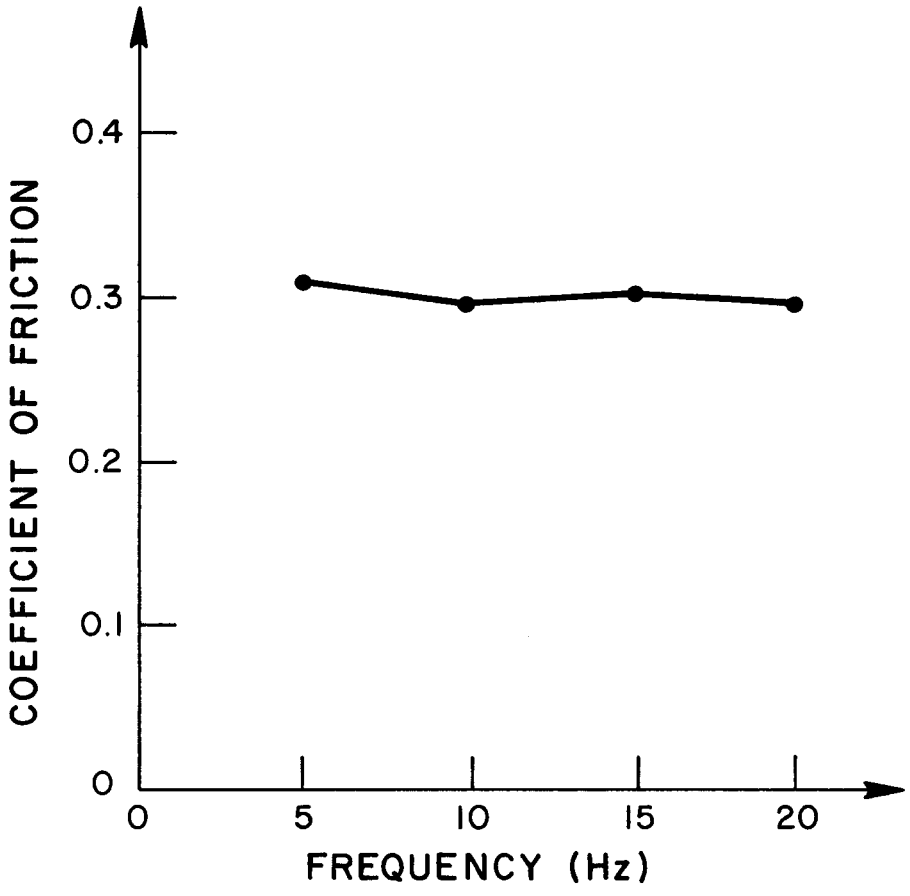

FIG. 3-9. VARIATION OF DYNAMIC COEFFICIENT OF FRICTION WITH FREQUENCY OF GROUND MOTION.

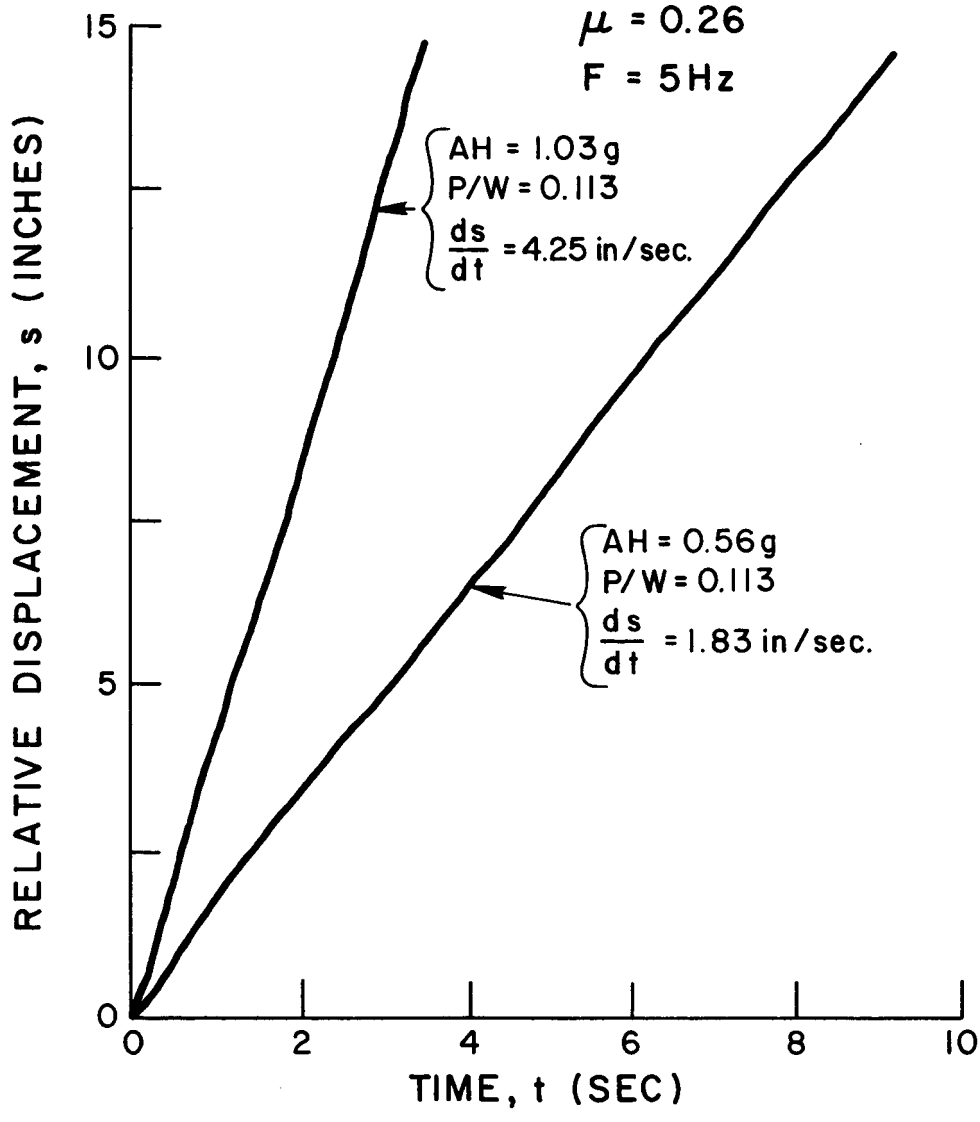

FIG. 3-10 (a). RELATIVE DISPLACEMENT VS TIME OF A RIGID BLOCK UNDER SINUSOIDAL HORIZONTAL ACCELERATION AND A HORIZONTAL FORCE (TEST).

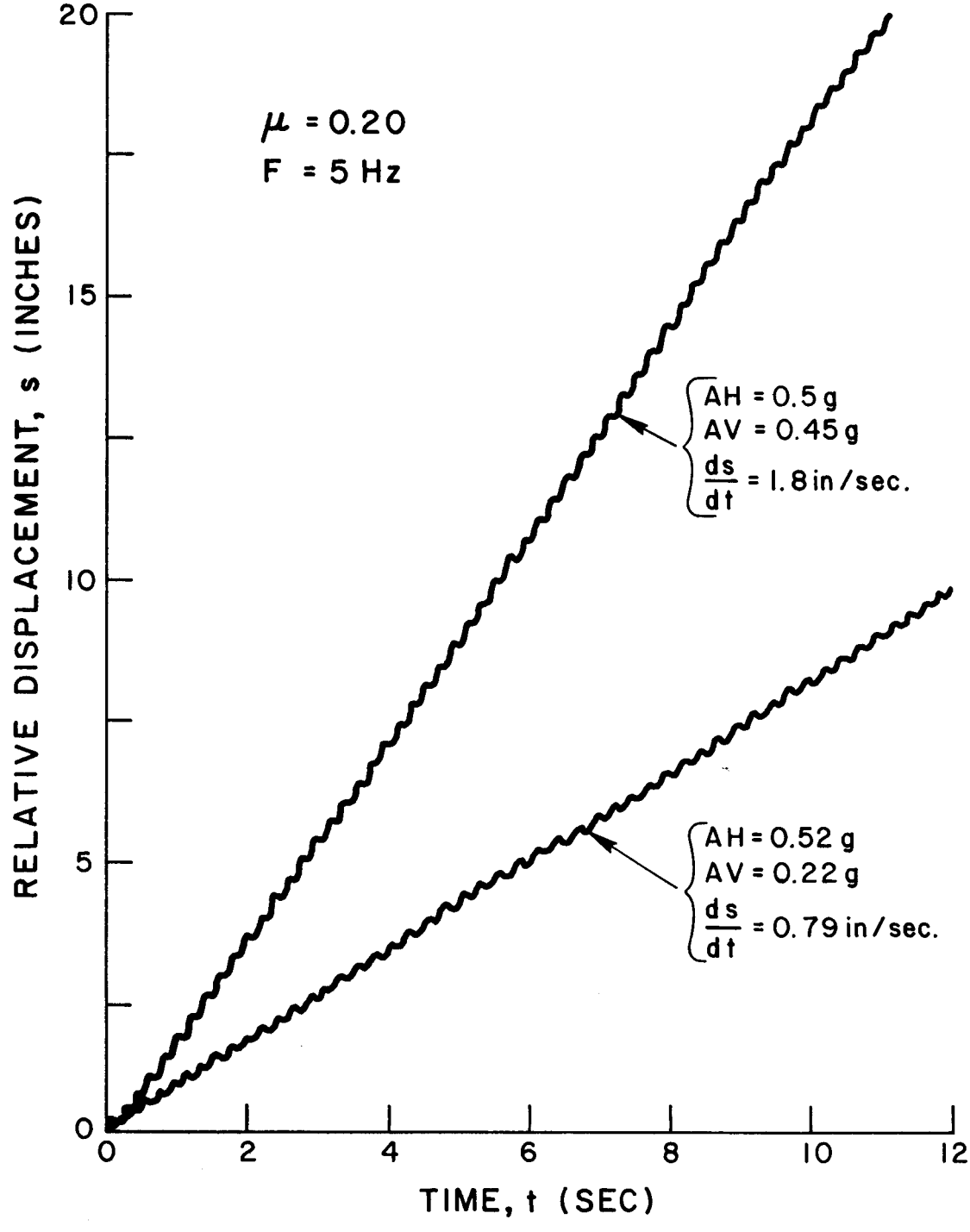

FIG. 3-10 (b). RELATIVE DISPLACEMENT VS TIME OF A RIGID BLOCK UNDER SINUSOIDAL HORIZONTAL AND VERTICAL ACCELERATION.(TEST).

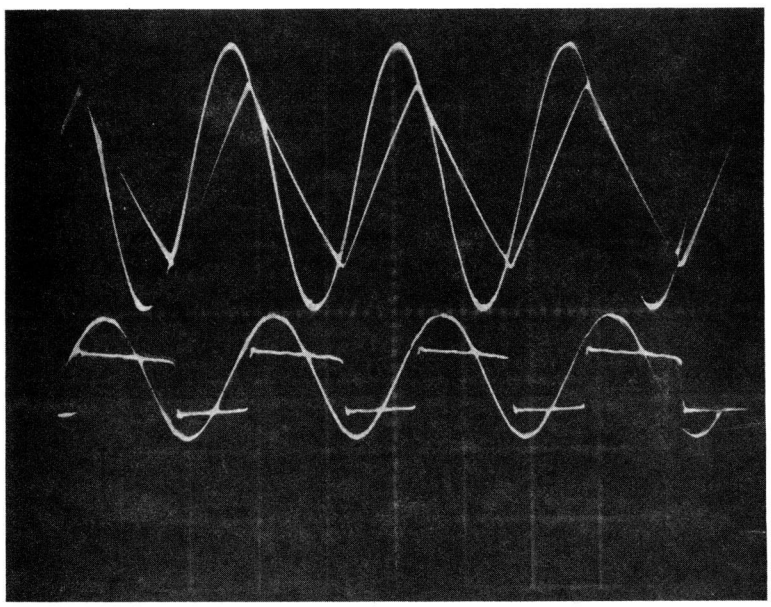

FIG. 3-11. SUPERIMPOSED ACCELERATIONS AND VELOCITY TRACES OF SHAKING TABLE AND BLOCK UNDER SINUSOIDAL ACCELERATION AND A FORCE.

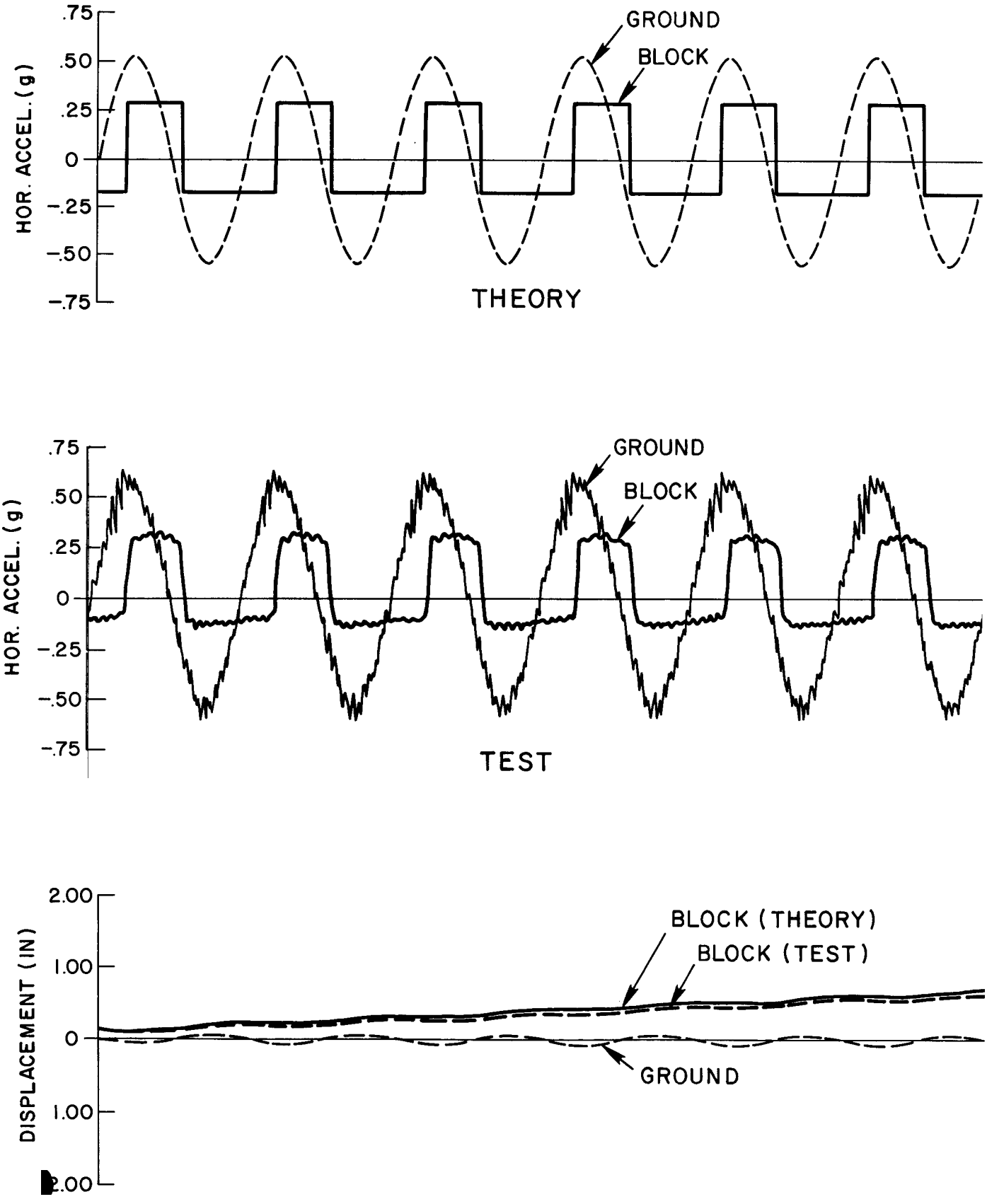

FIG. 3-12. COMPARISON OF TEST AND THEORETICAL SLIDING RESPONSE OF A RIGID BLOCK UNDER SINUSOIDAL HORIZONTAL ACCELERATION AND A HORIZONTAL FORCE (AH = 0.54 g, P/W = 0.058, FREQ = 5 Hz).

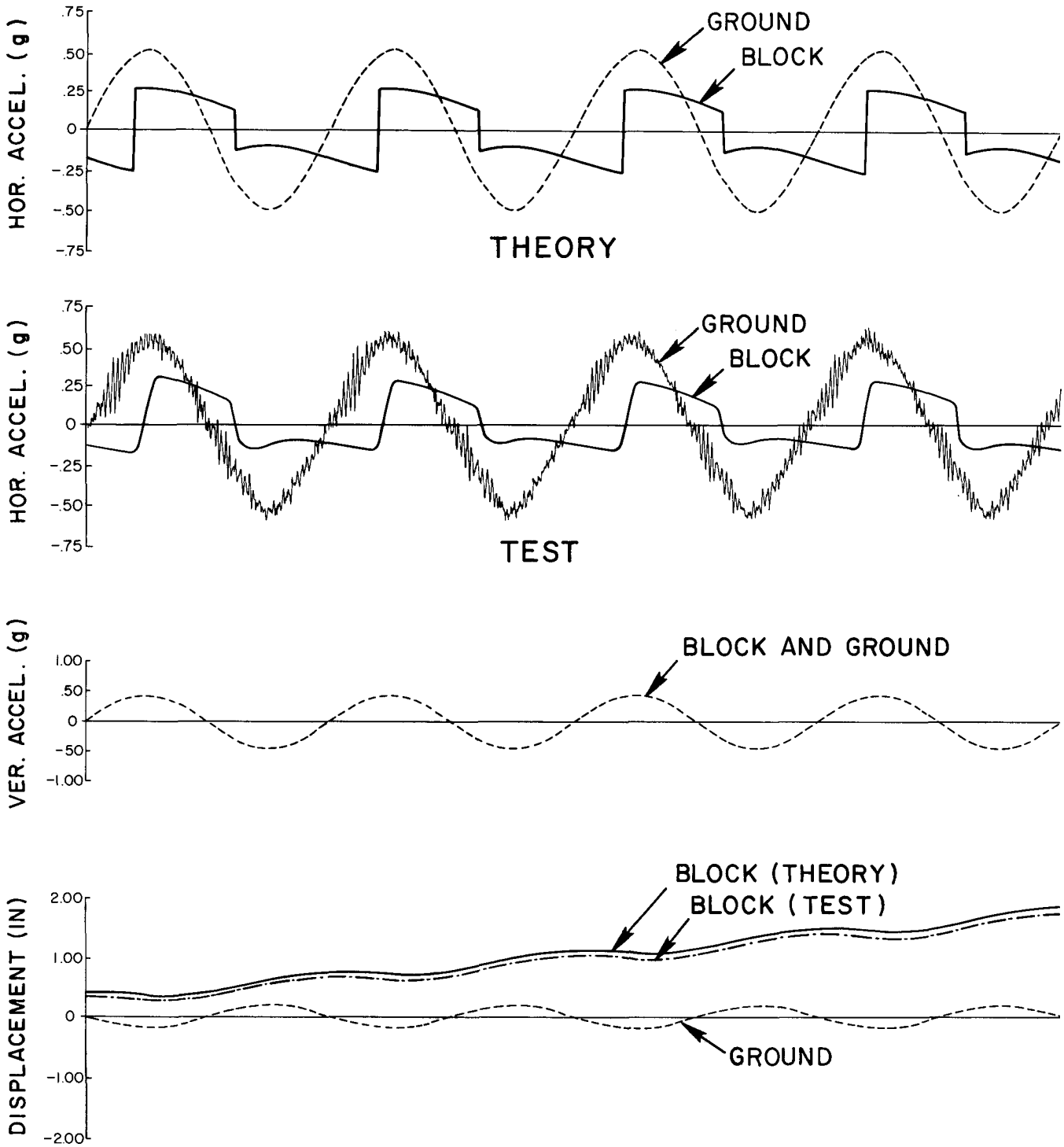

FIG. 3-13. COMPARISON OF TEST AND THEORETICAL SLIDING RESPONSE OF A RIGID BLOCK UNDER SINUSOIDAL HORIZONTAL AND VERTICAL GROUND ACCELERATIONS (AH = 0.5 g, AV = 0.45 g, FREQ = 5 Hz).

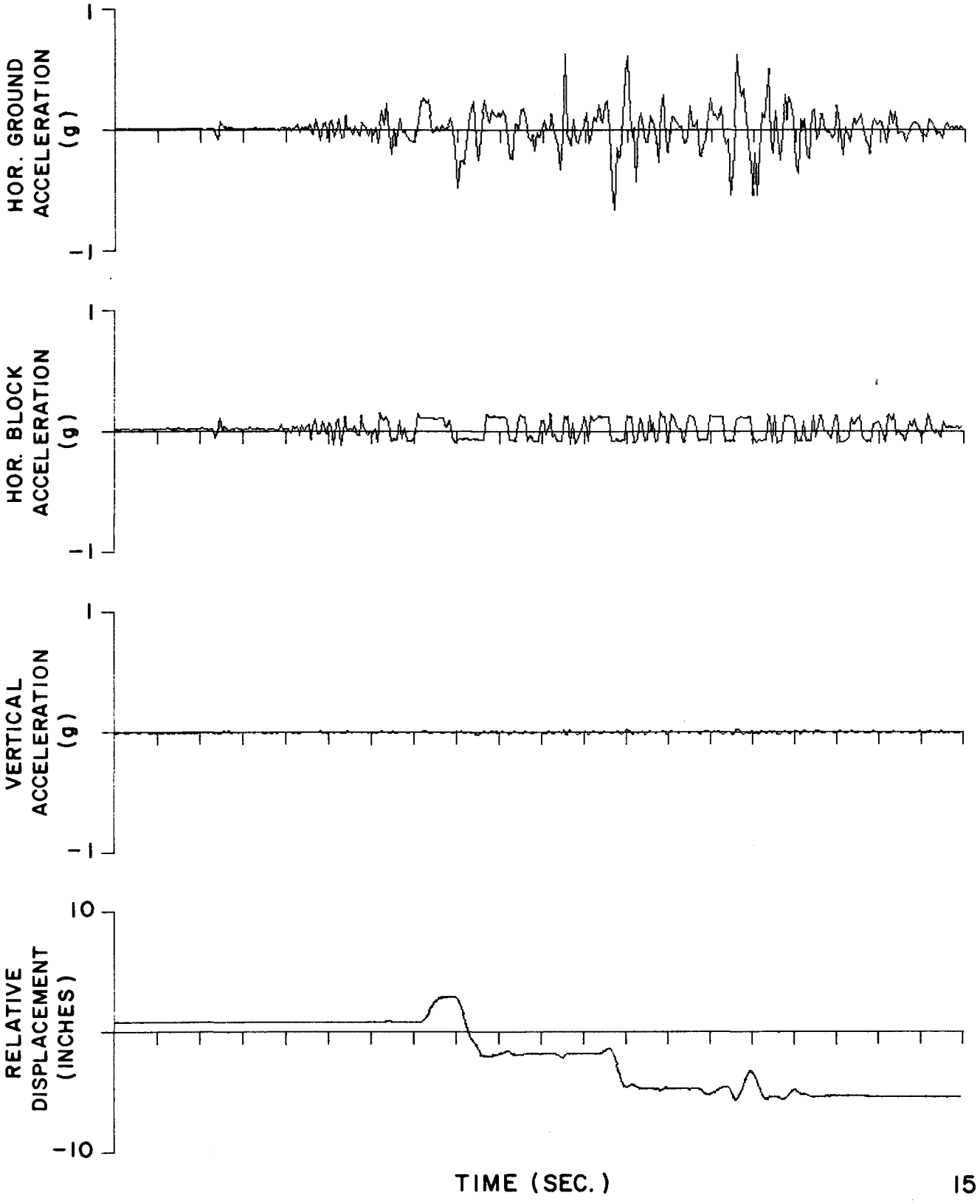

FIG. 3-14. EXPERIMENTAL SLIDING RESPONSE OF A RIGID BLOCK UNDER 80% INTENSITY OF PACOIMA DAM S74°W ACCELEROGRAM OF 1971.

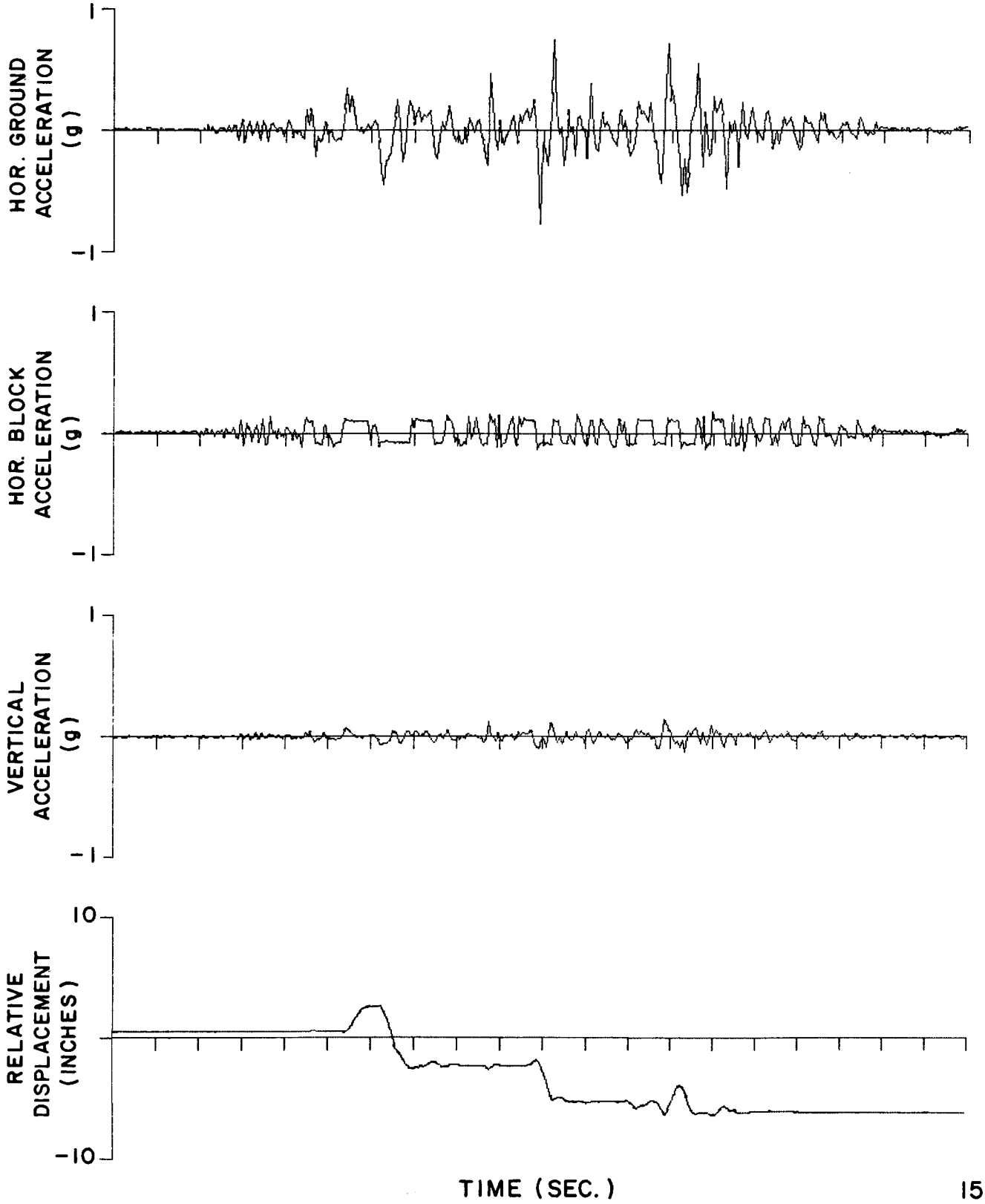

FIG. 3-15. EXPERIMENTAL SLIDING RESPONSE OF A RIGID BLOCK UNDER HORIZONTAL ACCELERATION (80% INTENSITY OF PACOIMA DAM S74^{O}W) AND VERTAL ACCELERATION (10% INTENSITY OF PACOIMA DAM S74^{O}W RECORD).

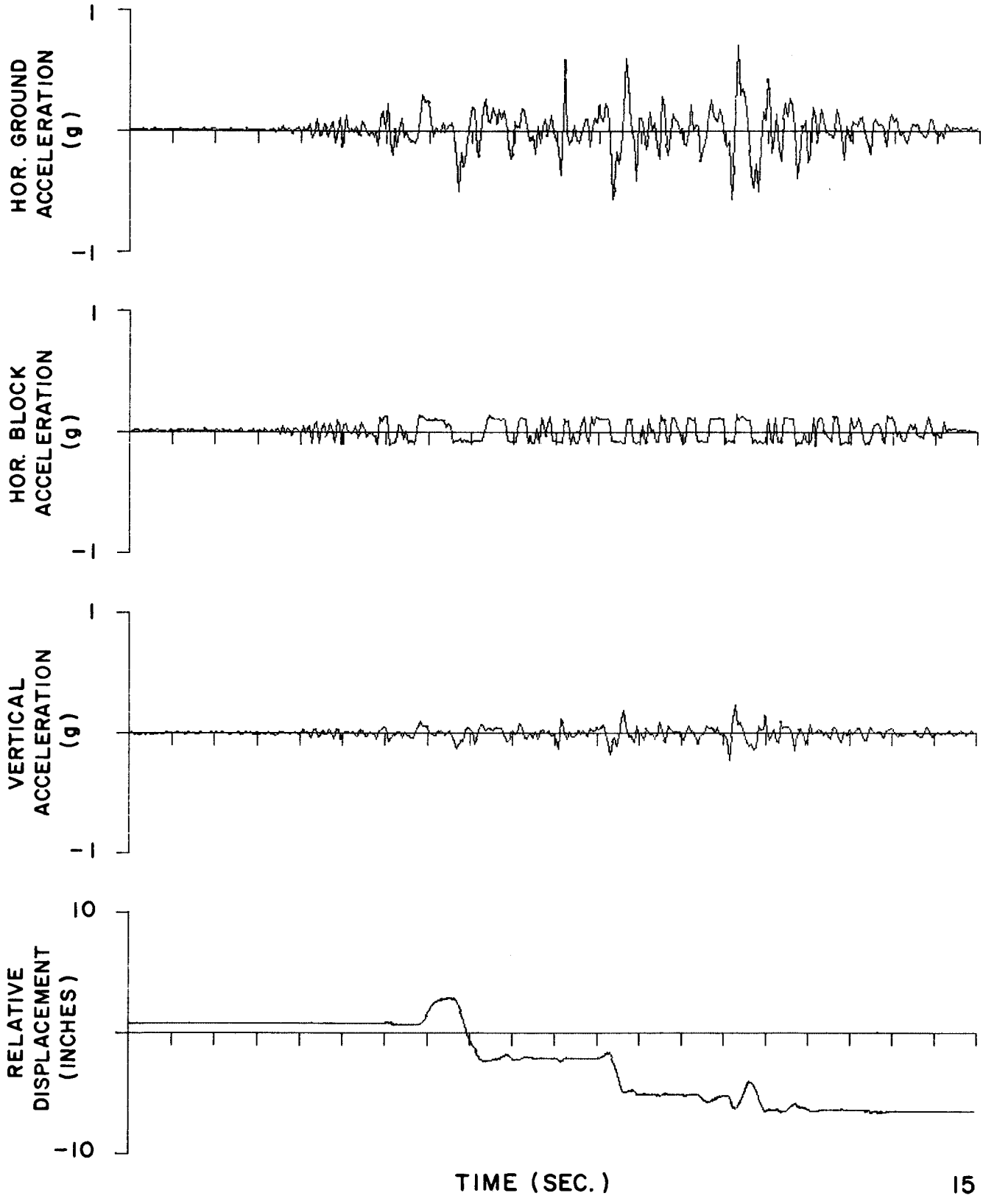

FIG. 3-16. EXPERIMENTAL SLIDING RESPONSE OF A RIGID BLOCK UNDER HORIZONTAL ACCELERATION (80% INTENSITY OF PACOIMA DAM S74^{O}W) AND VERTICAL ACCELERATION (20% INTENSITY OF PACOIMA DAM S74^{O}W) RECORD).

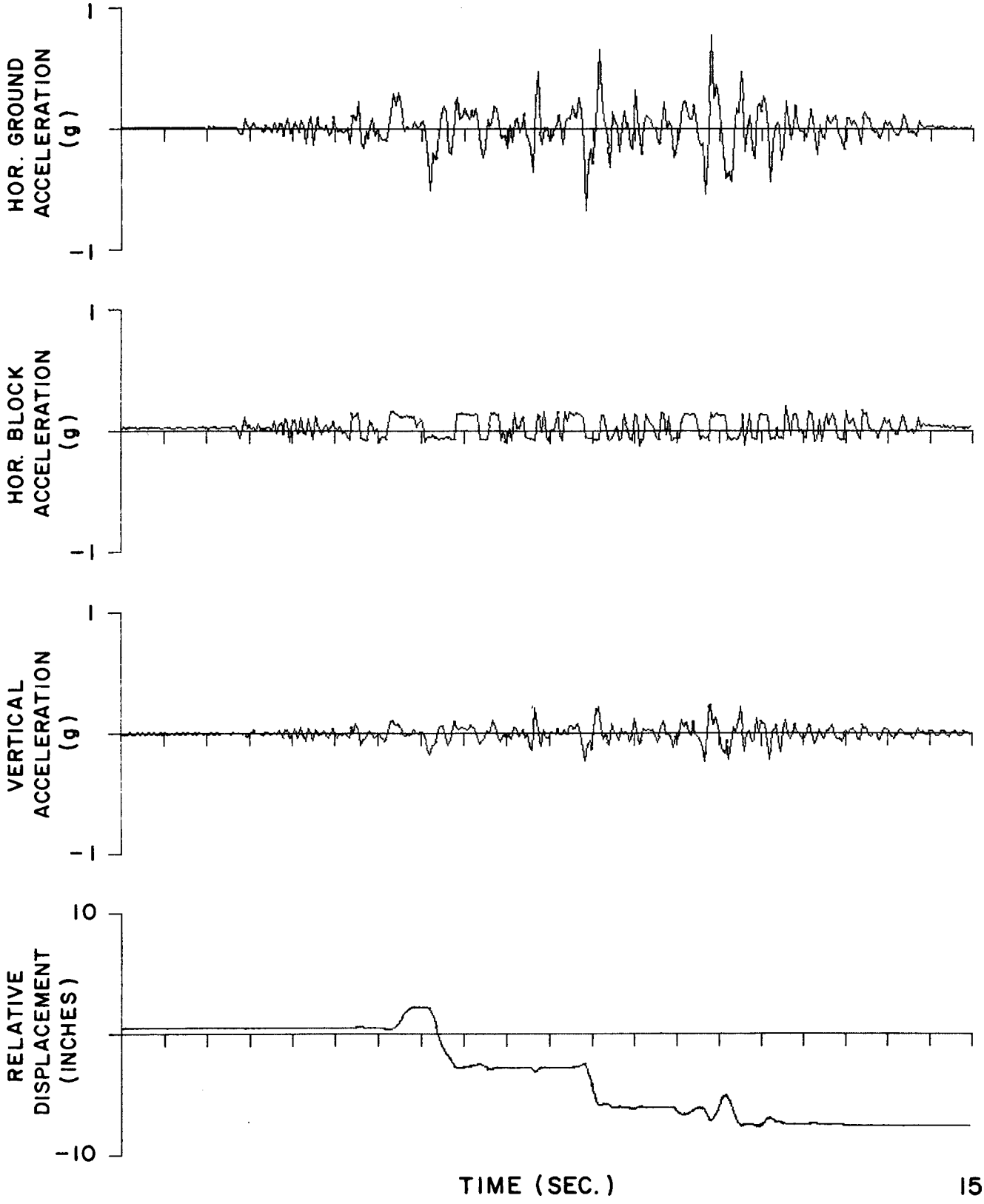

FIG. 3-17. EXPERIMENTAL SLIDING RESPONSE OF A RIGID BLOCK UNDER HORIZONTAL ACCELERATION (80% INTENSITY OF PACOIMA DAM S74°W) AND VERTICAL ACCELERATION (30% INTENSITY OF PACOIMA DAM S74°W RECORD).

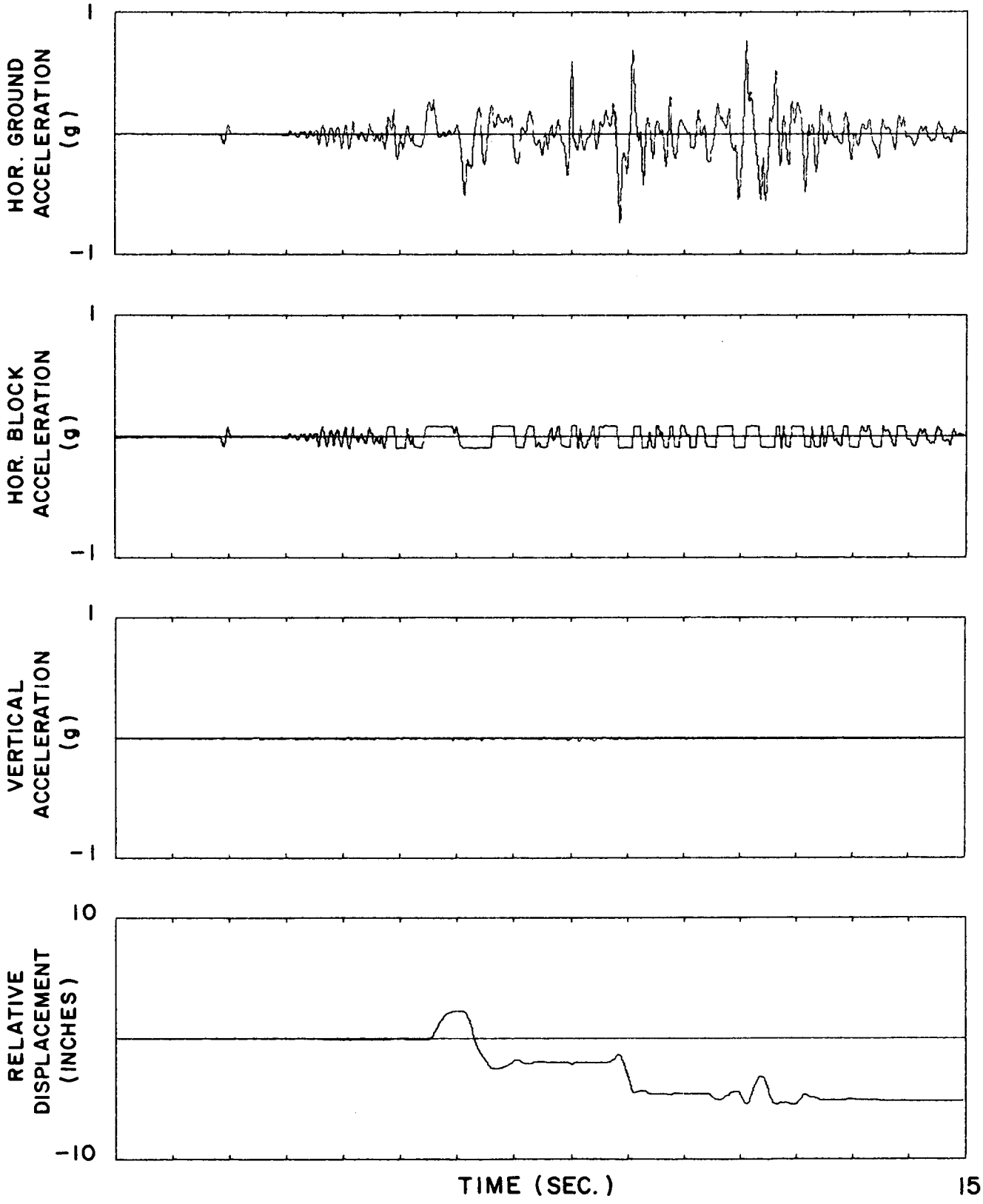

FIG. 3-18. THEORETICAL SLIDING RESPONSE OF A RIGID BLOCK UNDER 80% INTENSITY OF PACOIMA DAM S74°W ACCELEROGRAM OF 1971.

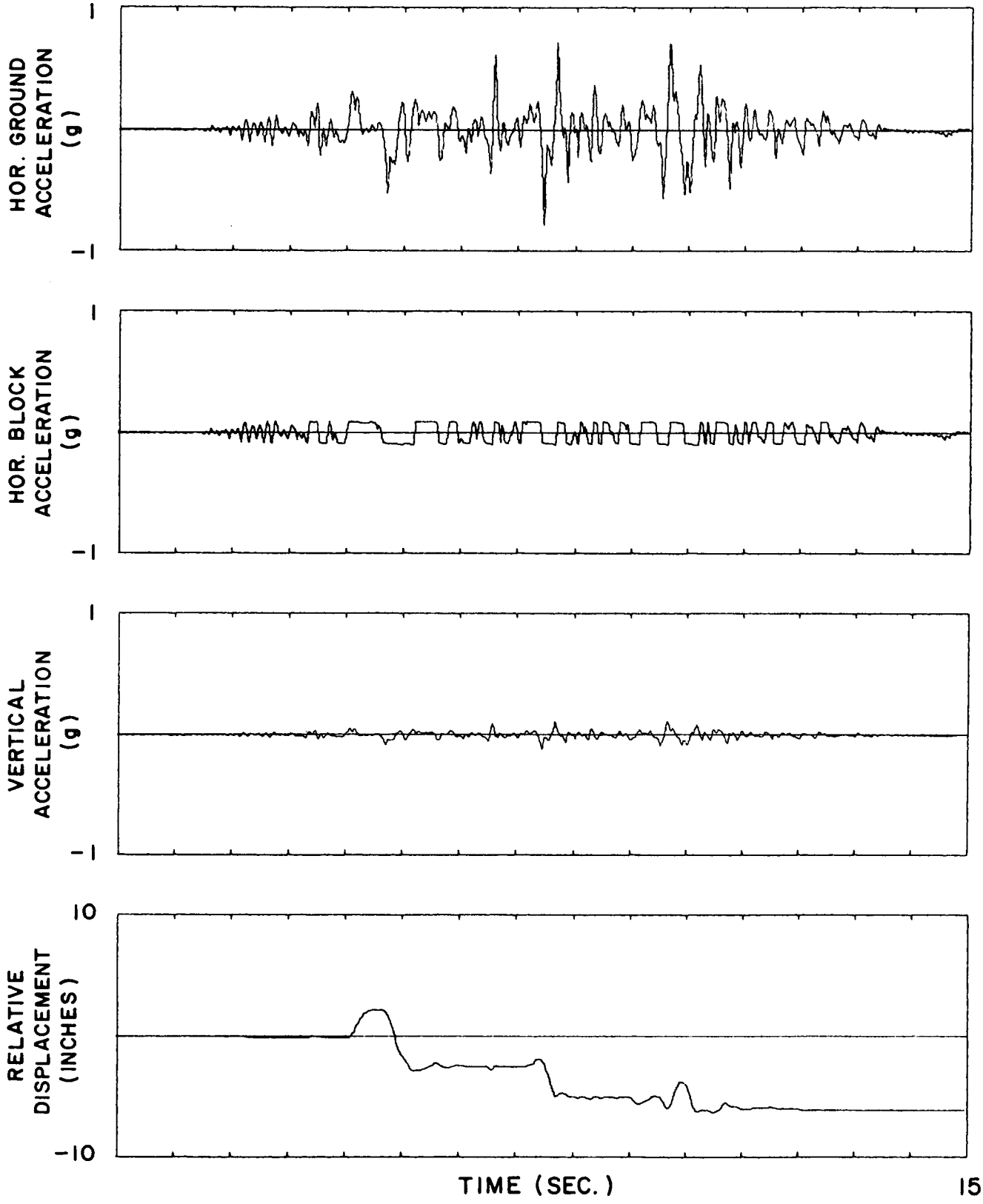

FIG. 3-19. THEORETICAL SLIDING RESPONSE OF A RIGID BLOCK UNDER HORIZONTAL ACCELERATION (80% INTENSITY OF PACOIMA DAM S74^{O}W RECORD) AND VERTICAL ACCELERATION (10% INTENSITY OF PACOIMA DAM S74^{O}W RECORD).

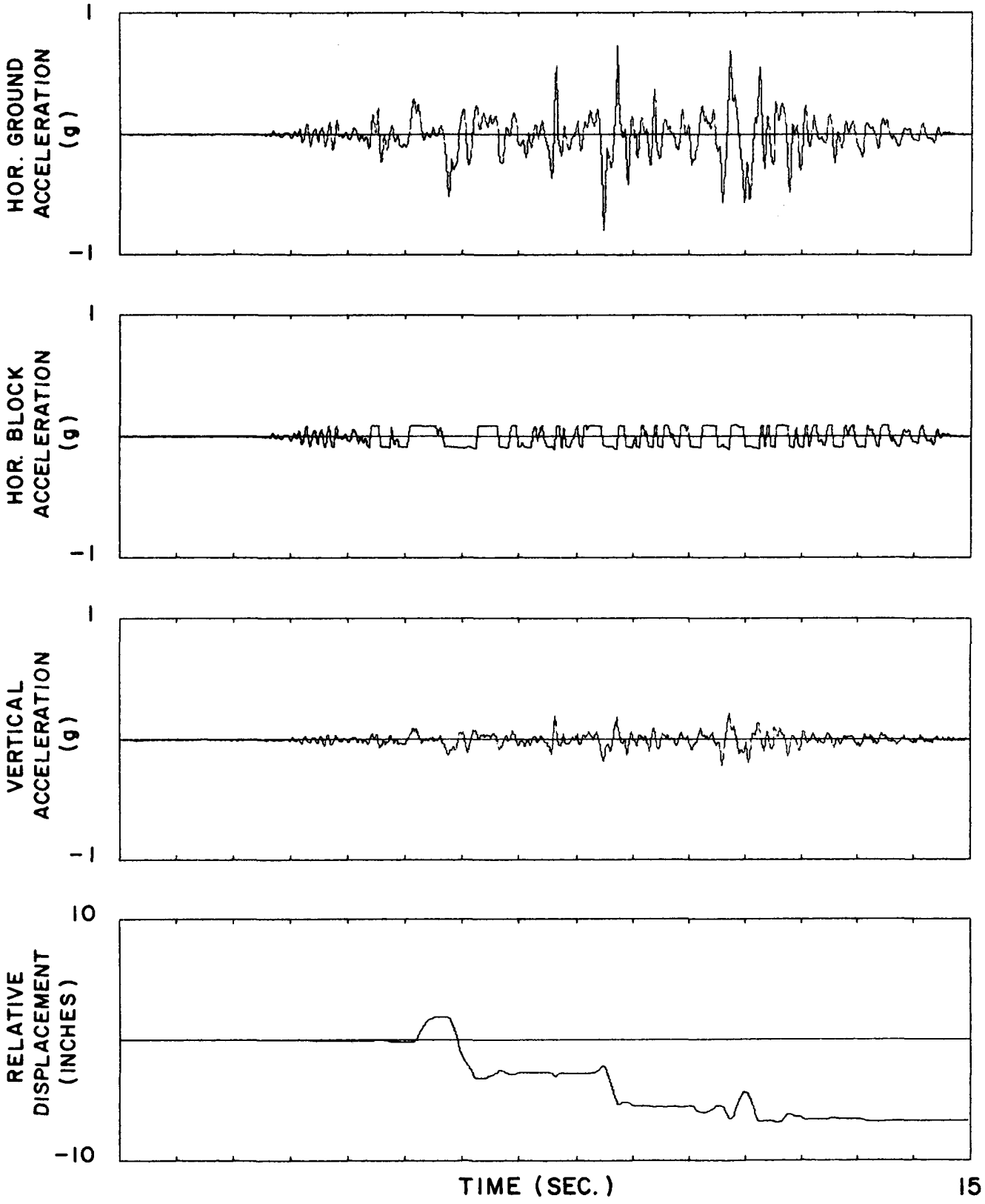

FIG. 3-20. THEORETICAL SLIDING RESPONSE OF A RIGID BLOCK UNDER HORIZONTAL ACCELERATION (80% INTENSITY OF PACOIMA DAM S74°W RECORD) AND VERTICAL ACCELERATION (20% INTENSITY OF PACOIMA DAM S74°W RECORD).

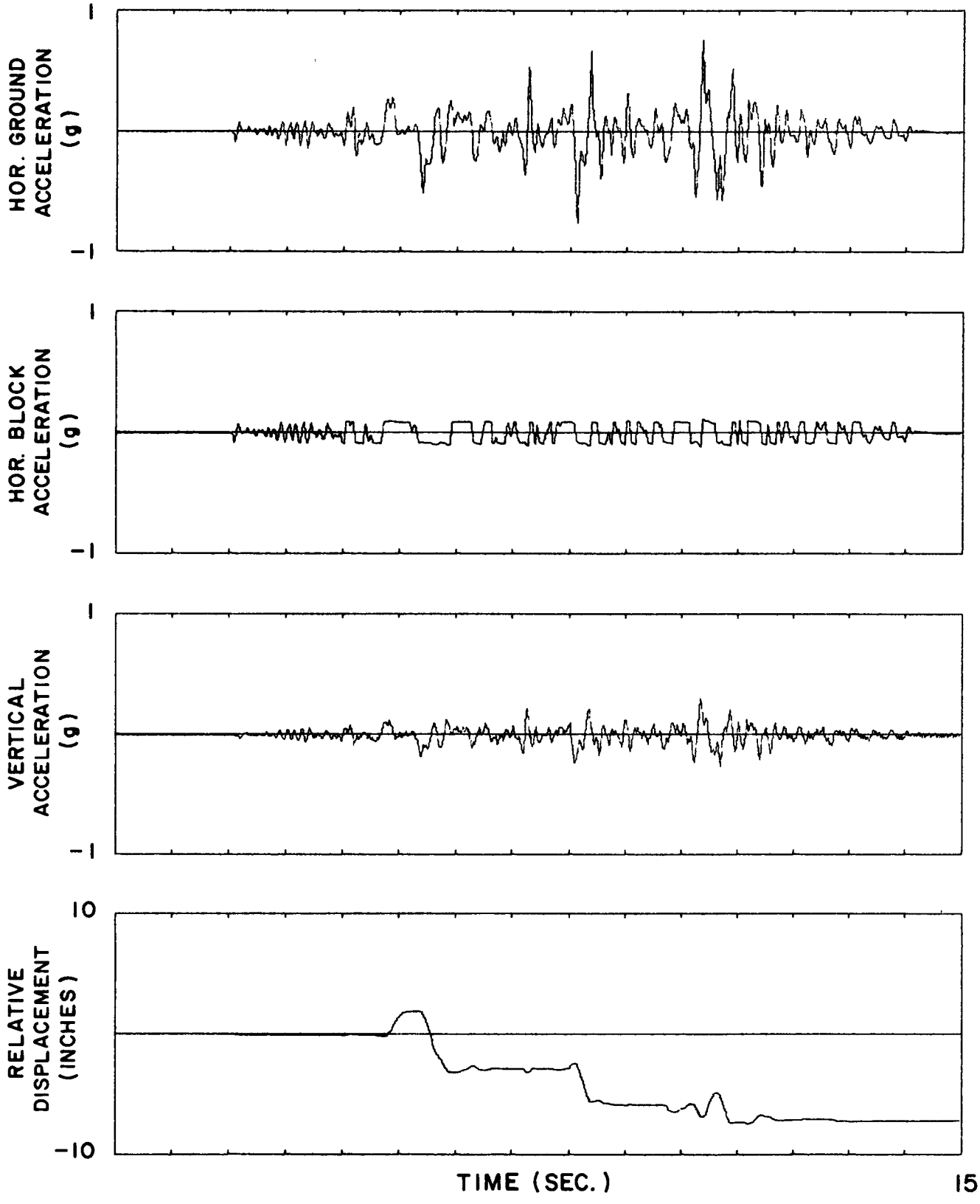

FIG. 3-21. THEORETICAL SLIDING RESPONSE OF A RIGID BLOCK UNDER HORIZONTAL ACCELERATION (80% INTENSITY OF PACOIMA DAM S74°W RECORD) AND VERTICAL ACCELERATION (30% INTENSITY OF PACOIMA DAM S74°W RECORD).

SECTION 4

SLIDING RESPONSE OF SHIELDING BLOCKS UNDER EARTHQUAKE GROUND MOTIONS

4.1 General

It has been shown in Section 3 that the sliding response of a rigid block can be successfully predicted under earthquake ground motion. Using the same computer program as was used for theoretical predictions in Section 3, a study was made of the relative displacements of a rigid block, with different values of μ, when subjected to the various digitized earthquake records which are available in the SESM Computer Program Library at the University of California, Berkeley. The added effect of vertical ground acceleration was also studied on the relative displacement of the block. A horizontal linear spring was later added to the block, making it a single degree of freedom system with Coulomb damping. The linear spring was included as it was suggested as a means of reducing the final relative displacement of the block with respect to the ground. Response spectra for a single degree of freedom system with Coulomb damping was prepared for comparison with a system having viscous damping.

4.2 Sliding Response of a Rigid Block to Earthquake Motions

The sliding response of a rigid block was analyzed under various strong motion earthquakes by using the computer program whose reliability has been established in Section 3. Various real and artificially generated digitized earthquake records that were available were used, but an appreciable sliding was found, as expected, under those earthquake ground motions where accelerations were relatively higher compared with the value μg. The results presented here include the response of the

block under San Fernando Earthquake 1971 (accelerograms S16°E and S74°W recorded at Pacoima Dam) and four artificially generated earthquakes. In the case of the Pacoima records, these were studied both with and without the measured vertical ground motion component. The artificially generated earthquakes were used without a vertical ground motion. It is suggested that the maximum relative displacements of a block due to the Pacoima ground motion represent an upper extreme and the probability of the relative displacements of a sliding block exceeding the maximum values given in Tables 4-1 and 4-2 for a given value of μ would be low in future earthquake events.

Tables 4-1 and 4-2 show the maximum values of acceleration of the block, maximum relative velocity and relative displacements of the block, and residual relative displacements of the block under Pacoima Dam Earthquake Records S16°E and S74°W respectively, with and without the actual measured vertical acceleration component. The coefficient of friction was varied from 0.05 to 0.30. Results of Table 4-1 are also shown in Figs. 4-1 and 4-2 and those of Table 4-2 in Figs. 4-3 and 4-4.

Time history analysis of the sliding response of the block for values of μ equal to 0.10, 0.15, 0.20, and 0.30 are also shown in Calcomp plots of Figs. 4-5 through 4-8 and Figs. 4-9 through 4-12 for Pacoima Dam records S16°E and 74°W respectively. From top to bottom the quantities plotted in these figures are horizontal accelerations, vertical accelerations, horizontal velocities and horizontal displacements of the ground and the block superimposed in each case. The block response in the velocity and displacement plots are represented by the thicker lines. K is the stiffness of the linear spring which is zero in this case. Values of acceleration, velocity and displacements are given in terms of g, inches/second, and inches respectively.

The sliding response analysis was also carried out under four artificially generated strong motion accelerograms [1] named A-1, A-2, B-1 and B-2. The artificial accelerograms are sections of a random process with a prescribed power spectral density, multiplied by envelope functions chosen to model the changing intensity at the beginning and end of a real earthquake accelerogram. The artificially generated earthquake accelerograms A and B were supposed to represent the shaking in the vicinity of the causative fault in earthquakes of Richter Magnitudes of 8 and 7 respectively. The maximum acceleration in the A type accelerogram is of the order of 0.5 g. However, the accelerations recorded in San Fernando Earthquake (1971) were as high as 1.25 g even though the Richter Magnitude was only 6.5. The artificial earthquake accelerograms were generated to represent the horizontal ground accelerations only, and the effect of vertical accelerogram, therefore, was not studied.

Table 4-3 shows maximum and residual relative displacements of a rigid block under the artificial ground motion accelerograms A-1 and A-2 for μ values of 0.10, 0.15, 0.20 and 0.30 while Table 4-4 shows the same for accelerograms B-1 and B-2. Time history response analysis of the block under accelerograms A-1, A-2, B-1 and B-2 for the same values of μ is shown in Calcomp plots of Figs. 4-13 through 4-28. From top to bottom in these plots are the horizontal acceleration of the ground, horizontal acceleration of the block, velocities of the block and the ground, and displacements of the ground and the block. It may be mentioned that the acceleration, velocity, and displacement values of the block and ground in these plots are all absolute values. The velocity and displacement curves of the block and the ground are superimposed. The relative velocity between the block and the ground in

Figs. 4-13 through 4-28 is usually small, and because of the relatively compressed time scale, the block and ground velocity curves look like a single curve. The displacement curve for the block is represented by the thicker line.

From Tables 4-1 through 4-4, the following observations can be made regarding the sliding response of a block under earthquake ground motions.

(1) Maximum relative displacement of the block does not necessarily occur at a minimum value of μ for a given earthquake accelerogram as may be seen from Table 4-2 or Fig. 4-3. Table 4-2 shows that the maximum relative displacement for the Pacoima Dam S74°W accelerogram occurs for a μ value of 0.14 and not for a μ value of 0.05.

(2) Tables 4-1 and 4-2 and Figs. 4-1 through 4-4 show the effect of vertical ground acceleration on the sliding response of the block when the block is subjected to the San Fernando Earthquake 1971 (Pacoima Dam Record). It will be seen that vertical ground motion may increase or decrease the relative displacement of the block. Table 4-2 and Fig. 4-3 show that the introduction of vertical ground motion increases the relative displacement of the block for all values of μ between 0.05 and 0.30 for S74°W component of Pacoima Dam accelerogram. The effect is particularly significant for μ values higher than 0.2. Table 4-1 and Fig. 4-1 show that the introduction of vertical ground motions may increase or decrease the relative displacement of the block under S16°E component of Pacoima Dam accelerogram depending upon the value of μ, e.g., the maximum relative displacement of the block decreases from 19.08 in. to 17.09 in. for μ of 0.10, whereas it

increases from 2.66 in. to 3.00 in. for $\mu = 0.25$ under the influence of vertical ground accelerogram recorded at Pacoima Dam.

(3) Out of all the available actual or artificial earthquake accelerograms, San Fernando Earthquake accelerogram of 1971 recorded at Pacoima Dam gives the highest relative displacements to a rigid block under pure sliding conditions, e.g., for a μ value of 0.10, the maximum relative displacement under Pacoima Dam accelerogram is 18.5 in. compared with maximum values of 12.0 in., 7.0 in., 5.8 in., 1.5 in. and less than 2 in. for accelerograms of earthquakes A-1, A-2, B-1, B-2 and El Centro (1940) respectively.

(4) For values of μ higher than 0.40 which is the case with most of the present radiation shielding blocks, it is estimated that under pure sliding conditions, there may not be any significant relative displacement of the blocks due to sliding even under very strong earthquake ground motions.

4.3 Effect of a Linear Spring on the Response of Block

A linear spring was introduced between the block and the ground in such a manner that the spring could exert a horizontal force proportional to the relative displacements. The block and spring system behaves as a single degree of freedom system with Coulomb damping (friction) as shown in Fig. 4-29. The method of analysis is explained in Section 2, and using the computer program BLOKSLD, the effect of a linear spring was studied on the response of the block under the San Fernando and the four artificial accelerograms for μ values of 0.10, 0.15, 0.20 and 0.30.

Maximum and residual values of relative displacement are summarized in Tables 4-5, 4-6 and 4-7 for comparison with Tables 4-1

through 4-4. It may be noted that the values in Table 4-5 for the Pacoima Dam accelerogram include the effect of the vertical accelerogram. The stiffness of the spring K was varied from 0.005W/in. to 0.20W/in. for each value of μ. Time history analysis was carried out and the block and table accelerations, velocities and displacements were plotted by Calcomp plotter. Representative plots for each accelerogram are shown in Figs. 4-30 through 4-37.

The following observations were made from Tables 4-5, 4-6, 4-7 and Calcomp plots regarding the influence of a linear spring on the response of a sliding block under earthquake ground motions.

(1) The introduction of a linear spring is very effective in reducing the relative residual displacement of the block because the elastic spring force will always push or pull the block towards its original position depending upon the sign of the relative displacement. This may be seen by comparing the values of residual displacements in Tables 4-5, 4-6 and 4-7 with the corresponding values of Tables 4-1 through 4-4, e.g., the residual displacement in Table 4-5 under the S16°E component of acceleration of the ground, for μ and K values of 0.10 and 0.01W/in. respectively, is only 1.32 in., compared with a value of 16.7 in. in Table 4-1 when K = 0.

(2) The presence of a spring may not necessarily decrease the maximum relative displacement of the block, e.g., in Table 4-5 under the S16°E component of acceleration of the ground for μ and K values of 0.20 and 0.01W/in., the value of maximum relative displacement is 6.34 in. compared with a value of 4.36 in. only when K = 0, as may be seen in Table 4-1. Such a situation could arise under resonance conditions where the system would start vibrating with its natural period T ($T = 2\pi\sqrt{M/K}$).

This point may further be illustrated by comparing Figs. 4-30 and 4-31, which show the sliding response of a block under the same ground motions and coefficient of friction but different spring stiffness values of K. Contrary to expectation, the maximum relative displacement values are 13.2 and 12.3 in. for a K value of 0.05W/in. and 0.01W/in. respectively as shown in Table 4-5. It can be seen in Fig. 4-31 that when K = 0.05W/in., the block is vibrating with its natural period T (T = 1.4 sec). It can be seen that the spring and mass system is vibrating with its natural frequency, resulting in block accelerations as high as 3.4 g.

(3) A careful review of Tables 4-1 through 4-7 will show that a spring of stiffness 0.01W/in. would be a good compromise between economics and minimizing residual displacements if it becomes absolutely necessary to reduce the residual displacements. A spring of this stiffness would give a natural period of greater than 3.0 seconds and the probability of resonance would be remote. It can be seen in Tables 4-1 through 4-7 that the maximum value of residual displacement for a μ value of 0.1 and K value of 0.01W/in. is 3.5 in. compared with a maximum residual displacement of 16.7 in. in the absence of a spring.

It is suggested that a spring of stiffness higher than 0.01W/in. should not be used so that the natural period of the system remains greater than 3 seconds.

(4) As noted earlier, there may not be any virtue in using an expensive spring system in shielding systems, as it is not quite effective in reducing the maximum relative displacements.

(5) It has been assumed all along that the response of the block is only in the sliding mode, even when the spring is present. It should however be noted that the introduction of a spring may change the

phenomenon from sliding to rocking even though $\mu_s < B/H$. This can be understood from the condition for sliding in the presence of a spring of stiffness K. It can be shown that the condition

$$\ddot{u} > \mu_s g\,(1 + \ddot{v}/g) + \frac{K}{M}\,s$$

must be met for sliding to take place, where S is the displacement of the block relative to ground.

If the spring is placed at ground level, the condition for rocking still remains the same as shown in Section 2 i.e.,

$$\ddot{u} > (B/H)g(1 + \ddot{v}/g)$$

It is clear from the above two conditions that even though μ_s may be less than (B/H), it is still possible for the block to go into the rocking mode in the presence of a spring depending on the magnitude of the displacement(s) of the block relative to the ground which is a function of the ground acceleration and thus remains an unknown.

Because of this danger of rocking in the presence of a spring, the possibility of rocking must be studied before using such a restraining device to reduce the residual relative displacements of shielding blocks. This applies particularly to free standing block stacks with a potentially high aspect ratio.

4.4 Response Spectra for San Fernando Earthquake (1971)

Relative velocity response spectra with Coulomb damping (friction) for San Fernando Earthquake 1971 (Pacoima Dam Accelerograms) are shown in Fig. 4-38 for comparison with the response spectra with viscous damping shown in Fig. 4-39. Response spectra with Coulomb damping were determined using the same basic computer program as the

one used to analyze the sliding response of the block under earthquake motion in Sections 2 and 4. The values for response spectra in Fig. 4-38 were determined at time period intervals of 0.10 seconds as long as the period of vibration T was less than 2.0 seconds, and the time period interval was increased to 0.5 seconds and 1.0 seconds for periods of vibration higher than 2.0 seconds and 4.0 seconds respectively, to reduce the computer time. Response spectra for viscous damping was taken directly from Ref. 2 and was plotted independently using another computer program for 0, 2, 5, 10 and 20% damping, as shown in Fig. 4-39. Response spectra with Coulomb damping were plotted for μ values of 0, 0.05, 0.10, 0.15, 0.20, 0.25 and 0.30 (Fig. 4-38).

Corresponding response spectra curves in Fig. 4-38 for $\mu = 0$ and in Fig. 4-39 for viscous damping equal to zero agree with each other with small differences at few points because the values in Fig. 4-38 were not plotted at the same time periods and the interval of plotted points was also different than in Fig. 4-39.

A noticeable difference between the two relative velocity response spectra in Figs. 4-38 and 4-39 is that whereas the relative velocity spectra become relatively independent of viscous damping at periods greater than 3.0 seconds (Fig. 4-39), this is not so for Coulomb damping; as may be seen in Fig. 4-38.

Relative displacement spectra of Pacoima Dam Accelerogram (1971) with Coulomb damping for μ values of 0.0, 0.05, 0.10, 0.15, 0.20, 0.25 and 0.30 are shown in Fig. 4-40.

TABLE 4-1 EFFECT OF VERTICAL ACCELEROGRAM (PACOIMA DAM RECORD) ON THE SLIDING RESPONSE OF A BLOCK UNDER SAN FERNANDO EARTHQUAKE 1971 (PACOIMA DAM S16°E ACCELEROGRAM)

	RESPONSE OF A RIGID BLOCK UNDER PACOIMA DAM SITE ACCELEROGRAM OF 1971							
	WITHOUT VERTICAL ACCELERATION				WITH VERTICAL ACCELERATION			
COEFFICIENT OF FRICTION	MAXIMUM BLOCK ACCELERATION (g,S)	MAXIMUM RELATIVE VELOCITY (INCHES/SEC)	MAXIMUM RELATIVE DISPLACEMENT (INCHES)	RESIDUAL RELATIVE DISPLACEMENT (INCHES)	MAXIMUM BLOCK ACCELERATION (g,S)	MAXIMUM RELATIVE VELOCITY (INCHES/SEC)	MAXIMUM RELATIVE DISPLACEMENT (INCHES)	RESIDUAL RELATIVE DISPLACEMENT (INCHES)
.0500	.0500	45.5161	27.4662	25.9207	.0833	46.1749	29.2262	27.8734
.0600	.0600	44.2066	26.4952	25.1812	.1000	45.0333	27.9249	26.7260
.0700	.0700	43.0145	24.8474	23.7653	.1167	43.7200	25.7615	24.8687
.0800	.0800	41.5086	23.1650	22.3840	.1333	42.1370	23.2815	22.6094
.0900	.0900	39.9149	21.8404	21.2045	.1500	40.1443	21.1500	20.6271
.1000	.1000	37.7595	19.0796	18.5370	.1667	37.7371	17.0891	16.6742
.1100	.1100	35.5776	16.3793	15.8870	.1833	35.3943	14.5791	13.6878
.1200	.1200	33.1861	13.8114	13.3490	.2000	33.0669	13.2111	11.2329
.1300	.1300	30.8780	12.5044	11.7849	.2167	30.7477	11.8896	8.8684
.1400	.1400	28.5711	11.2625	9.9976	.2333	28.4324	10.6342	6.8377
.1500	.1500	26.2885	10.0929	8.8314	.2500	26.1434	9.4641	5.6789
.1600	.1600	24.0129	8.9720	7.8968	.2667	24.7765	8.3406	4.4962
.1700	.1700	21.7734	7.9045	6.8714	.2833	24.5715	7.2631	3.3846
.1800	.1800	20.8857	6.8749	5.7083	.3000	24.1223	6.2375	2.5345
.1900	.1900	20.4015	5.8774	4.6317	.3167	23.8827	5.2455	1.3791
.2000	.2000	20.2382	4.9188	3.0123	.3333	23.6279	4.3644	.6100
.2100	.2100	19.9300	3.9884	1.8619	.3500	23.3846	4.5105	.1176
.2200	.2200	19.5251	3.3580	1.0114	.3667	22.3941	4.1264	.1777
.2300	.2300	18.0390	2.8390	1.2462	.3833	21.2010	3.6985	.4628
.2400	.2400	16.8664	2.5828	1.4998	.4000	20.2161	3.3413	.7259
.2500	.2500	16.4539	2.6569	1.6479	.4167	19.4521	2.9994	.9659
.2600	.2600	16.6309	2.7780	1.8358	.4333	19.4370	2.7142	1.0037
.2700	.2700	16.6690	2.8268	1.8959	.4500	19.4054	2.4891	1.1882
.2800	.2800	16.6433	2.9427	2.1178	.4667	19.1745	2.4886	1.0685
.2900	.2900	16.5160	3.0973	2.3433	.4829	18.8876	2.2344	1.1837
.3000	.3000	15.9195	3.1092	2.3823	.4906	18.6017	2.1104	1.1773

TABLE 4-2 EFFECT OF VERTICAL ACCELEROGRAM (PACOIMA DAM RECORD) ON THE SLIDING RESPONSE OF A BLOCK UNDER SAN FERNANDO EARTHQUAKE (PACOIMA DAM S74°W ACCELEROGRAM) 1971

	RESPONSE OF A RIGID BLOCK UNDER PACOIMA DAM S74°W ACCELEROGRAM OF 1971							
	WITHOUT VERTICAL ACCELERATION				WITH VERTICAL ACCELERATION			
COEFFICIENT OF FRICTION	MAXIMUM BLOCK ACCELERATION (g)	MAXIMUM RELATIVE VELOCITY (INCHES/SEC)	MAXIMUM RELATIVE DISPLACEMENT (INCHES)	RESIDUAL RELATIVE DISPLACEMENT (INCHES)	MAXIMUM BLOCK ACCELERATION (g)	MAXIMUM RELATIVE VELOCITY (INCHES/SEC)	MAXIMUM RELATIVE DISPLACEMENT (INCHES)	RESIDUAL RELATIVE DISPLACEMENT (INCHES)
.0500	.0500	20.2876	6.3810	.5052	.0829	20.7477	6.8231	.2268
.0600	.0600	19.6033	6.3695	.0111	.0995	19.8114	6.8375	.9797
.0700	.0700	19.6807	5.9822	.8846	.1160	19.5313	6.5482	1.7807
.0800	.0800	19.7320	5.6821	1.4788	.1326	19.5400	6.2317	2.6631
.0900	.0900	19.8582	5.2970	2.0655	.1492	19.6819	5.8584	3.6194
.1000	.1000	19.4436	4.8163	3.3438	.1658	19.6588	5.5737	4.7232
.1100	.1100	19.5293	4.4870	3.6342	.1823	19.9924	6.5783	6.0688
.1200	.1200	19.6374	5.3936	4.8408	.1989	20.3196	7.7387	7.2946
.1300	.1300	19.0427	6.0783	5.3773	.2155	20.1957	8.7176	8.2743
.1400	.1400	19.0968	7.3966	6.6680	.2321	20.6689	9.7686	9.5223
.1500	.1500	19.5991	7.2028	6.1720	.2486	20.7057	9.7055	9.5046
.1600	.1600	18.8846	7.2332	6.3570	.2652	20.2312	9.4773	9.1196
.1700	.1700	18.8653	7.0574	6.0451	.2818	20.8400	9.6594	9.5880
.1800	.1800	18.8460	6.4515	5.2782	.2984	19.9303	9.1291	9.0778
.1900	.1900	18.0929	6.0903	5.4168	.3149	20.4317	8.9225	8.9225
.2000	.2000	18.0374	5.7633	4.7998	.3315	20.0101	8.7543	8.7542
.2100	.2100	17.9962	5.4493	4.5997	.3481	19.4950	8.7679	8.7673
.2200	.2200	17.5416	4.9759	4.0291	.3647	18.4666	7.6956	7.6944
.2300	.2300	17.0573	4.8414	4.0970	.3813	18.6029	7.2174	7.2170
.2400	.2400	17.0121	4.2186	3.4754	.3978	18.4459	6.8719	6.8712
.2500	.2500	16.9788	3.8200	3.0841	.4144	18.6032	6.8740	6.8739
.2600	.2600	16.4551	3.5577	2.6060	.4310	18.7488	6.8688	6.8679
.2700	.2700	15.9670	3.2972	2.4764	.4476	18.3978	6.3918	6.3913
.2800	.2800	15.9258	2.9863	2.0891	.4641	17.4538	5.9462	5.9460
.2900	.2900	15.8846	2.7280	1.8685	.4807	16.9981	5.4262	5.4261
.3000	.3000	15.3511	2.4812	1.6225	.4973	16.5520	5.1368	5.1367

TABLE 4-3 MAXIMUM AND RESIDUAL RELATIVE DISPLACEMENTS OF A RIGID BLOCK UNDER ARTIFICIAL EARTHQUAKES A-1 AND A-2

COEFFICIENT OF FRICTION	DISPLACEMENT FOR THE EARTHQUAKE (INCHES)			
	EARTHQUAKE A-1		EARTHQUAKE A-2	
	MAXIMUM RELATIVE DISPLACEMENT	RESIDUAL RELATIVE DISPLACEMENT	MAXIMUM RELATIVE DISPLACEMENT	RESIDUAL RELATIVE DISPLACEMENT
0.10	12.01	10.29	7.01	1.02
0.15	5.11	4.86	3.90	0.90
0.20	2.36	2.32	1.83	1.31
0.30	0.14	0.13	0.26	0.25

TABLE 4-4 MAXIMUM AND RESIDUAL RELATIVE DISPLACEMENTS OF A RIGID BLOCK UNDER ARTIFICIAL EARTHQUAKES B-1 AND B-2

COEFFICIENT OF FRICTION	RELATIVE DISPLACEMENT UNDER THE EARTHQUAKE (INCHES)			
	EARTHQUAKE B-1		EARTHQUAKE B-2	
	MAXIMUM DISPLACEMENT	RESIDUAL DISPLACEMENT	MAXIMUM DISPLACEMENT	RESIDUAL DISPLACEMENT
0.10	5.81	4.14	1.54	0.81
0.15	1.57	1.00	0.79	0.62
0.20	0.36	0.10	0.28	0.27
0.30	0.03	0.01	0.00	0.00

TABLE 4-5. EFFECT OF SPRING STIFFNESS ON MAXIMUM AND RESIDUAL RELATIVE DISPLACEMENTS OF A RIGID BLOCK UNDER SAN-FERNANDO EARTHQUAKE 1971 (PACOIMA DAM ACCELEROGRAMS SIG°E AND S74°W). VERTICAL GROUND ACCELERATION INCLUDED.

COEFFICIENT OF FRICTION (μ)	COEFFICIENT C WHERE C = K/W	RELATIVE DISPLACEMENT (INCHES)			
		S16°E		S74°W	
		MAXIMUM DISPLACEMENT	RESIDUAL DISPLACEMENT	MAXIMUM DISPLACEMENT	RESIDUAL DISPLACEMENT
0.10	0.005	13.73	3.43	5.45	2.41
0.10	0.010	12.31	1.32	5.32	0.93
0.10	0.050	13.19	0.04	6.11	0.02
0.10	0.100	9.16	0.01	4.12	0.02
0.15	0.010	7.70	1.60	5.08	2.29
0.15	0.050	9.54	0.37	3.73	0.09
0.15	0.100	6.61	0.04	2.87	0.16
0.15	0.200	3.79	0.02	3.83	0.06
0.20	0.005	5.74	0.46	6.83	5.09
0.20	0.010	6.34	0.99	5.53	3.19
0.20	0.050	6.31	0.42	2.65	0.40
0.20	0.100	4.86	0.32	2.31	0.10
0.20	0.200	3.12	0.08	3.63	0.15
0.30	0.005	2.21	0.97	4.52	4.16
0.30	0.010	2.17	0.93	4.15	3.47
0.30	0.050	2.37	0.18	2.28	1.07
0.30	0.100	2.39	0.27	1.69	0.72
0.30	0.200	2.07	0.21	2.46	0.29
0.10	0.650	5.14	0.01		

TABLE 4-6. EFFECT OF SPRING STIFFNESS ON MAXIMUM AND RESIDUAL RELATIVE DISPLACEMENTS OF A RIGID BLOCK UNDER ARTIFICIAL EARTHQUAKES A-1 AND A-2.

COEFFICIENT OF FRICTION (μ)	COEFFICIENT C where C = K/W	RELATIVE DISPLACEMENT (INCHES)			
		EARTHQUAKE A-1		EARTHQUAKE A-2	
		MAXIMUM DISPLACEMENT	RESIDUAL DISPLACEMENT	MAXIMUM DISPLACEMENT	RESIDUAL DISPLACEMENT
0.10	0.005	5.23	0.59	4.96	0.19
0.10	0.010	4.83	0.46	4.17	0.12
0.10	0.050	3.14	0.25	2.86	0.03
0.10	0.100	2.32	0.14	2.15	0.03
0.10	0.200	1.64	0.08	1.54	0.03
0.15	0.005	3.08	1.34	3.41	0.54
0.15	0.010	2.47	0.60	3.07	0.45
0.15	0.050	1.80	0.10	1.92	0.01
0.15	0.100	1.37	0.04	1.68	0.02
0.15	0.200	0.98	0.04	1.54	0.02
0.20	0.005	1.80	1.61	1.72	0.71
0.20	0.010	1.53	1.16	1.63	0.37
0.20	0.050	0.78	0.25	1.15	0.01
0.20	0.100	0.68	0.14	0.87	0.02
0.20	0.200	0.52	0.06	0.64	0.02

TABLE 4-7. EFFECT OF SPRING STIFFNESS ON MAXIMUM AND RESIDUAL RELATIVE DISPLACEMENTS OF A RIGID BLOCK UNDER ARTIFICIAL EARTHQUAKES B-1 AND B-2.

COEFFICIENT OF FRICTION	COEFFICIENT C where C = K/W	RELATIVE DISPLACEMENT (INCHES)			
		EARTHQUAKE B-1		EARTHQUAKE B-2	
		MAXIMUM DISPLACEMENT	RESIDUAL DISPLACEMENT	MAXIMUM DISPLACEMENT	RESIDUAL DISPLACEMENT
0.10	0.005	4.35	0.08	1.38	0.35
0.10	0.010	3.91	0.33	1.44	0.16
0.10	0.050	2.31	0.04	1.03	0.22
0.10	0.100	1.66	0.10	0.86	0.15
0.10	0.200	1.27	0.08	0.85	0.02
0.15	0.005	1.48	0.63	0.65	0.45
0.15	0.010	1.40	0.36	0.59	0.36
0.15	0.050	1.00	0.13	0.45	0.11
0.15	0.100	0.81	0.13	0.41	0.00
0.15	0.200	0.62	0.07	0.35	0.04
0.20	0.005	0.36	0.09	0.26	0.26
0.20	0.010	0.36	0.08	0.25	0.25
0.20	0.050	0.34	0.01	0.18	0.16
0.20	0.100	0.31	0.04	0.17	0.11
0.20	0.200	0.29	0.04	0.16	0.08

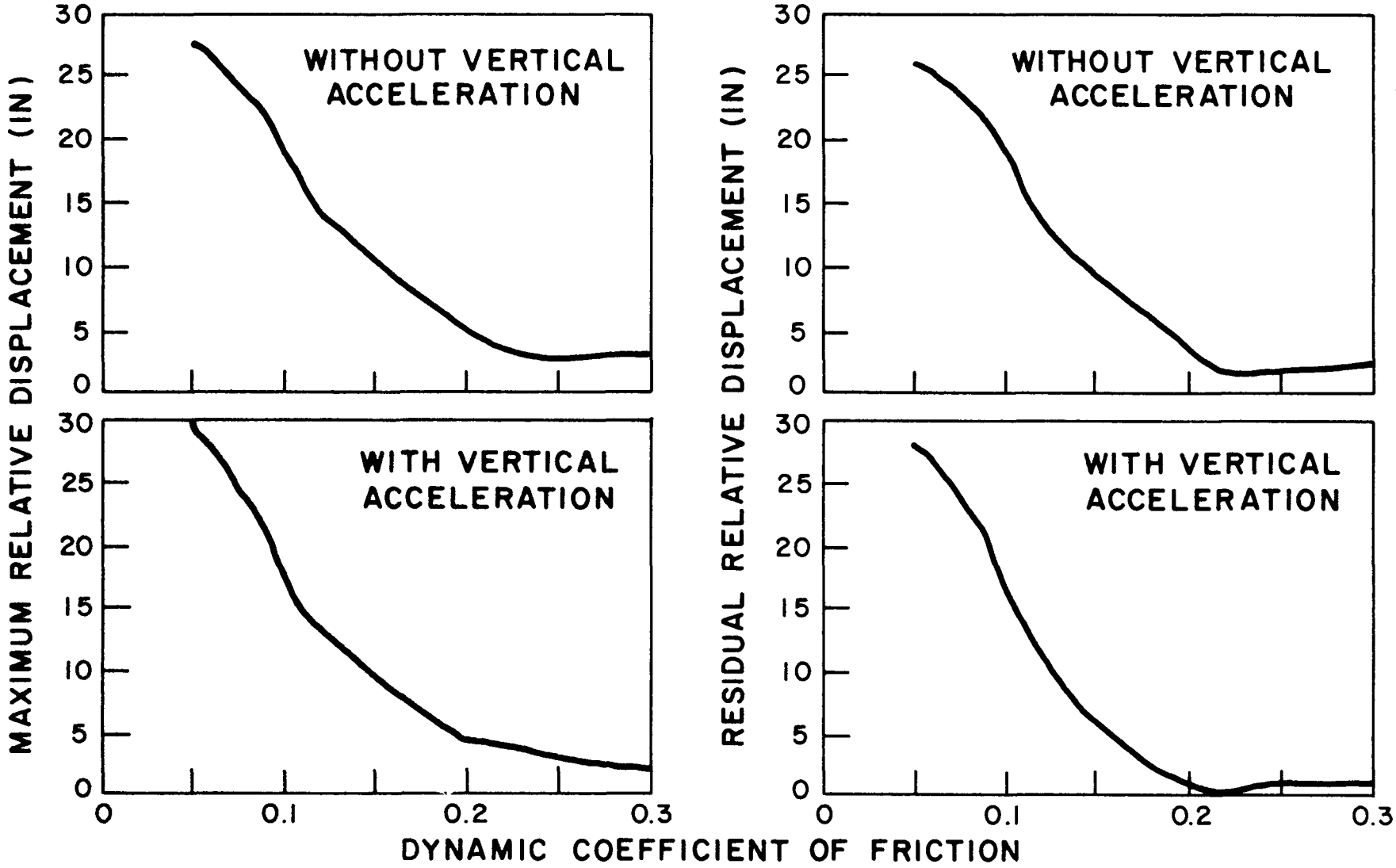

FIG. 4-1. EFFECT OF VERTICAL ACCELEROGRAM (PACOIMA DAM RECORD) ON THE SLIDING RESPONSE OF A BLOCK UNDER SAN FERNANDO EARTHQUAKE 1971 (PACOIMA DAM S16°E ACCELEROGRAM).

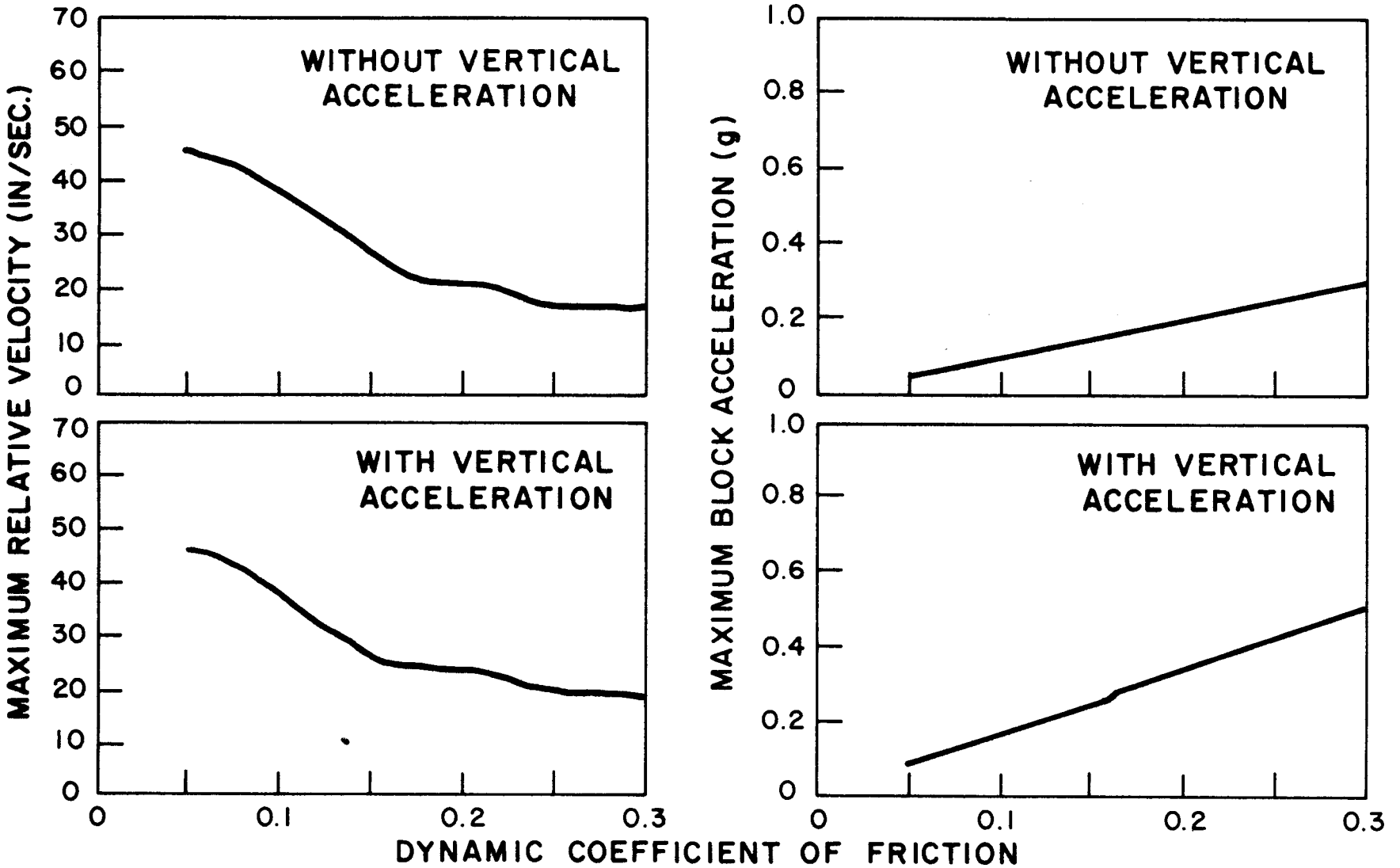

FIG. 4-2. EFFECT OF VERTICAL ACCELEROGRAM (PACOIMA DAM RECORD) ON THE SLIDING RESPONSE OF A BLOCK UNDER SAN FERNANDO EARTHQUAKE 1971 (PACOIMA DAM S16°E ACCELEROGRAM).

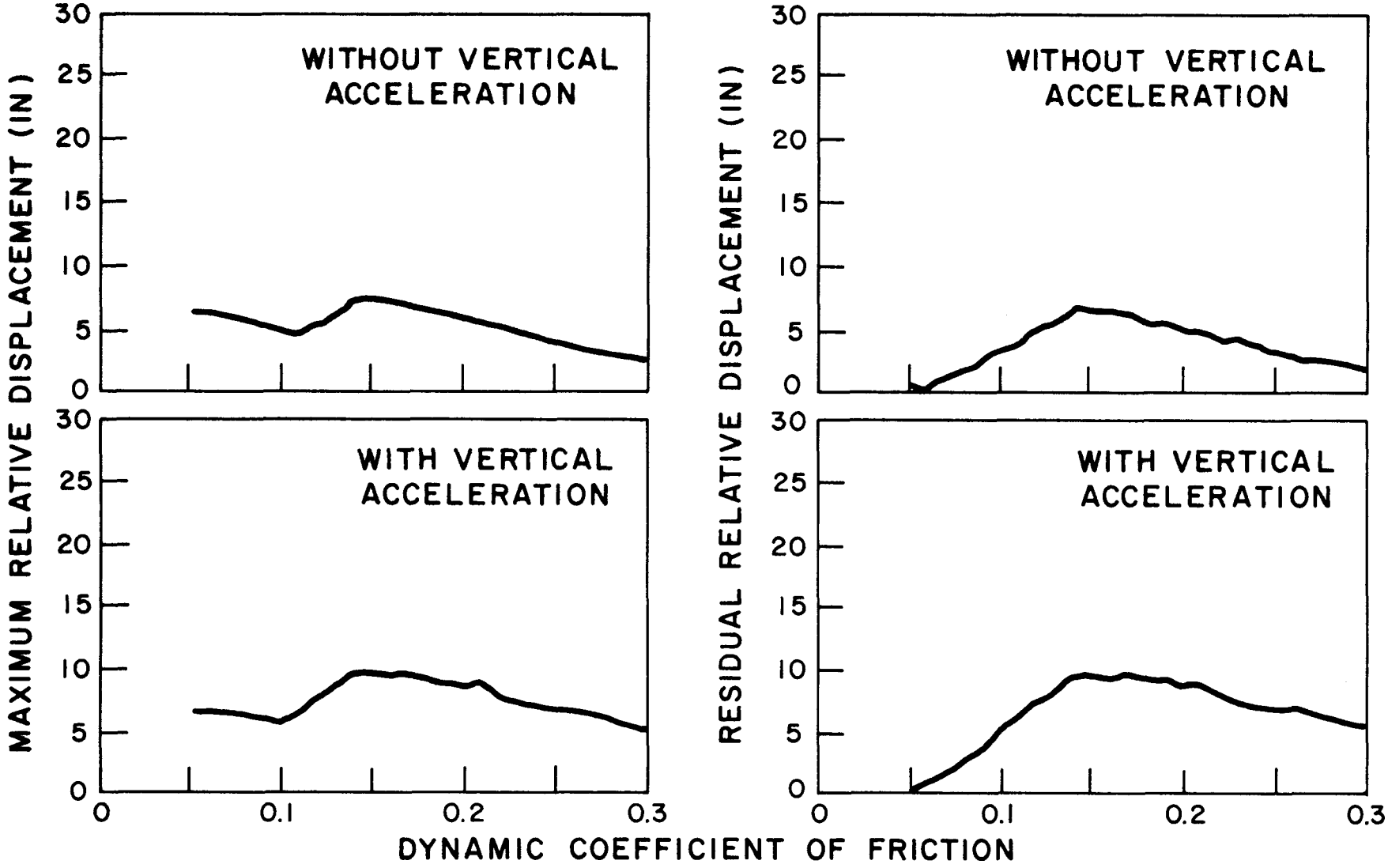

FIG. 4-3. EFFECT OF VERTICAL ACCELEROGRAM (PACOIMA DAM RECORD) ON THE SLIDING RESPONSE OF A BLOCK UNDER SAN FERNANDO EARTHQUAKE 1971 (PACOIMA DAM S74°W ACCELEROGRAM).

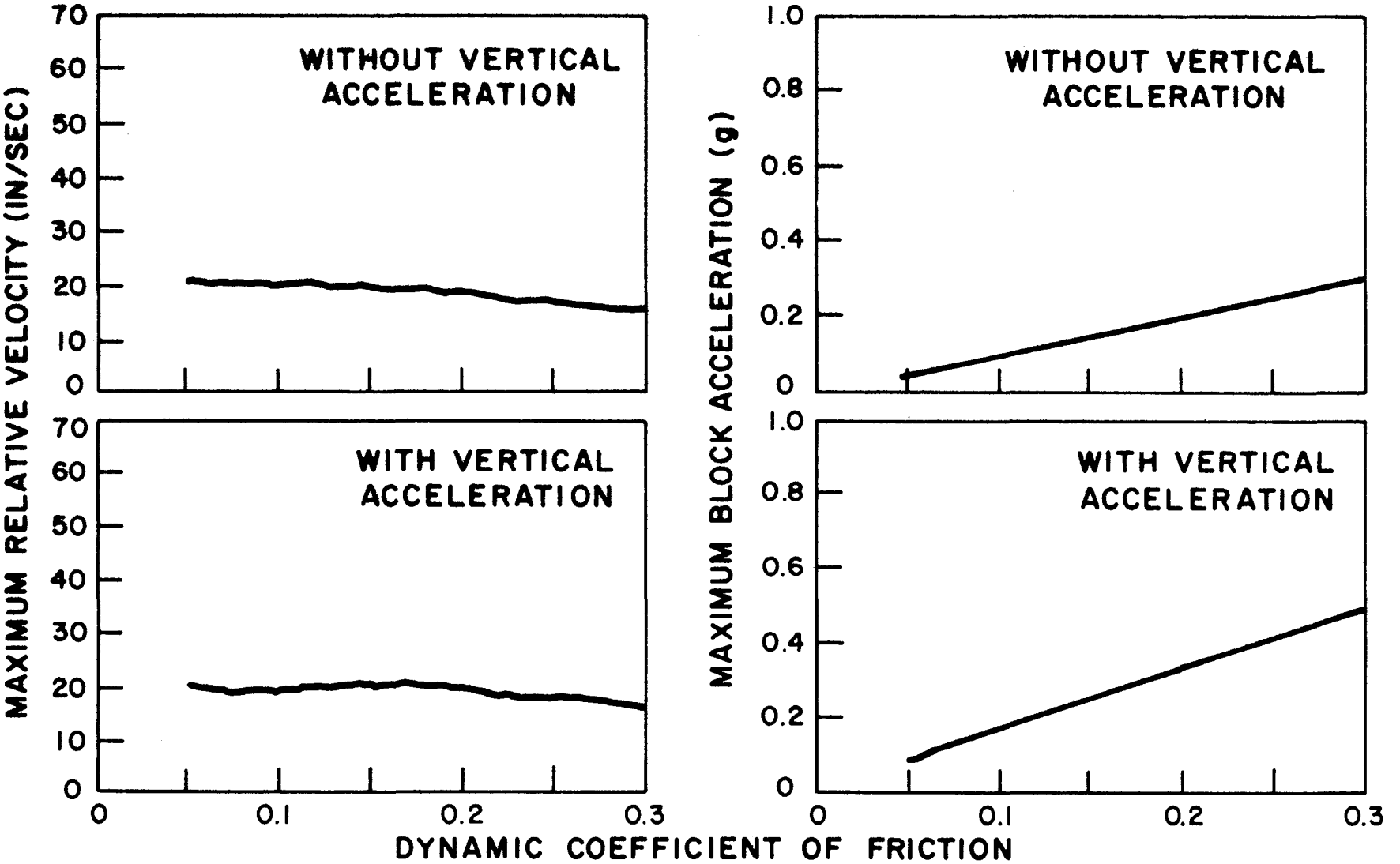

FIG. 4-4. EFFECT OF VERTICAL ACCELEROGRAM (PACOIMA DAM RECORD) ON THE SLIDING RESPONSE OF A BLOCK UNDER SAN FERNANDO EARTHQUAKE 1971 (PACOIMA DAM S74°W ACCELEROGRAM).

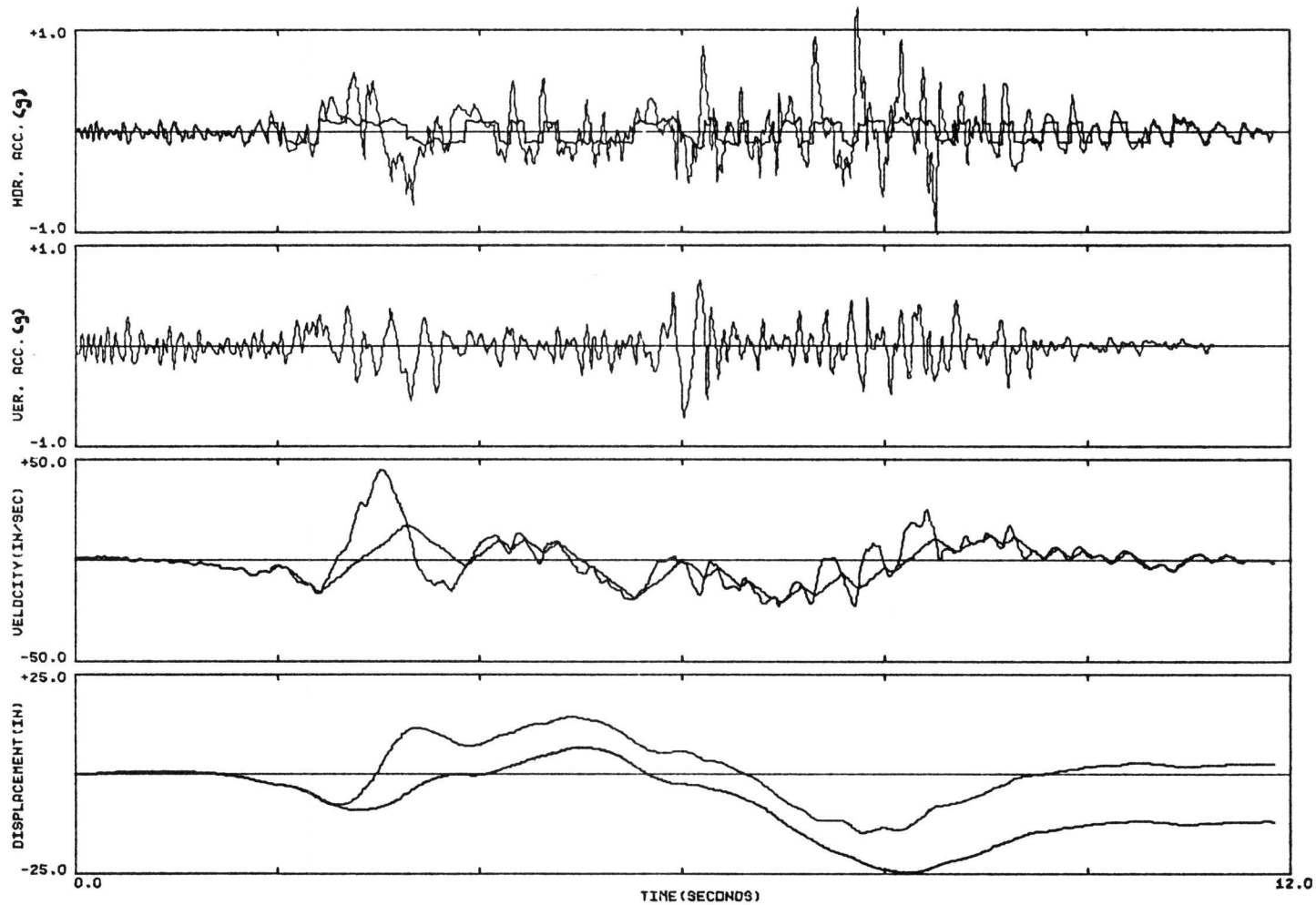

FIG. 4-5. MOTION OF A SHIELDING BLOCK SUBJECTED TO SAN-FERNANDO EARTHQUAKE 1971(PACOIMA DAM RECORD S16E)U=.10,K=.000W/IN

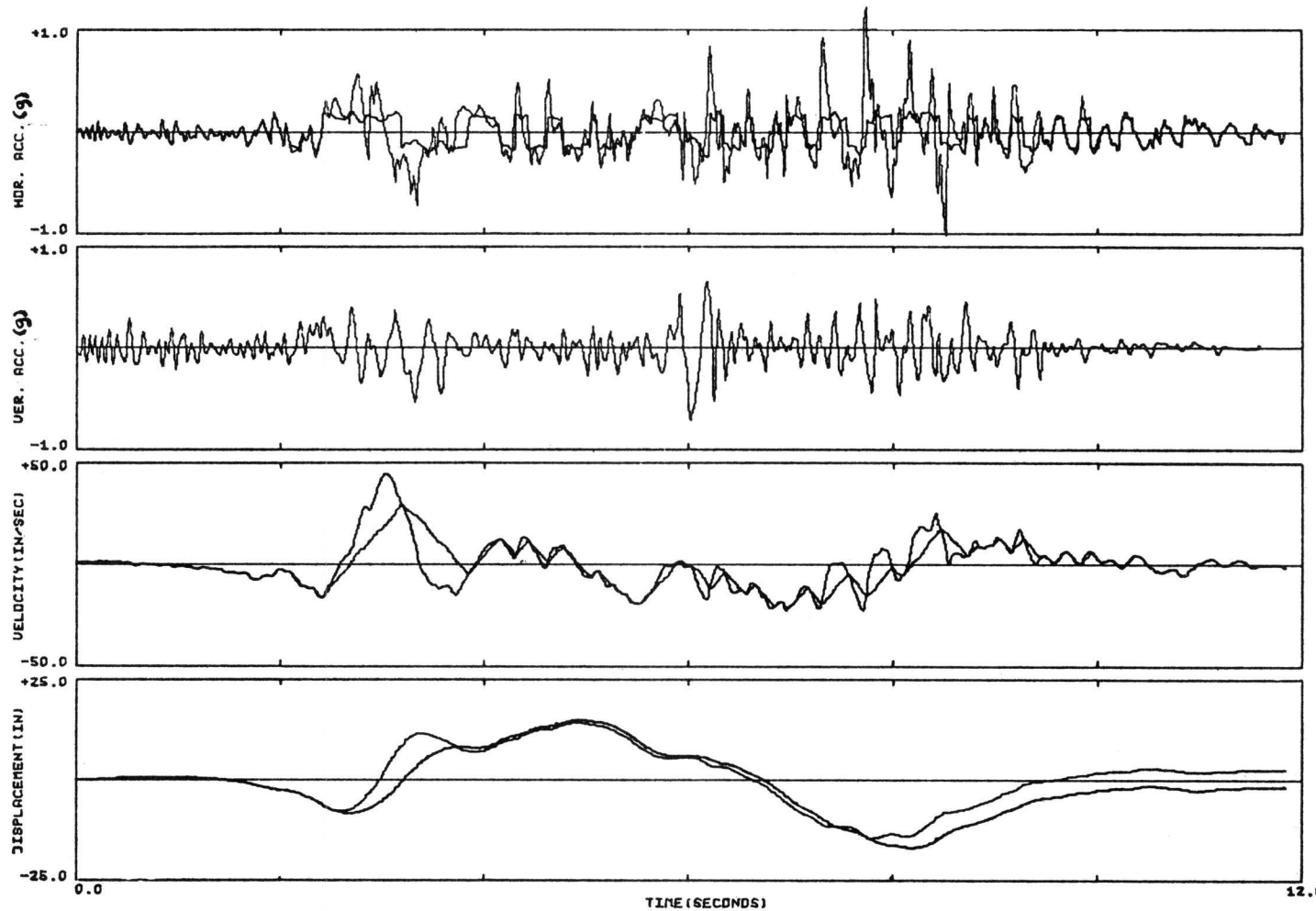

FIG. 4-6. MOTION OF A SHIELDING BLOCK SUBJECTED TO SAN-FERNANDO EARTHQUAKE 1971(PACOIMA DAM RECORD S16E)U=.15,K=.000W/IN

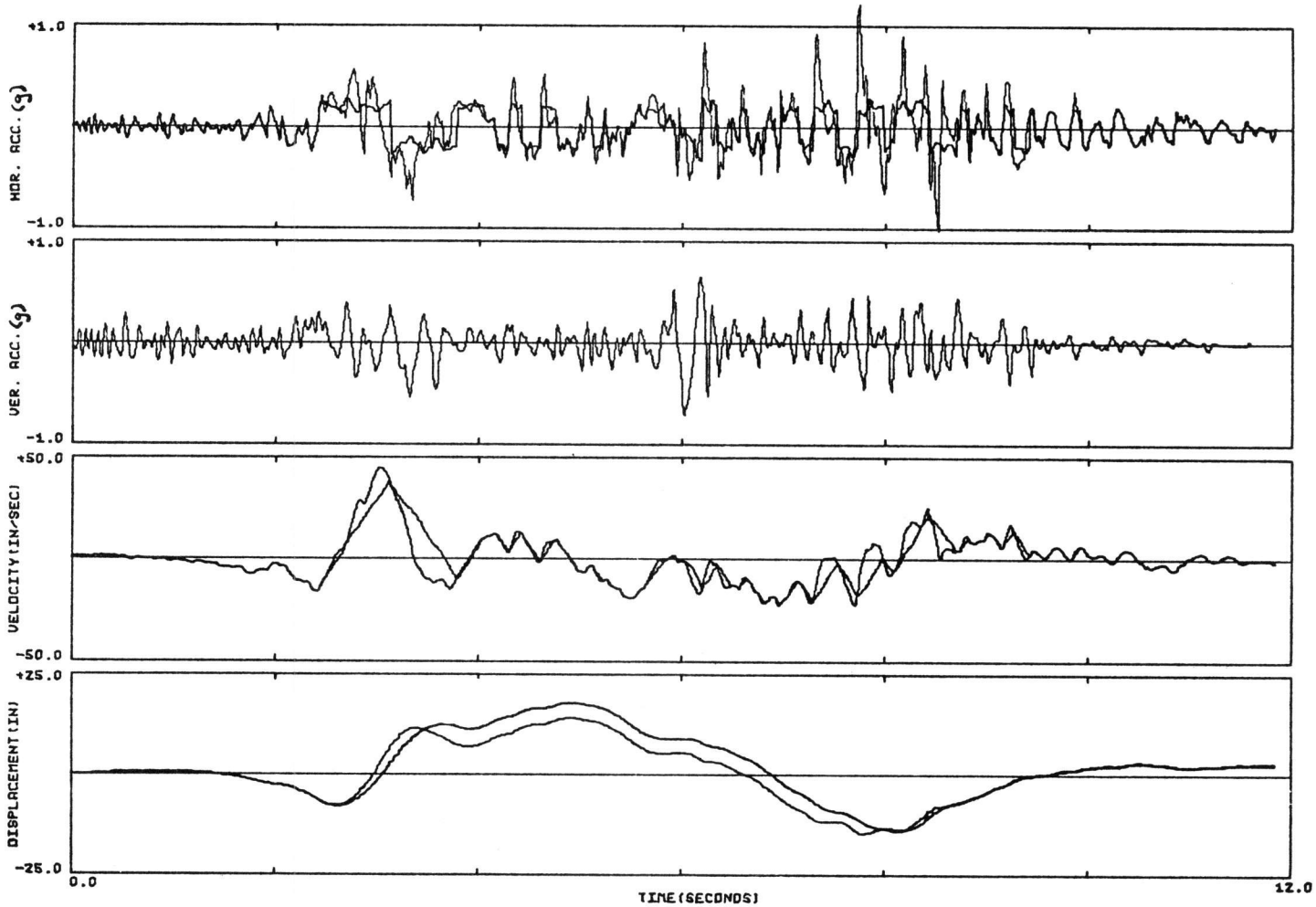

FIG. 4-7. MOTION OF A SHIELDING BLOCK SUBJECTED TO SAN-FERNANDO EARTHQUAKE 1971(PACOIMA DAM RECORD S16E)U=.20,K=.000W/IN

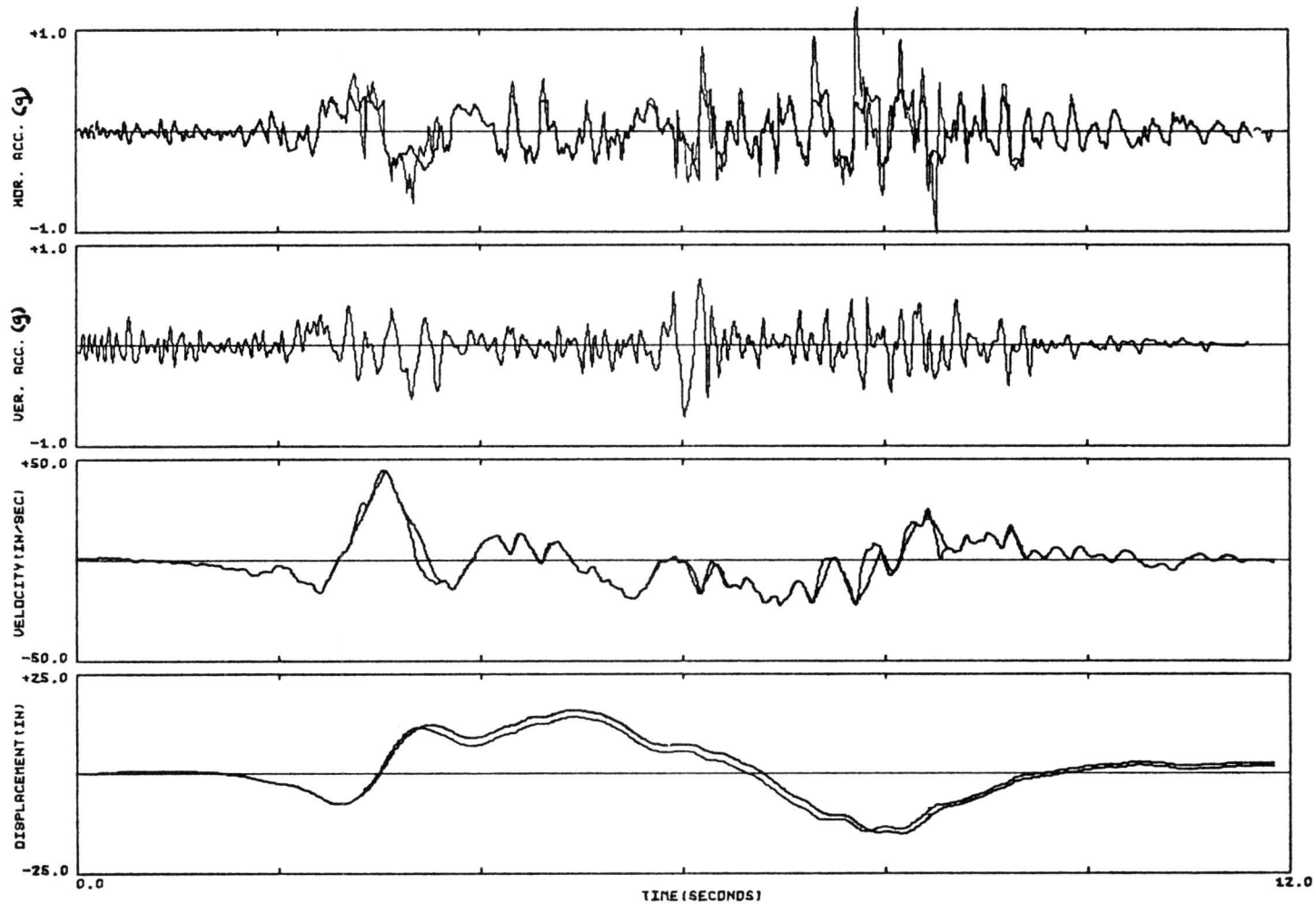

FIG. 4-8. MOTION OF A SHIELDING BLOCK SUBJECTED TO SAN-FERNANDO EARTHQUAKE 1971(PACOIMA DAM RECORD S16E)U=.30,K=.000W/IN

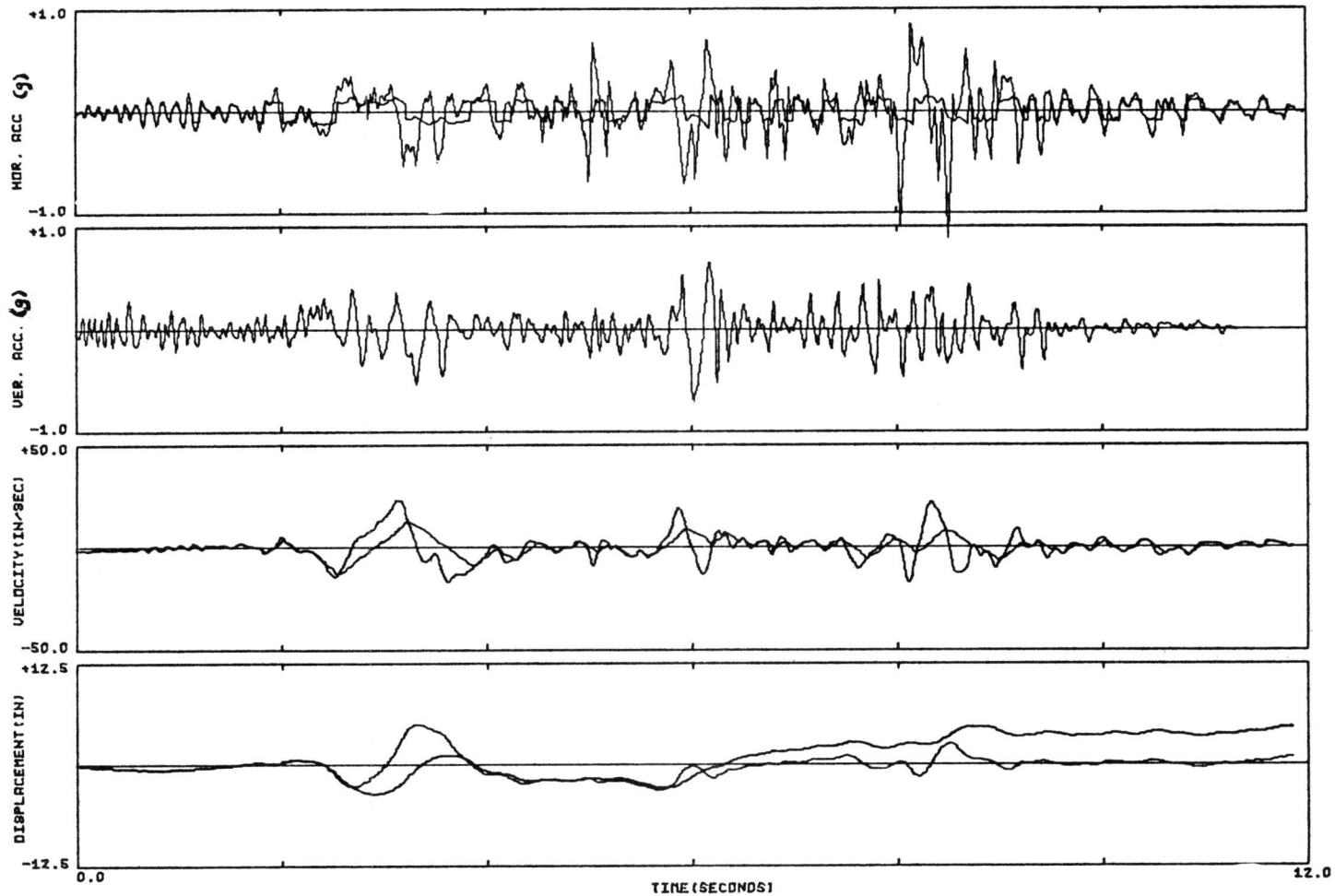

FIG. 4-9. MOTION OF A SHIELDING BLOCK SUBJECTED TO SAN-FERNANDO EARTHQUAKE 1971(PACOIMA DAM RECORD S74W)U=.10,K=.000W/IN

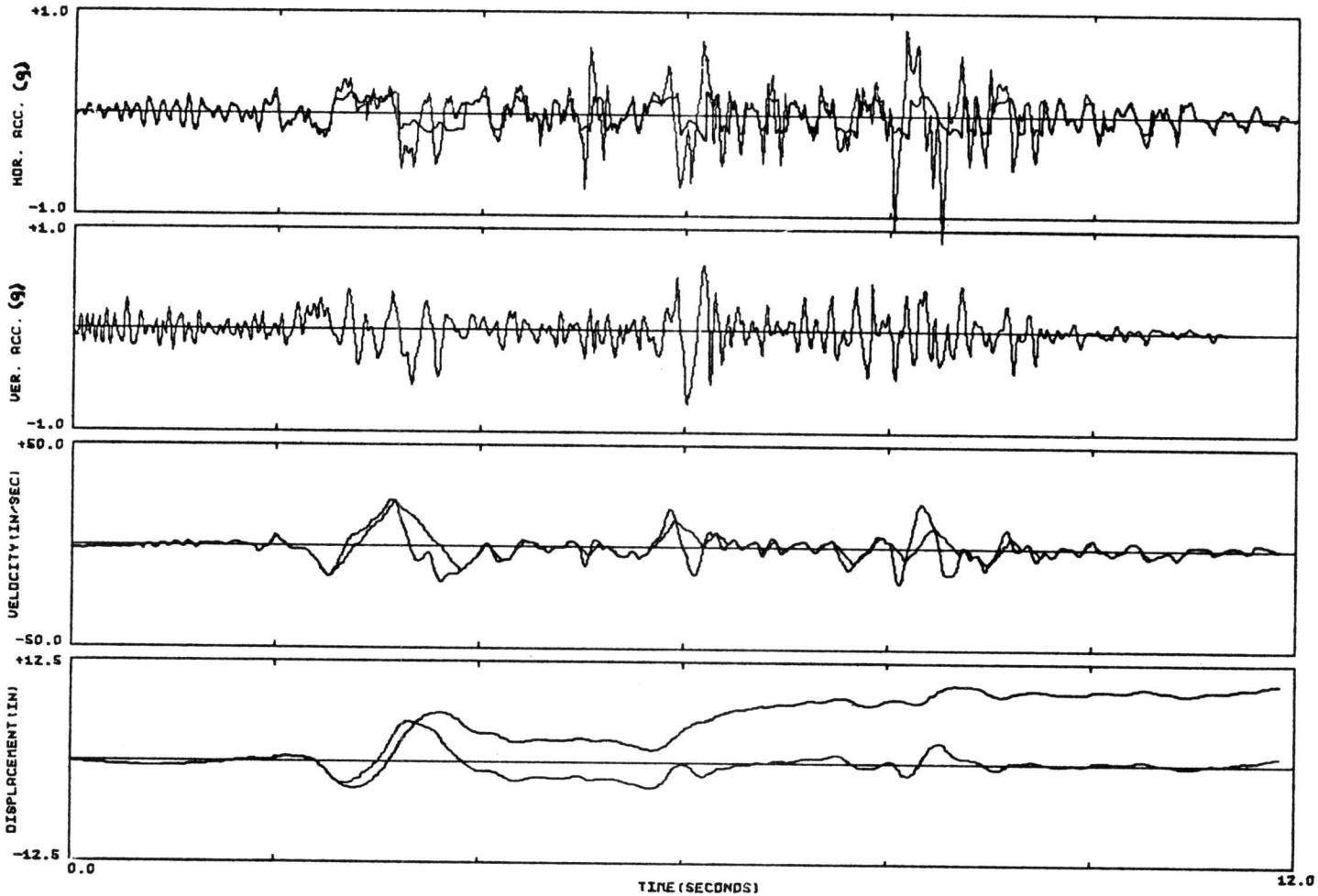

FIG. 4-10. MOTION OF A SHIELDING BLOCK SUBJECTED TO SAN-FERNANDO EARTHQUAKE 1971(PACOIMA DAM RECORD S74W)U=.15,K=.000W/IN

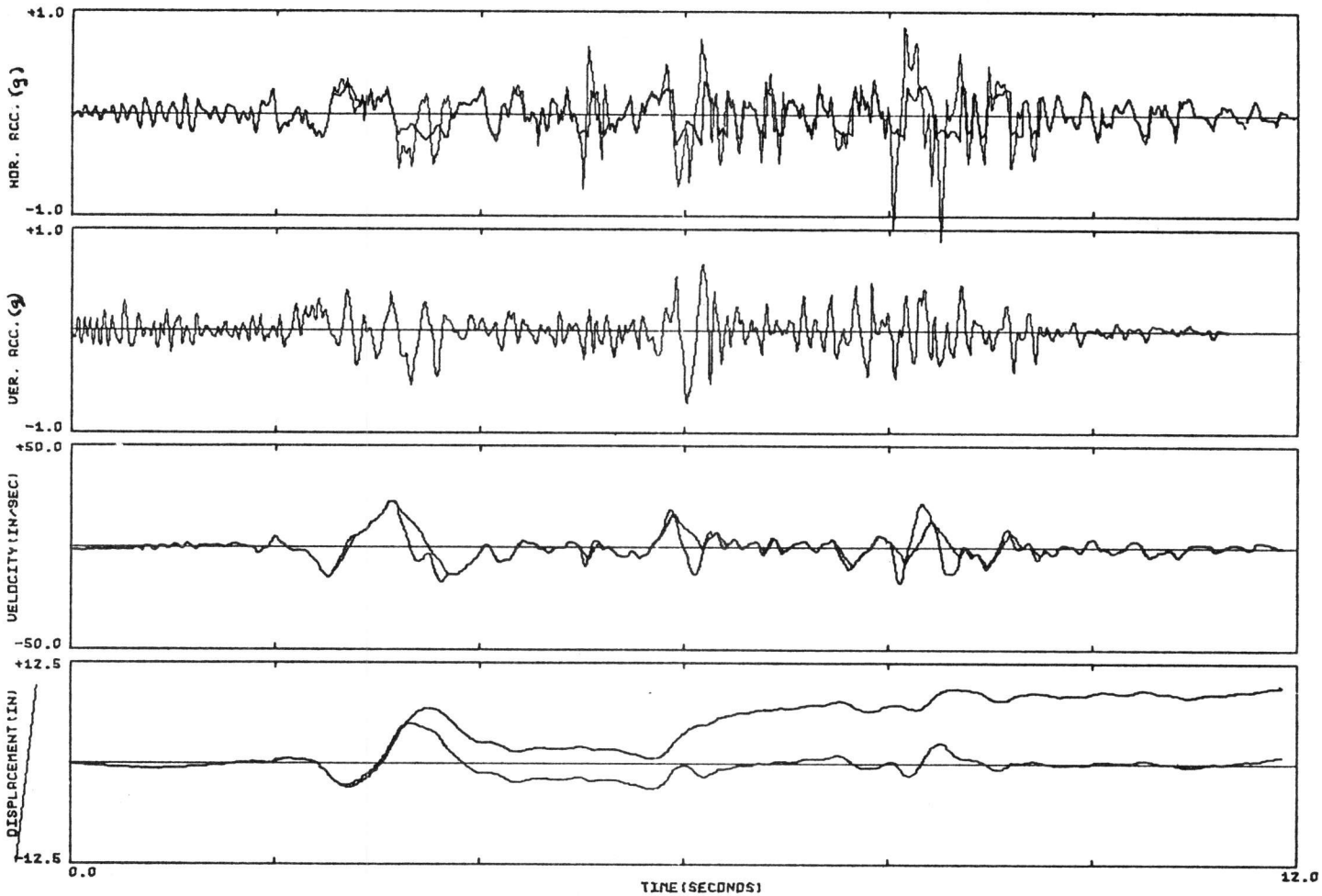

FIG. 4-11. MOTION OF A SHIELDING BLOCK SUBJECTED TO SAN-FERNANDO EARTHQUAKE 1971(PACOIMA DAM RECORD S74W)U=.20,K=.000W/IN

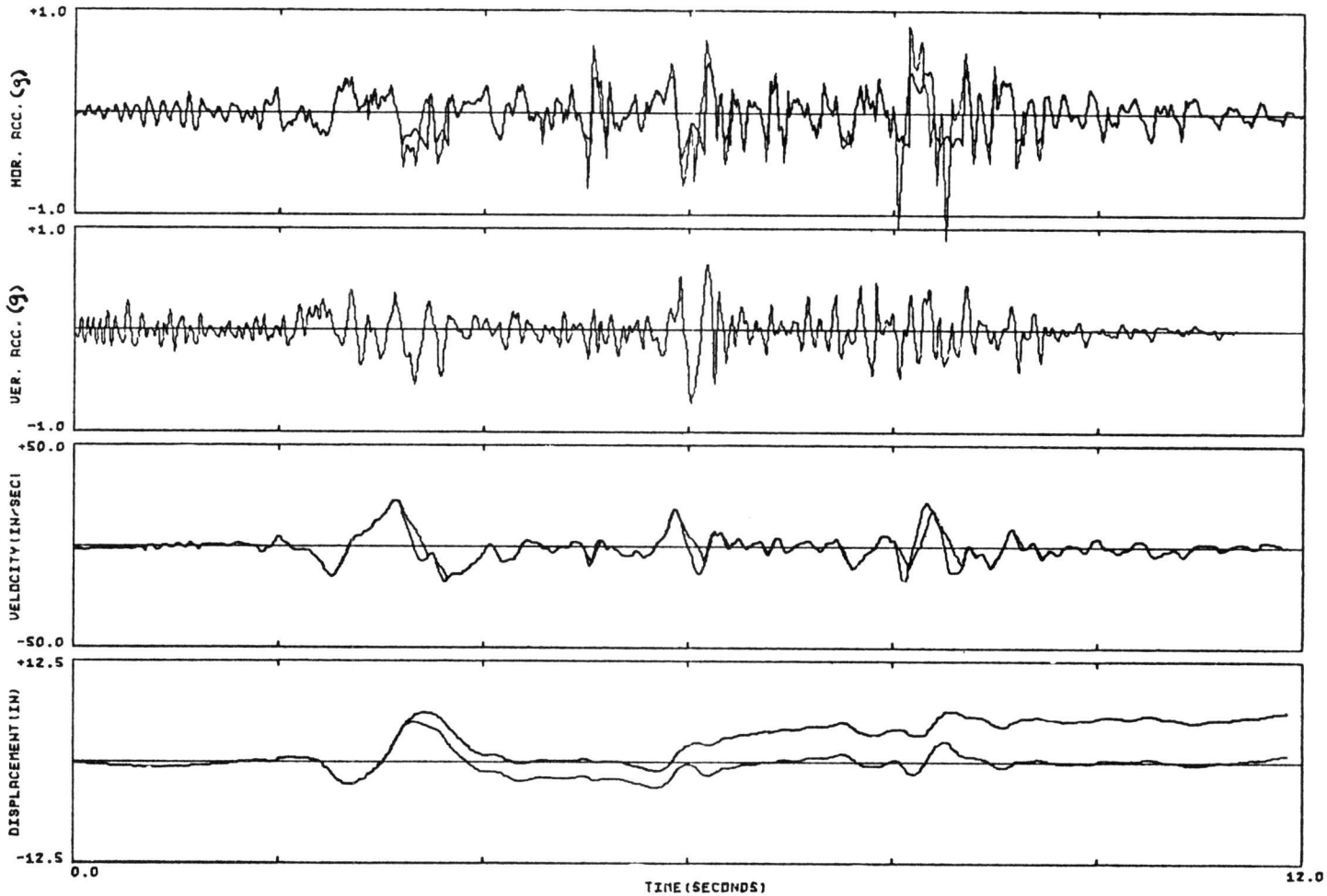

FIG. 4-12. MOTION OF A SHIELDING BLOCK SUBJECTED TO SAN-FERNANDO EARTHQUAKE 1971(PACOIMA DAM RECORD S74W)U=.30,K=.000W/IN

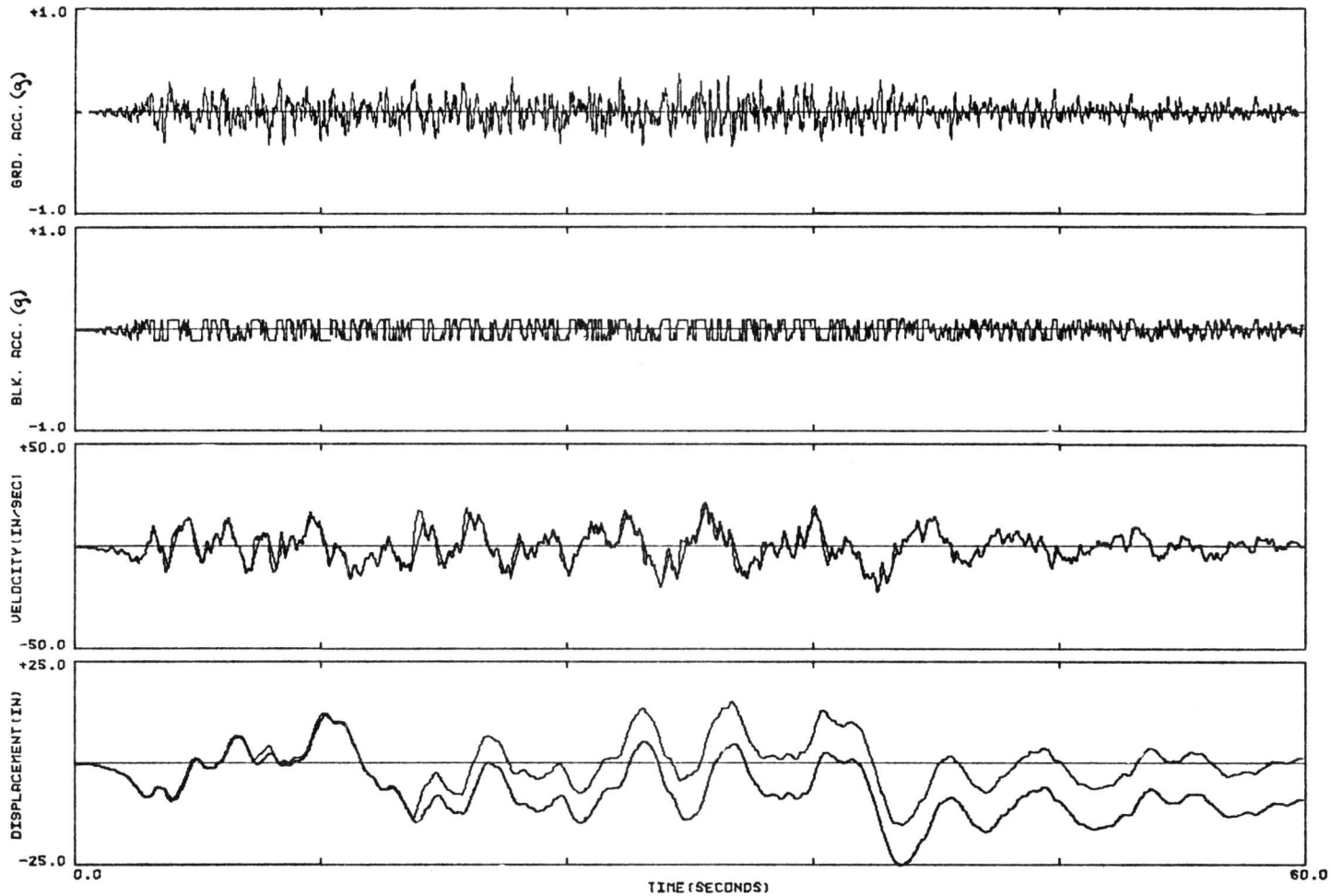

FIG. 4-13. MOTION OF A SHIELDING BLOCK SUBJECTED TO THE ARTIFICIAL EARTHQUAKE A-1, U=.10,K=.000W/IN

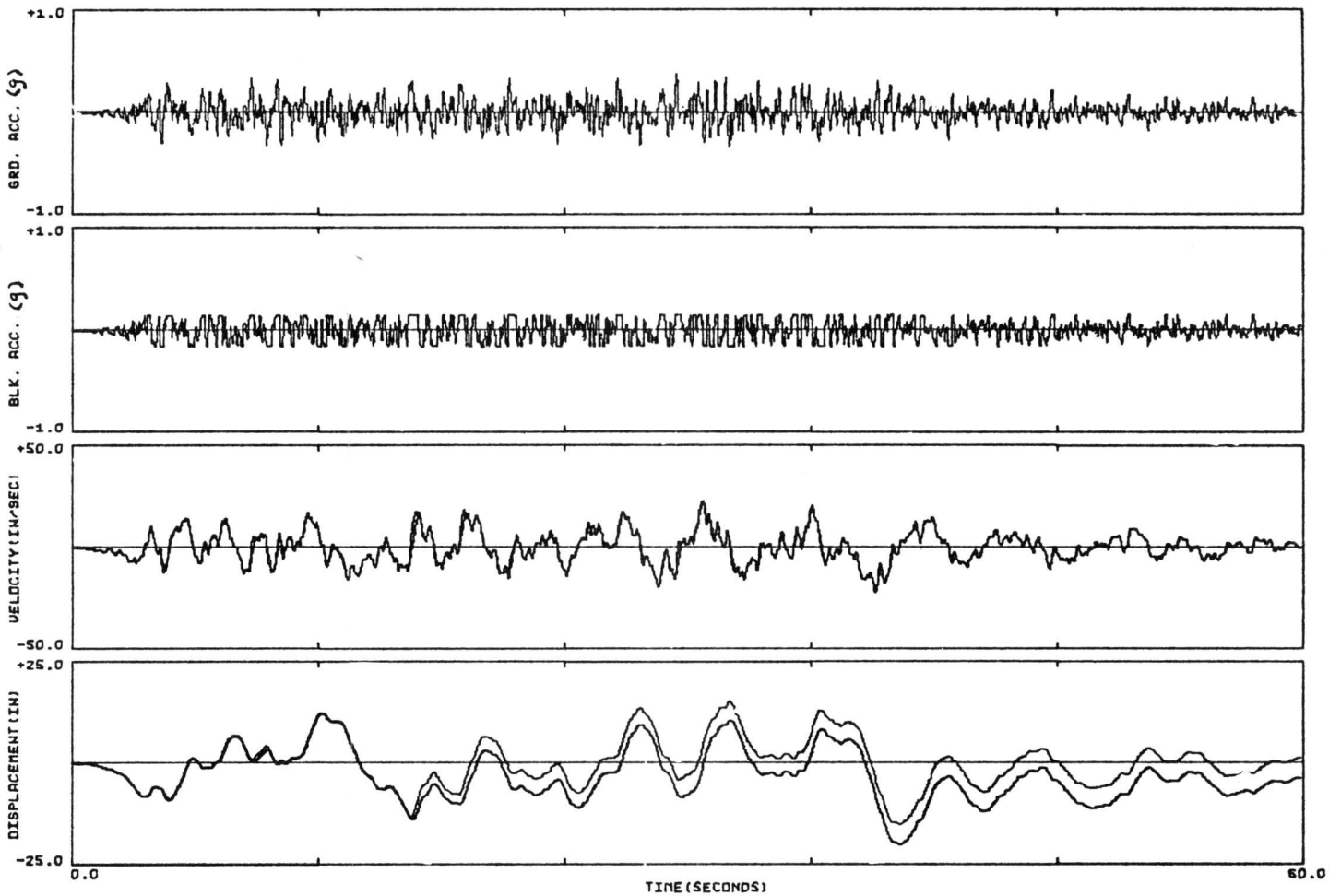

FIG. 4-14. MOTION OF A SHIELDING BLOCK SUBJECTED TO THE ARTIFICIAL EARTHQUAKE A-1, U=.15,K=.000W/IN

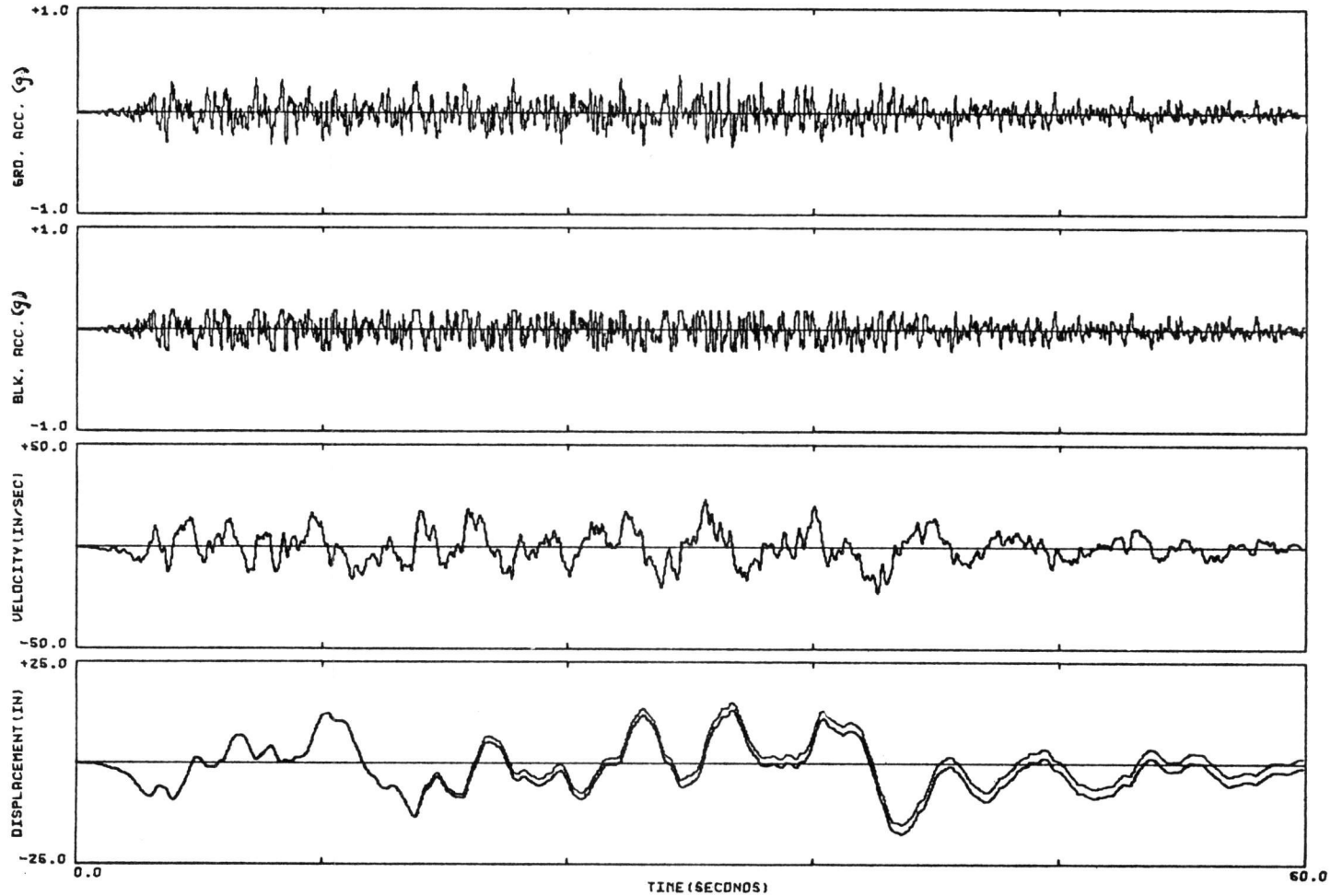

FIG. 4-15. MOTION OF A SHIELDING BLOCK SUBJECTED TO THE ARTIFICIAL EARTHQUAKE A-1, U=.20, K=.000W/IN

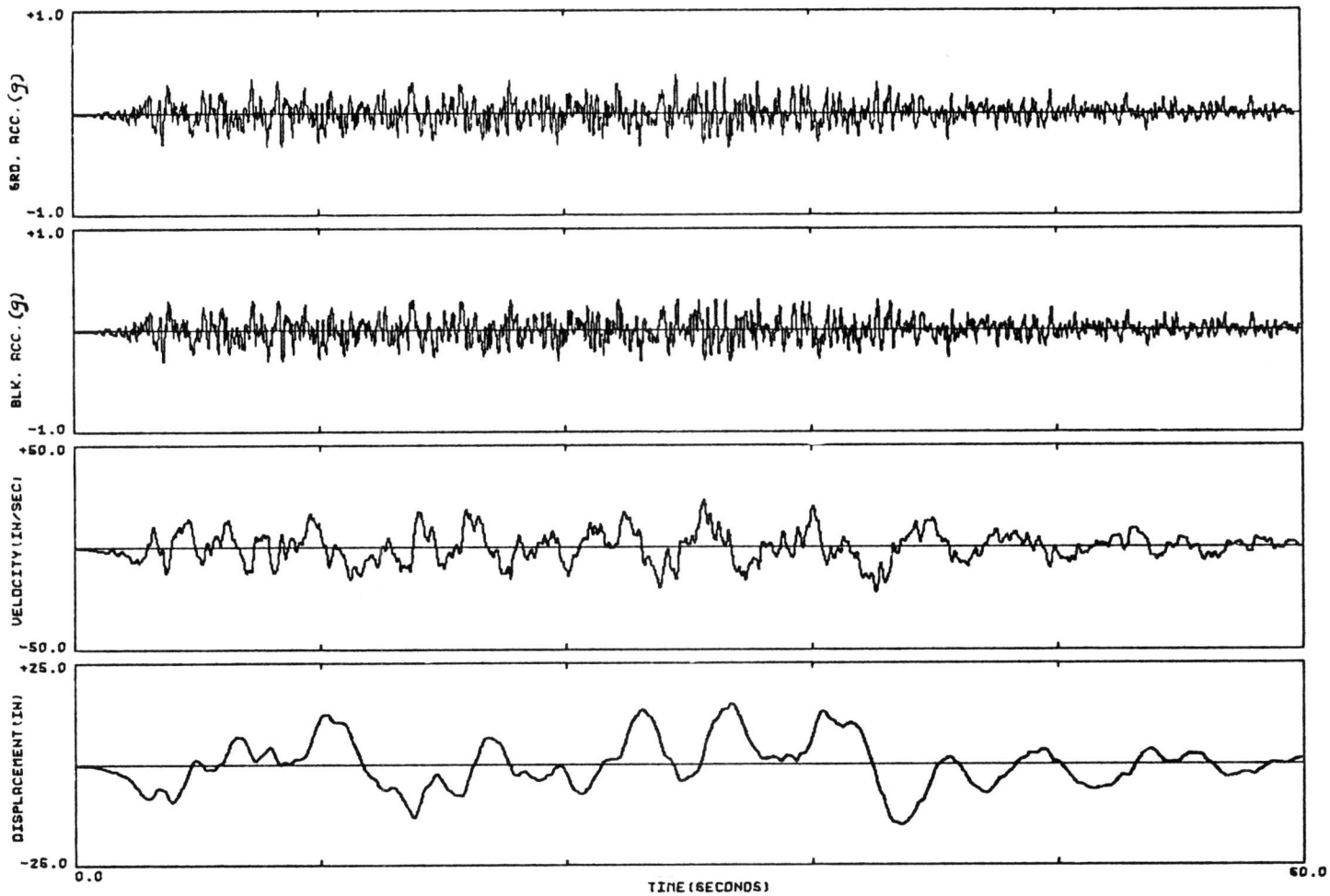

FIG. 4-16. MOTION OF A SHIELDING BLOCK SUBJECTED TO THE ARTIFICIAL EARTHQUAKE A-1, U=.30, K=.000W/IN

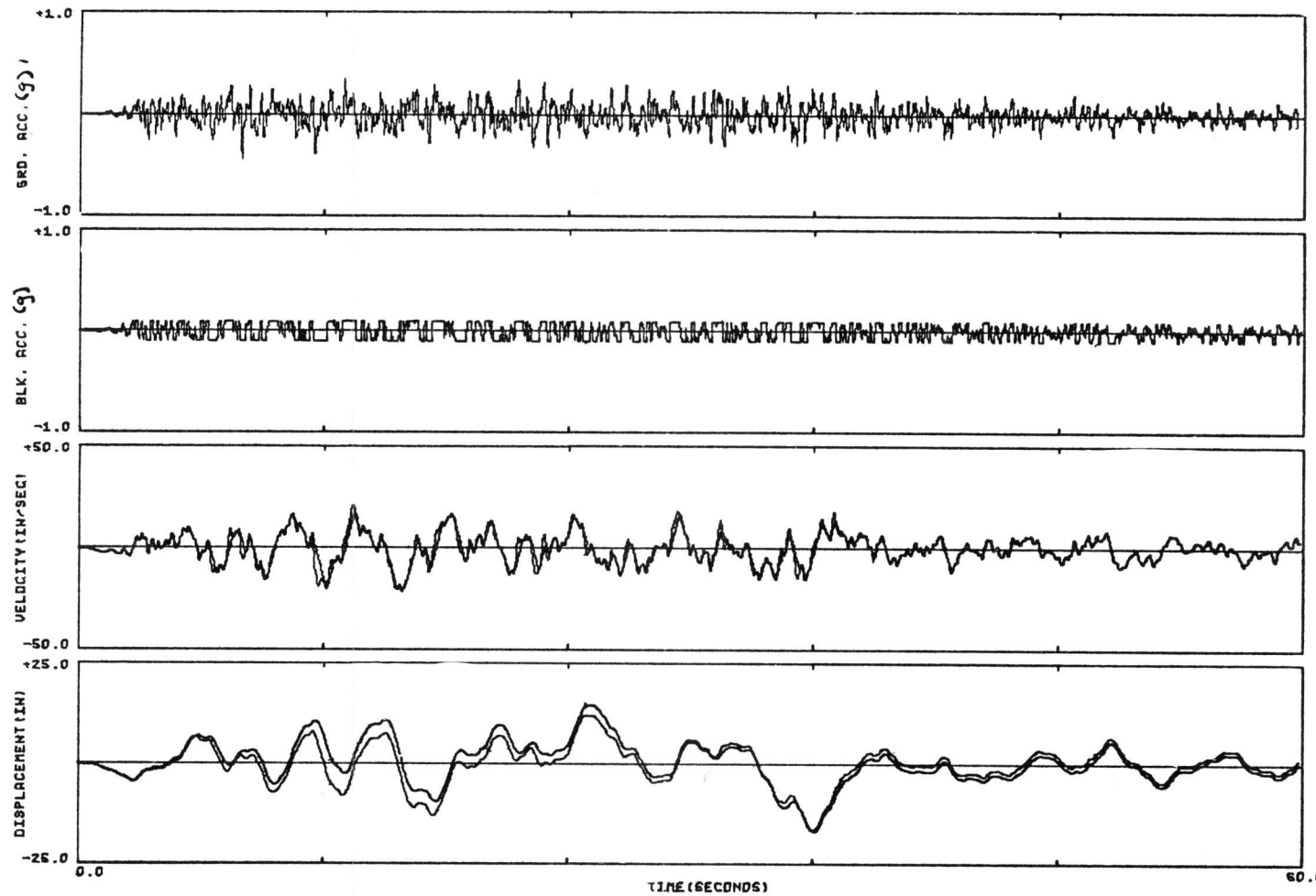

FIG. 4-17. MOTION OF A SHIELDING BLOCK SUBJECTED TO THE ARTIFICIAL EARTHQUAKE A-2, U=.10, K=.000W/IN

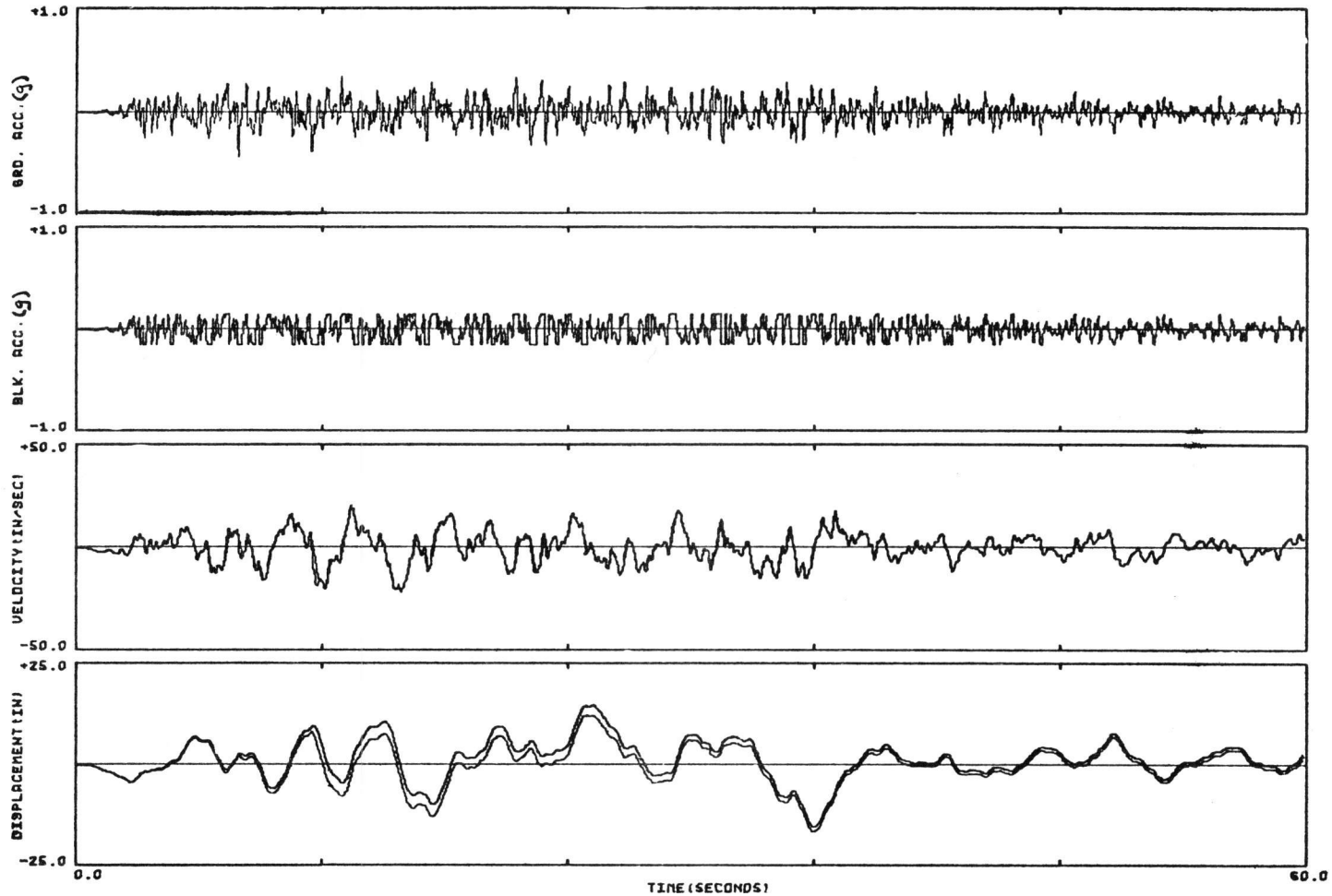

FIG. 4-18. MOTION OF A SHIELDING BLOCK SUBJECTED TO THE ARTIFICIAL EARTHQUAKE A-2, U=.15,K=.000W/IN

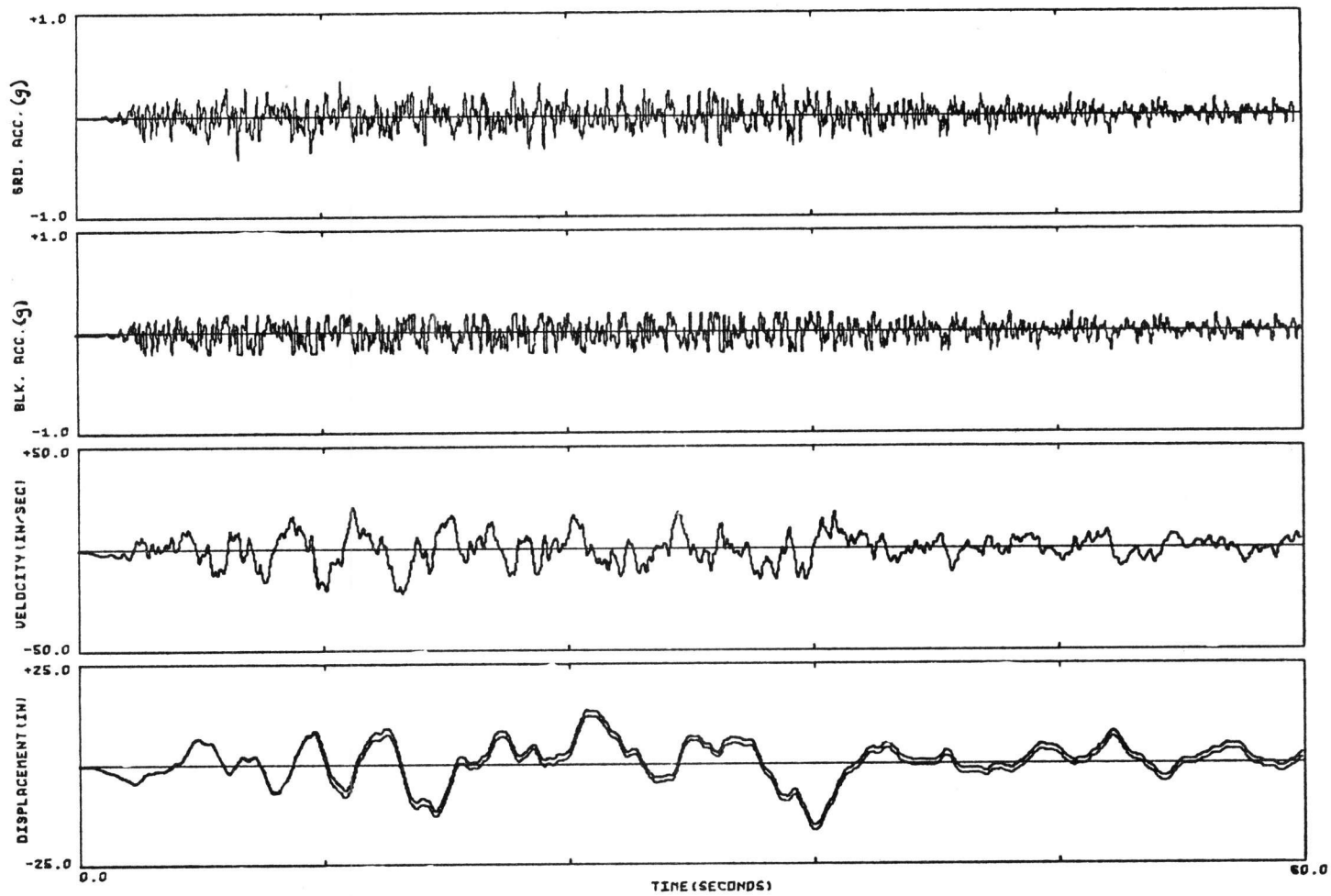

FIG. 4-19. MOTION OF A SHIELDING BLOCK SUBJECTED TO THE ARTIFICIAL EARTHQUAKE A-2, U=.20,K=.000W/IN

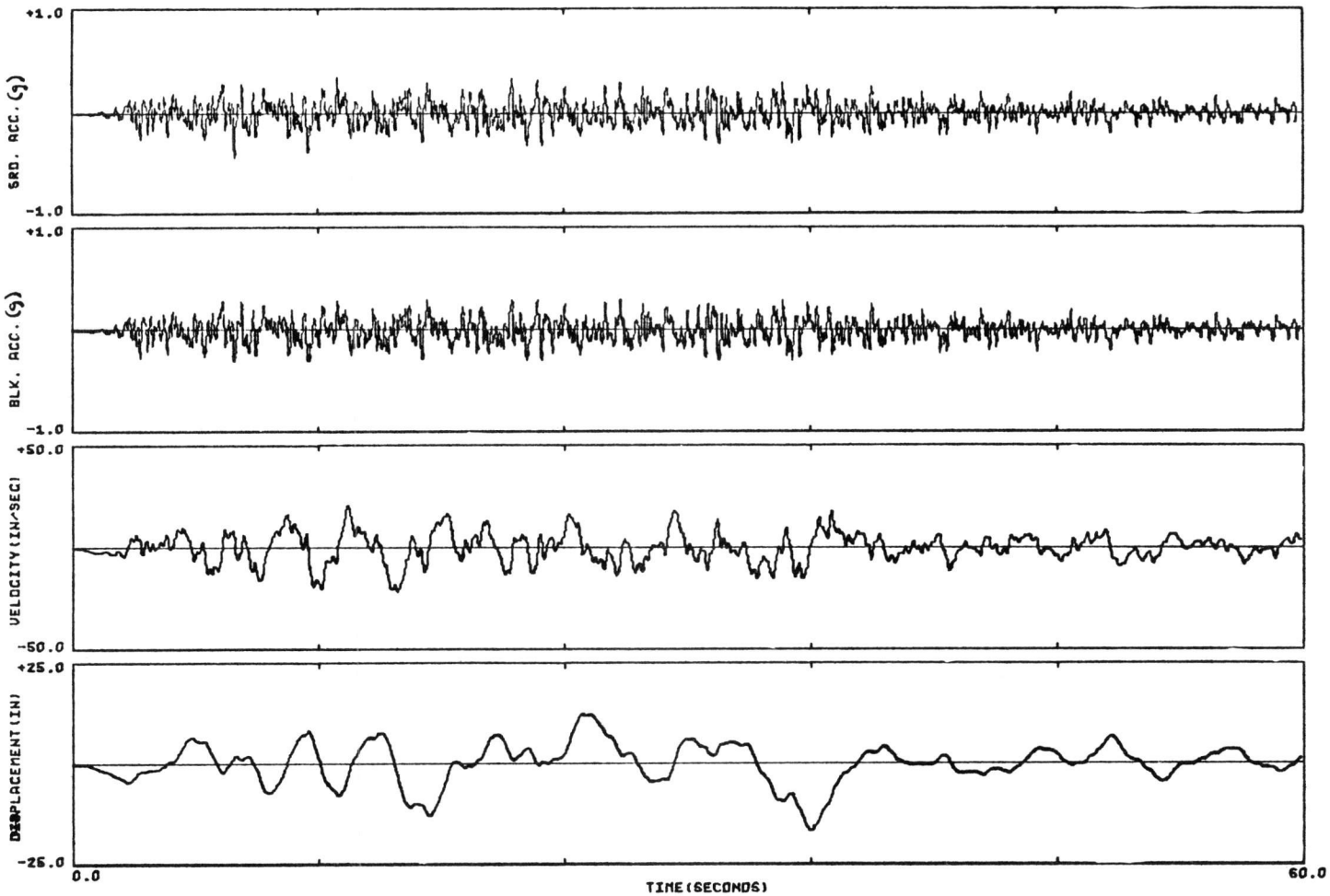

FIG. 4-20. MOTION OF A SHIELDING BLOCK SUBJECTED TO THE ARTIFICIAL EARTHQUAKE A-2, U=.30, K=.000W/IN

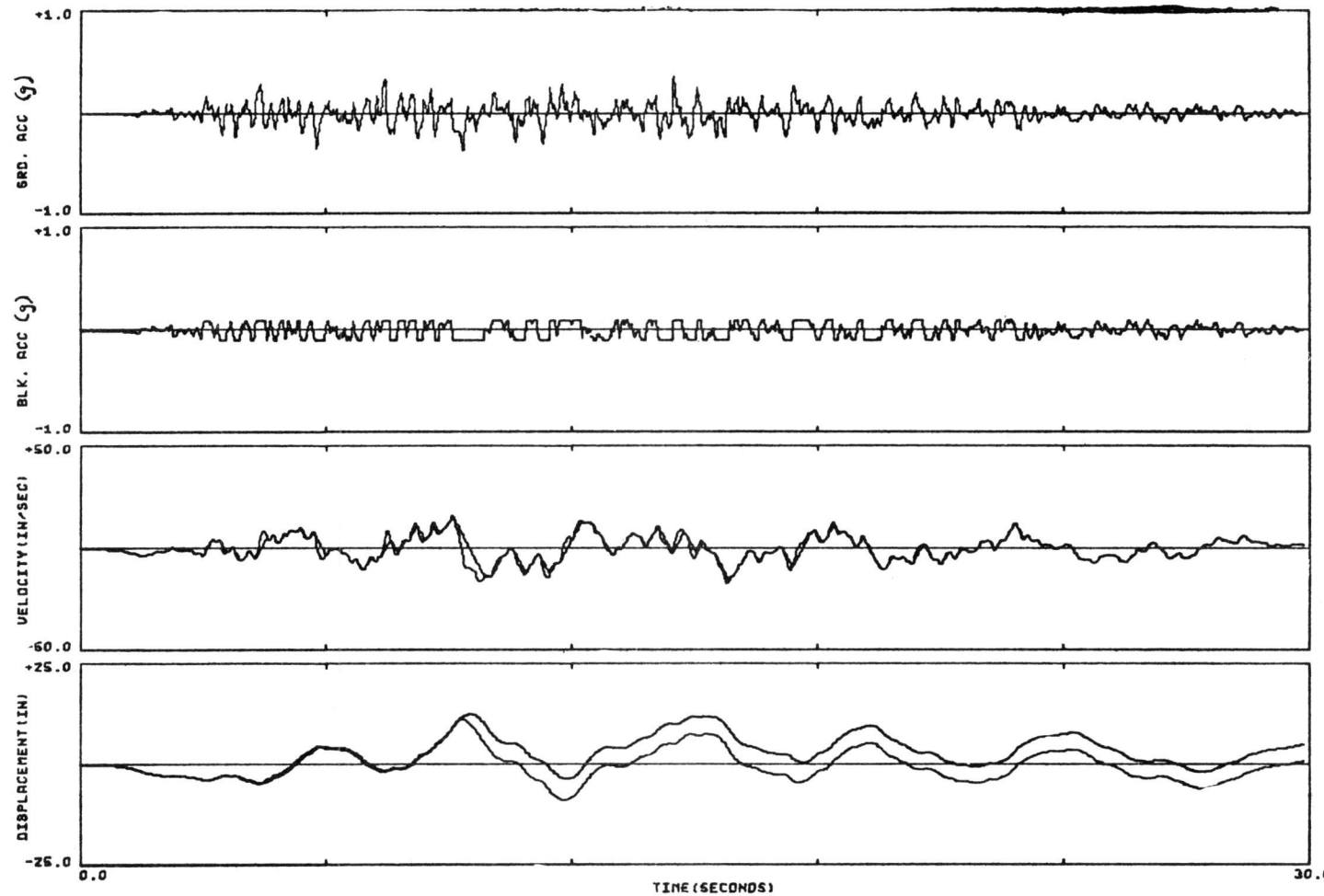

FIG. 4-21. MOTION OF A SHIELDING BLOCK SUBJECTED TO THE ARTIFICIAL EARTHQUAKE B-1, U=.10,K=.000W/IN

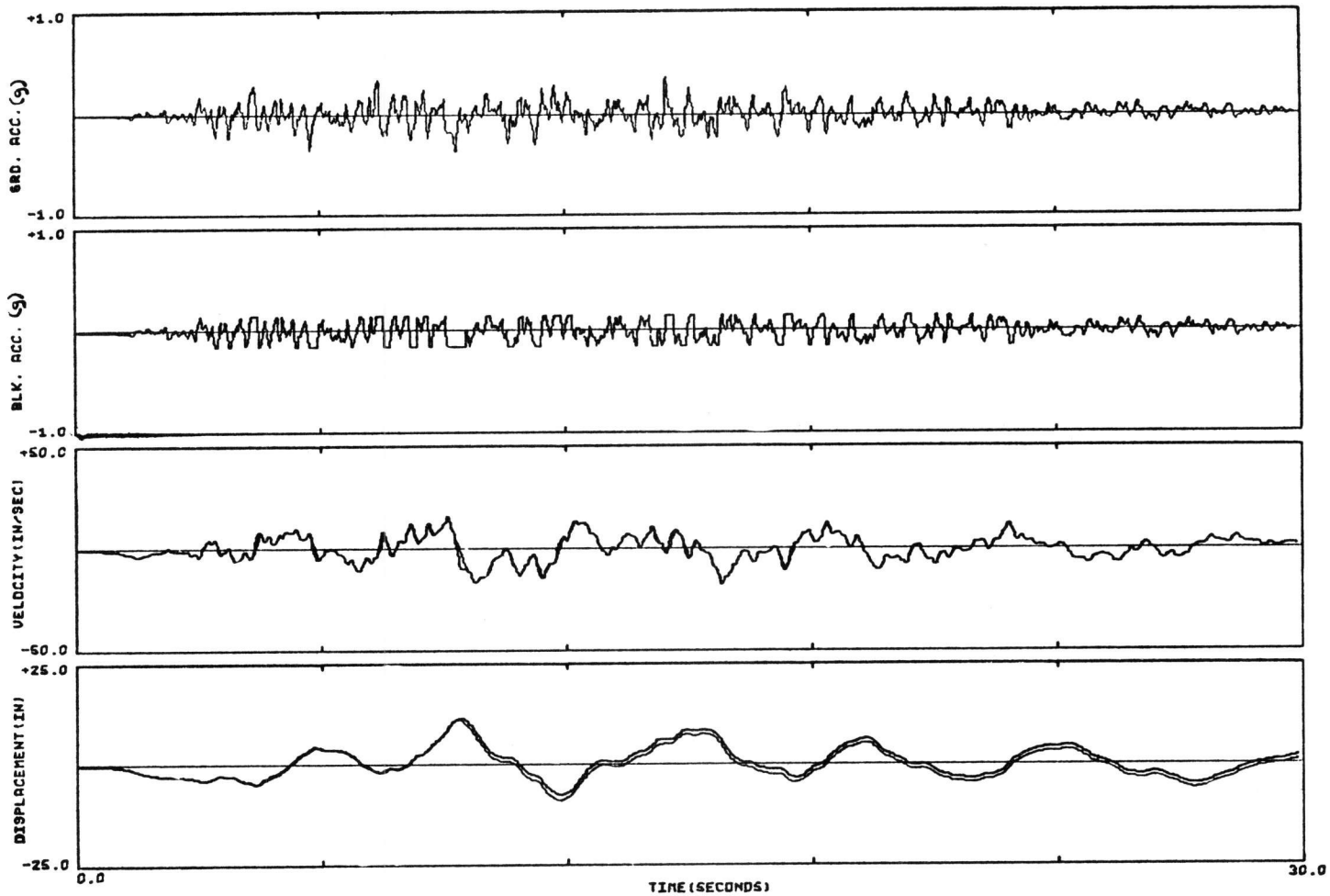

FIG. 4-22. MOTION OF A SHIELDING BLOCK SUBJECTED TO THE ARTIFICIAL EARTHQUAKE B-1, U=.15,K=.000W/IN

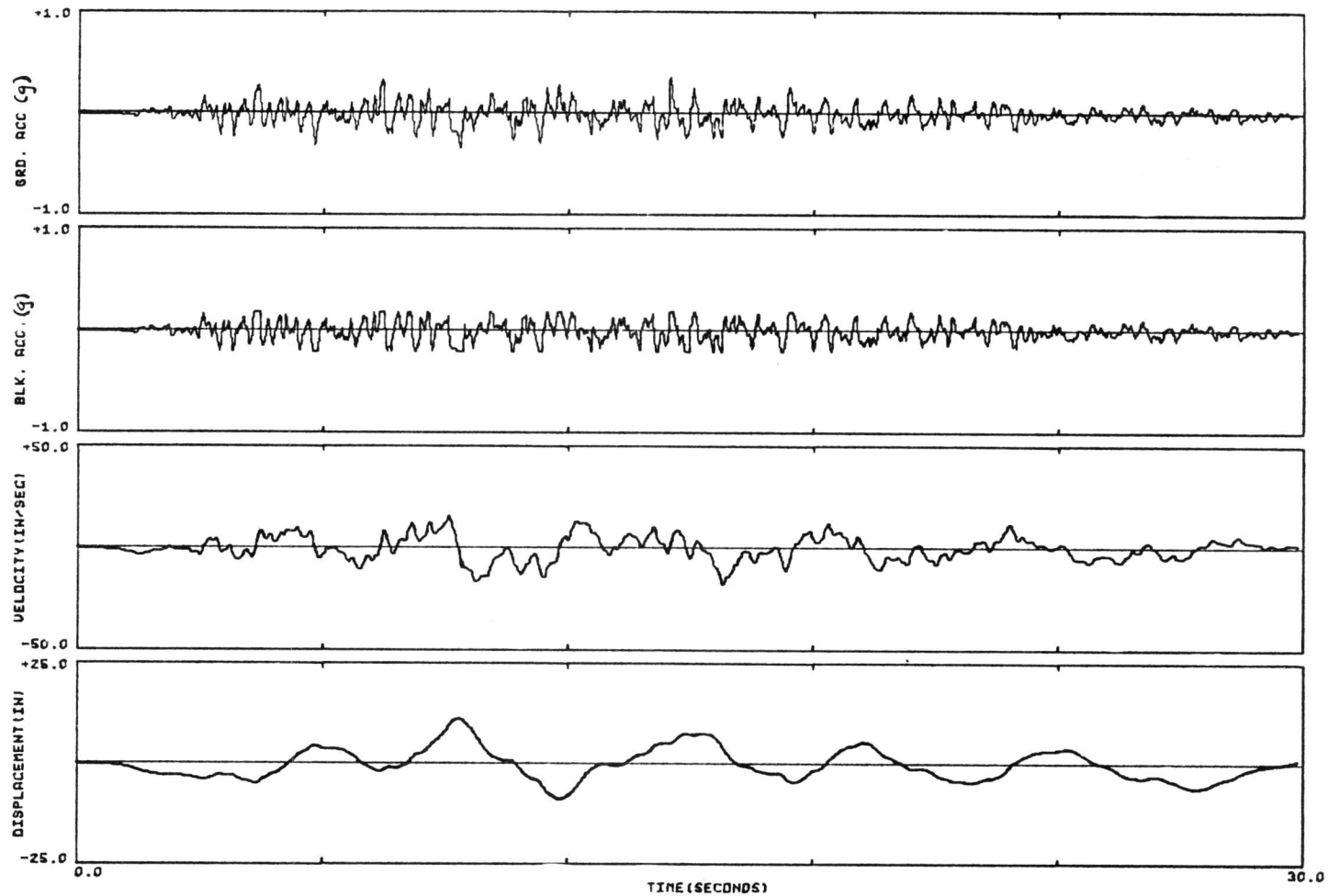

FIG. 4-23. MOTION OF A SHIELDING BLOCK SUBJECTED TO THE ARTIFICIAL EARTHQUAKE B-1, U=.20,K=.000W/IN

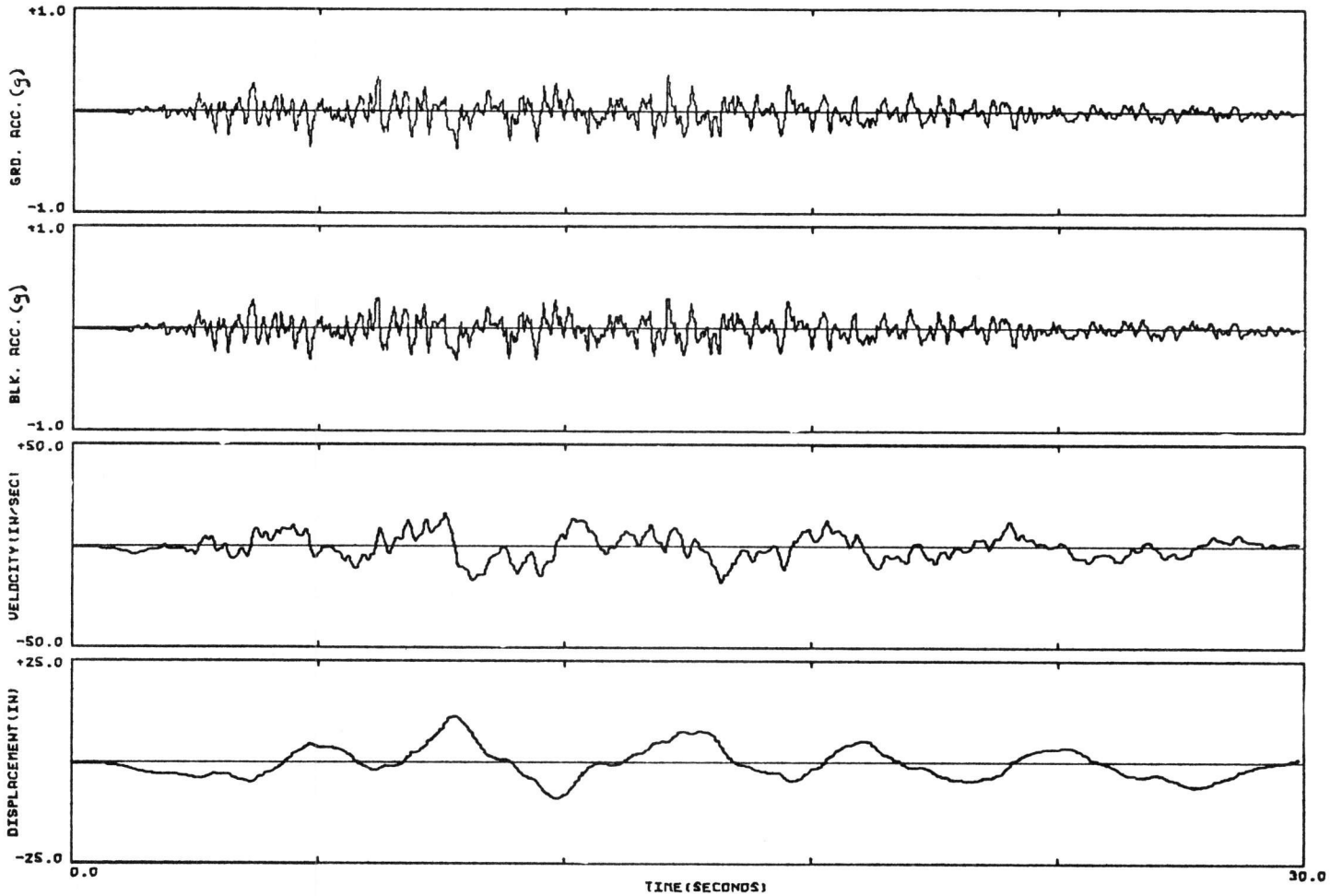

FIG. 4-24. MOTION OF A SHIELDING BLOCK SUBJECTED TO THE ARTIFICIAL EARTHQUAKE B-1, U=.30,K=.000W/IN

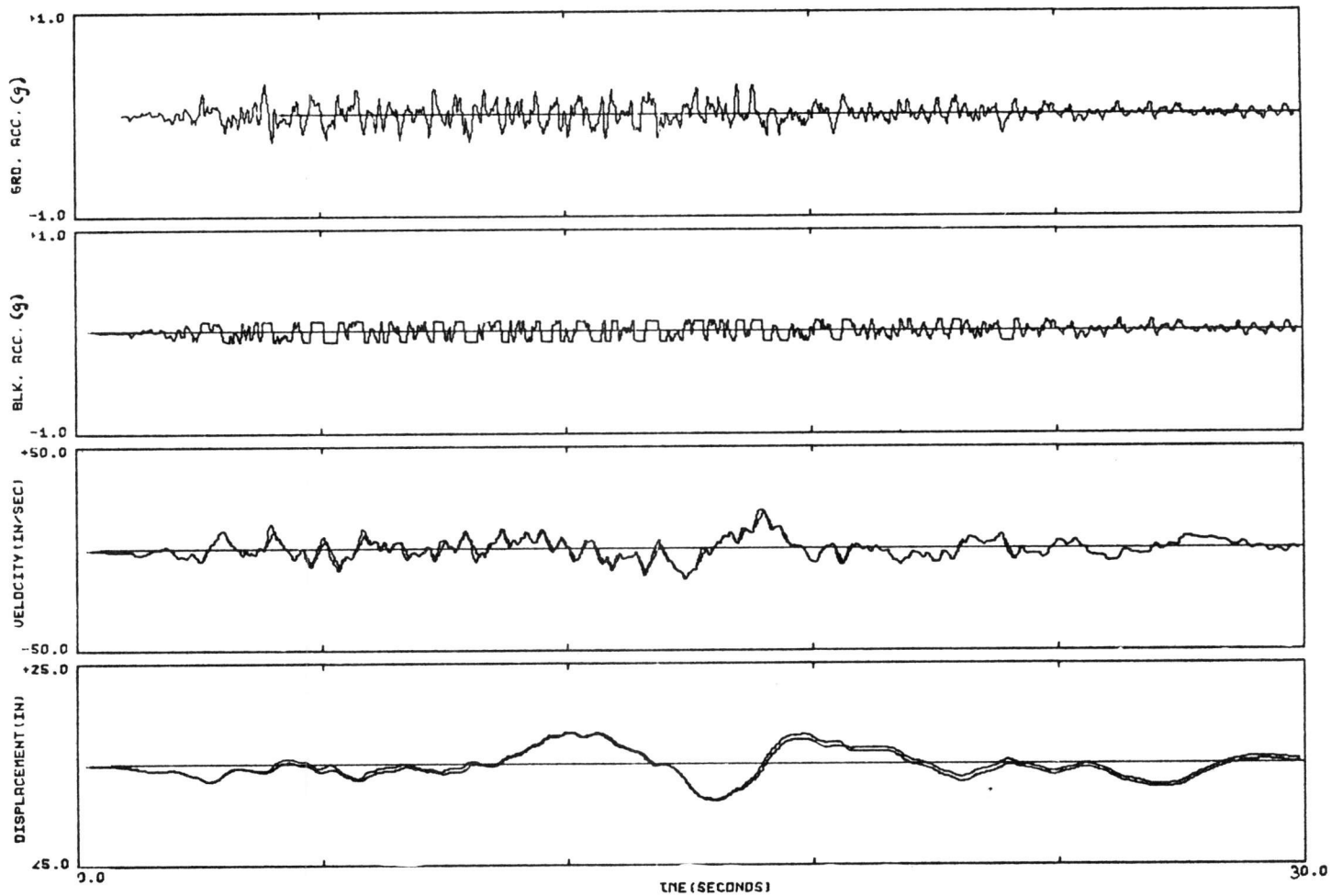

FIG. 4-25. MOTION OF A SHIELDING BLOCK SUBJECTED TO THE ARTIFICIAL EARTHQUAKE B-2, U=.10,K=.000W/IN

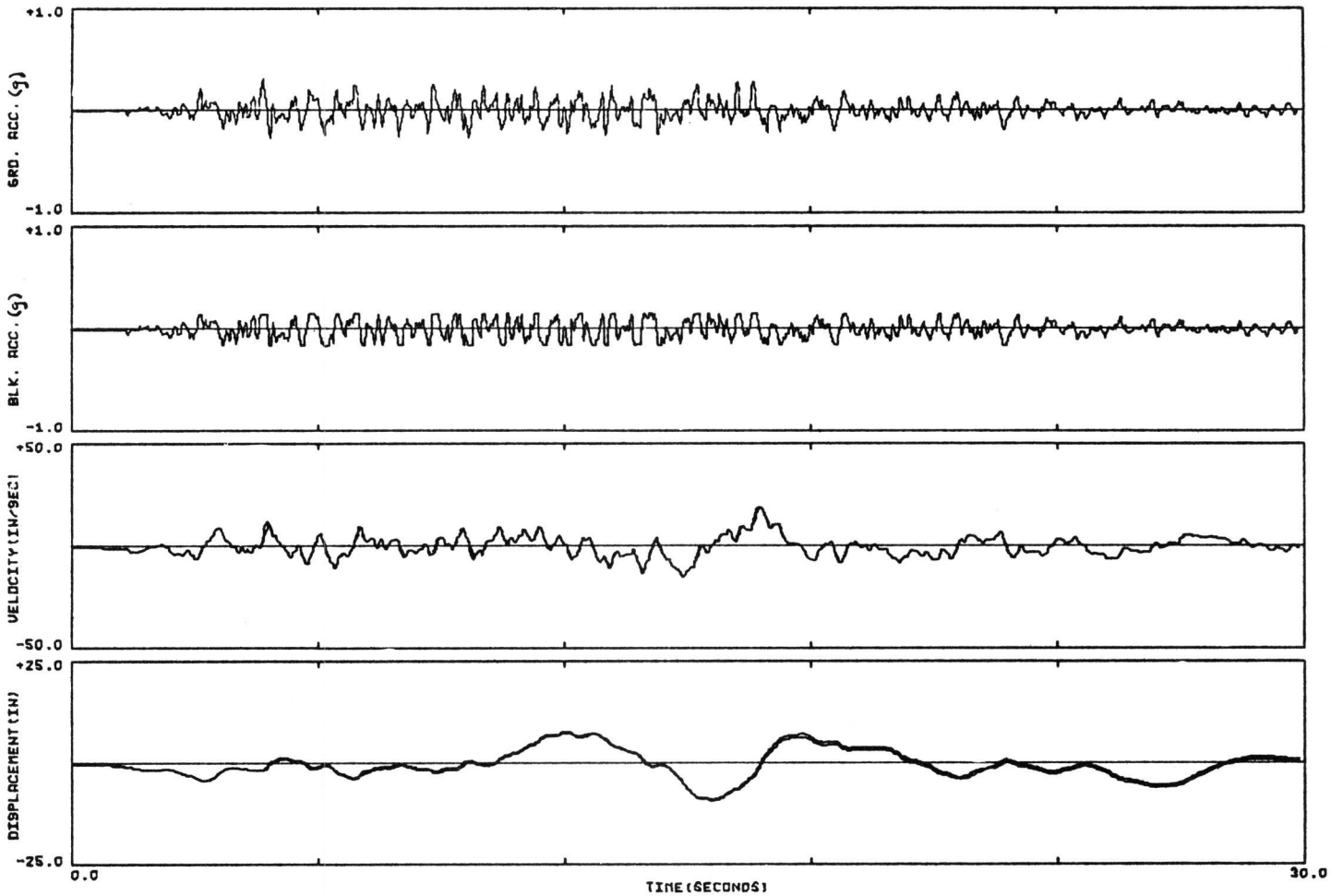

FIG. 4-26. MOTION OF A SHIELDING BLOCK SUBJECTED TO THE ARTIFICIAL EARTHQUAKE B-2, U=.15,K=.000W/IN

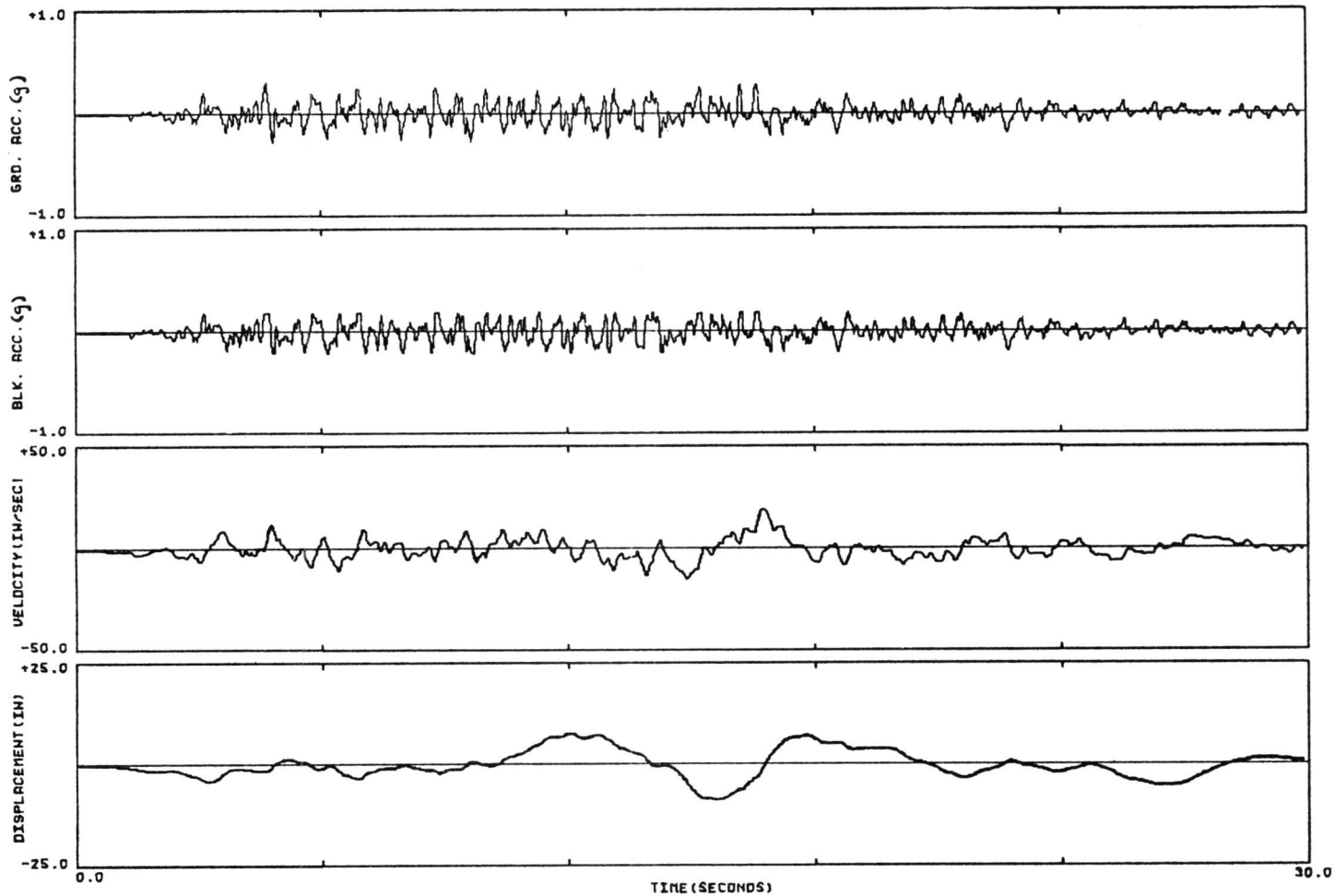

FIG. 4-27. MOTION OF A SHIELDING BLOCK SUBJECTED TO THE ARTIFICIAL EARTHQUAKE B-2, U=.20,K=.000W/IN

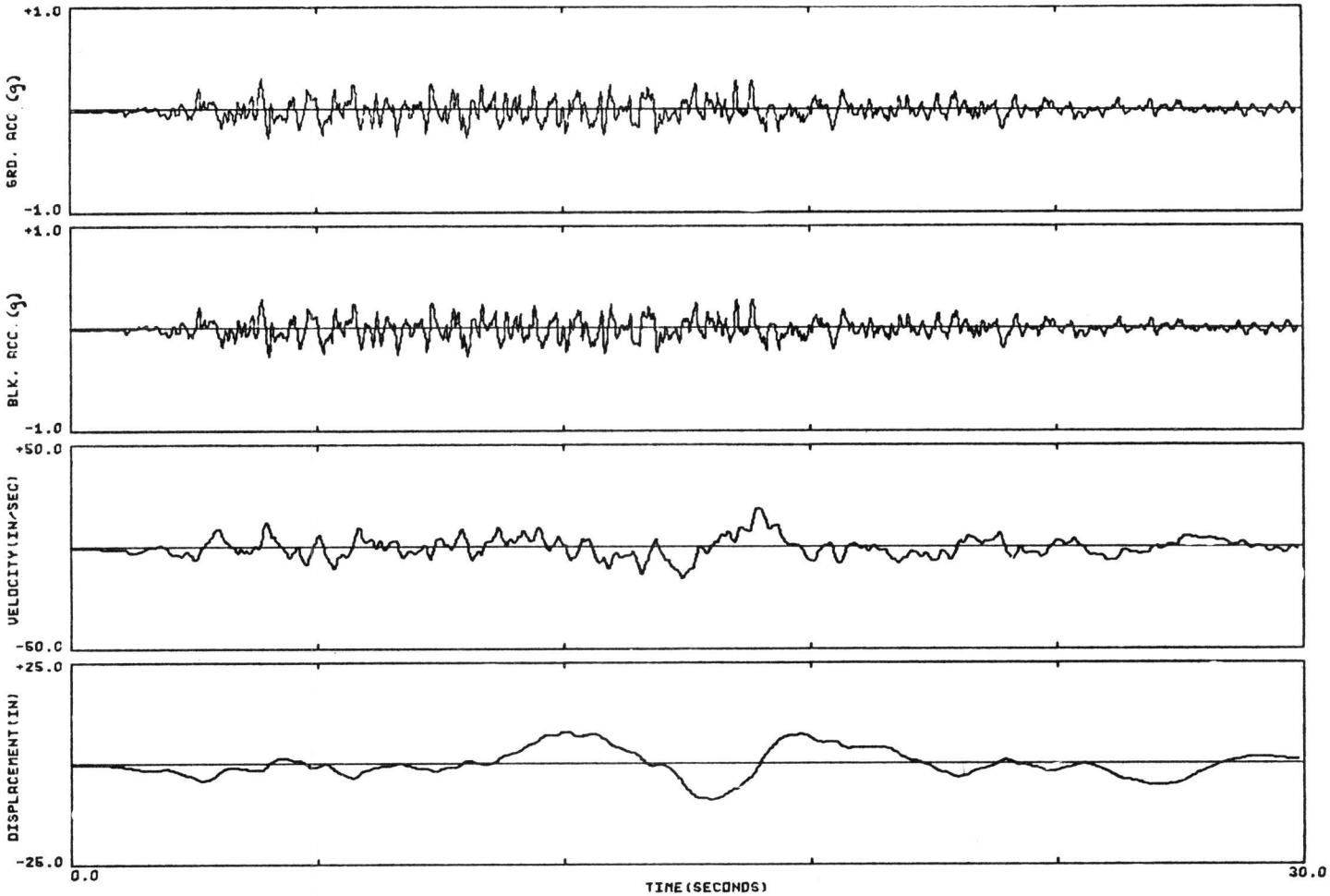

FIG. 4-28. MOTION OF A SHIELDING BLOCK SUBJECTED TO THE ARTIFICIAL EARTHQUAKE B-2, U=.30, K=.000W/IN

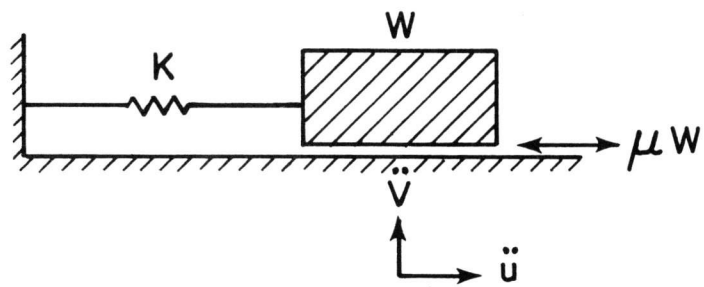

FIG. 4-29. SINGLE DEGREE OF FREEDOM SYSTEM WITH COULOMB DAMPING.

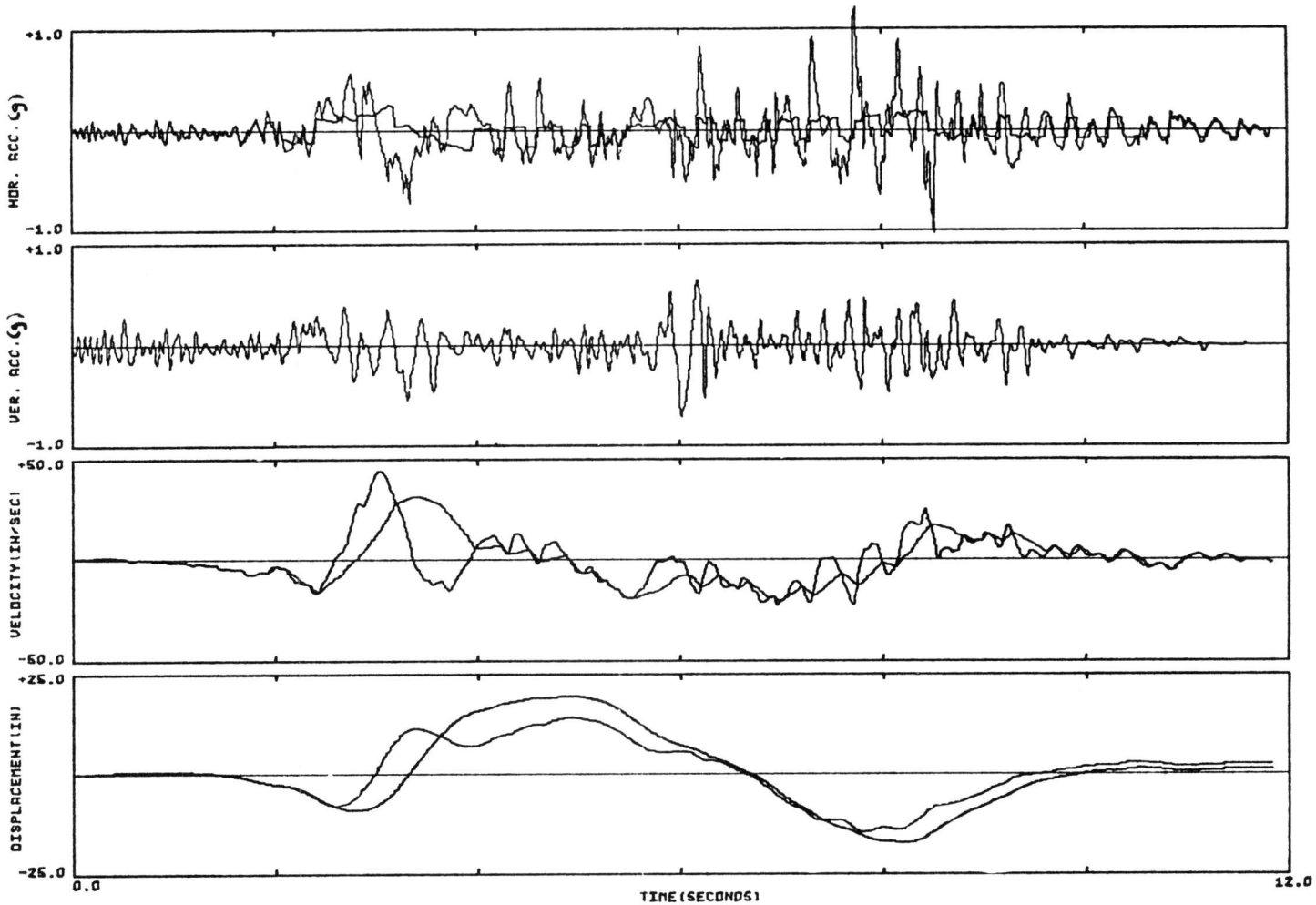

FIG. 4-30. MOTION OF A SHIELDING BLOCK SUBJECTED TO SAN-FERNANDO EARTHQUAKE 1971(PACOIMA DAM RECORD S16E)U=.10,K=.010W/IN

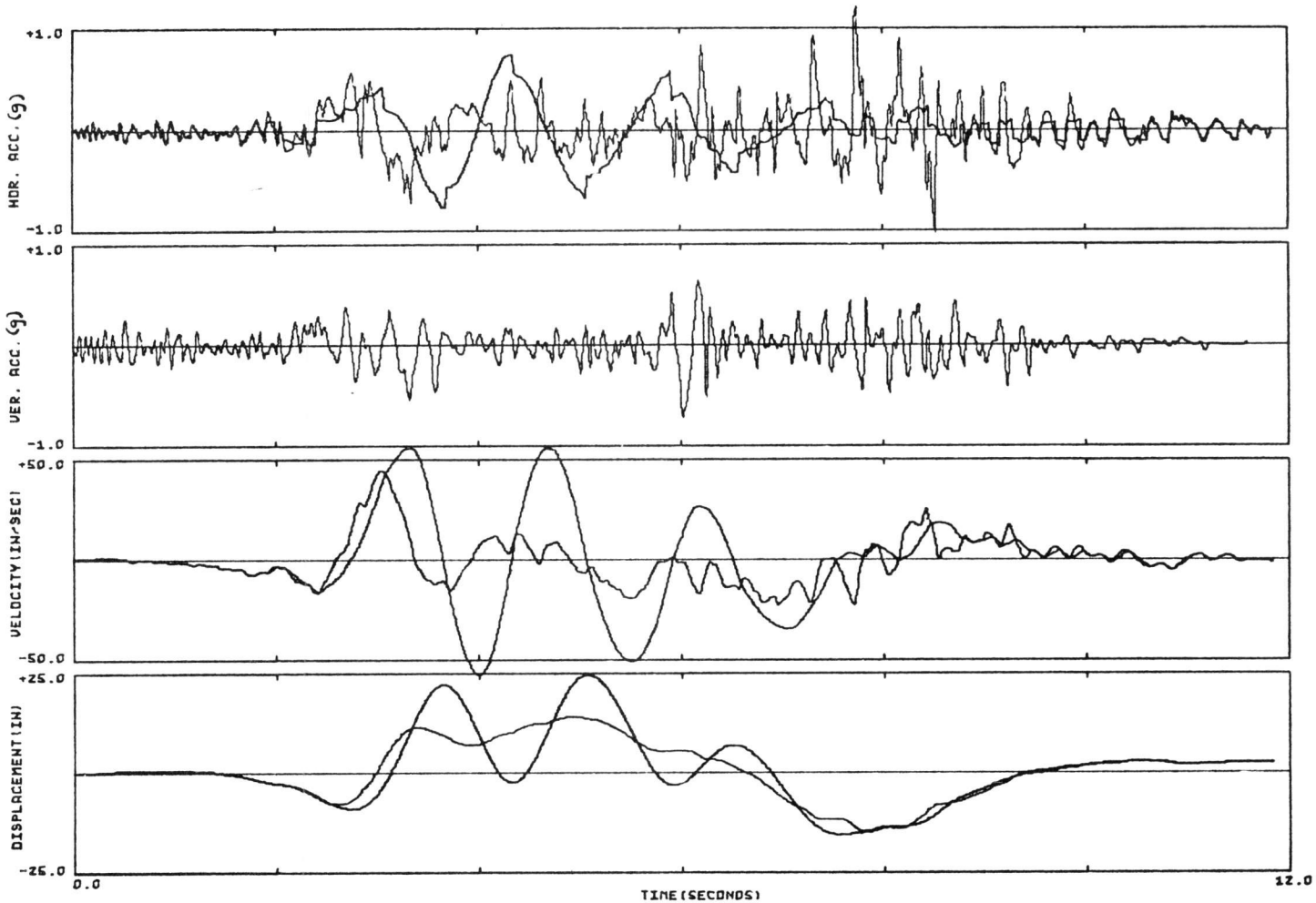

FIG. 4-31. MOTION OF A SHIELDING BLOCK SUBJECTED TO SAN-FERNANDO EARTHQUAKE 1971(PACOIMA DAM RECORD S16E)U=.10,K=.050W/IN

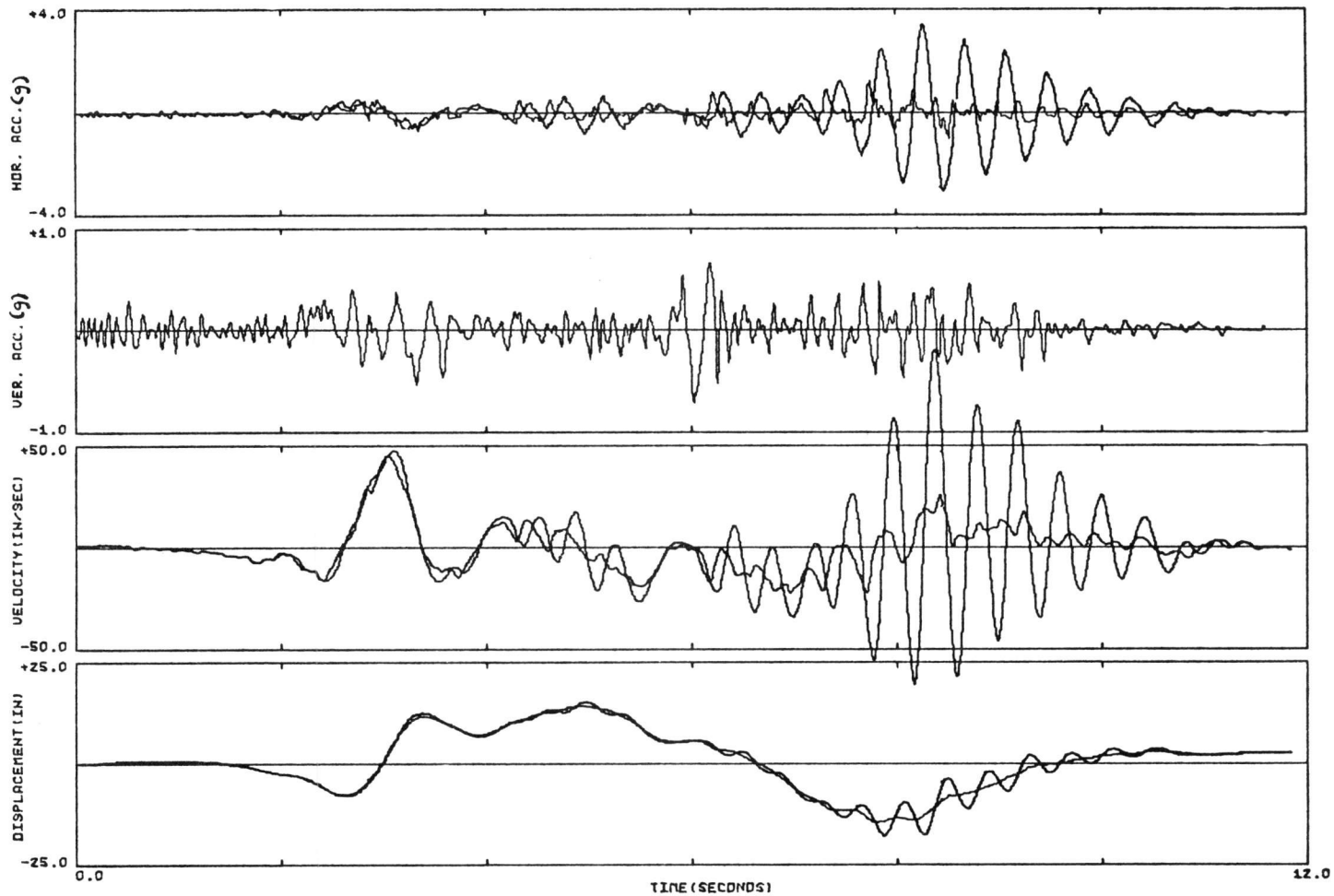

FIG. 4-32. MOTION OF A SHIELDING BLOCK SUBJECTED TO SAN-FERNANDO EARTHQUAKE 1971(PACOIMA DAM RECORD S16E)U=.10,K=.650W/IN

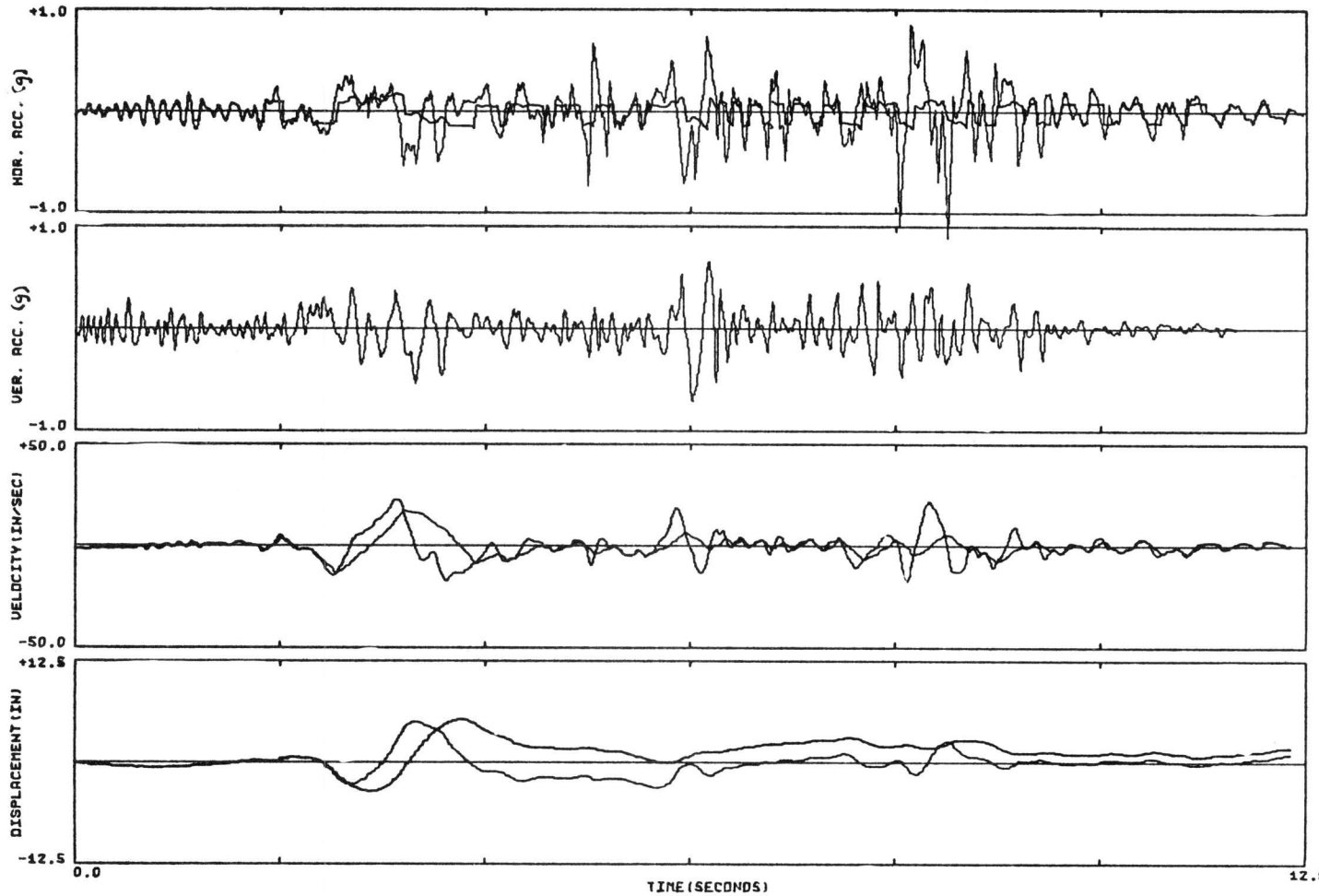

FIG. 4-33. MOTION OF A SHIELDING BLOCK SUBJECTED TO SAN-FERNANDO EARTHQUAKE 1971(PACOIMA DAM RECORD S74W)U=.10,K=.010W/IN

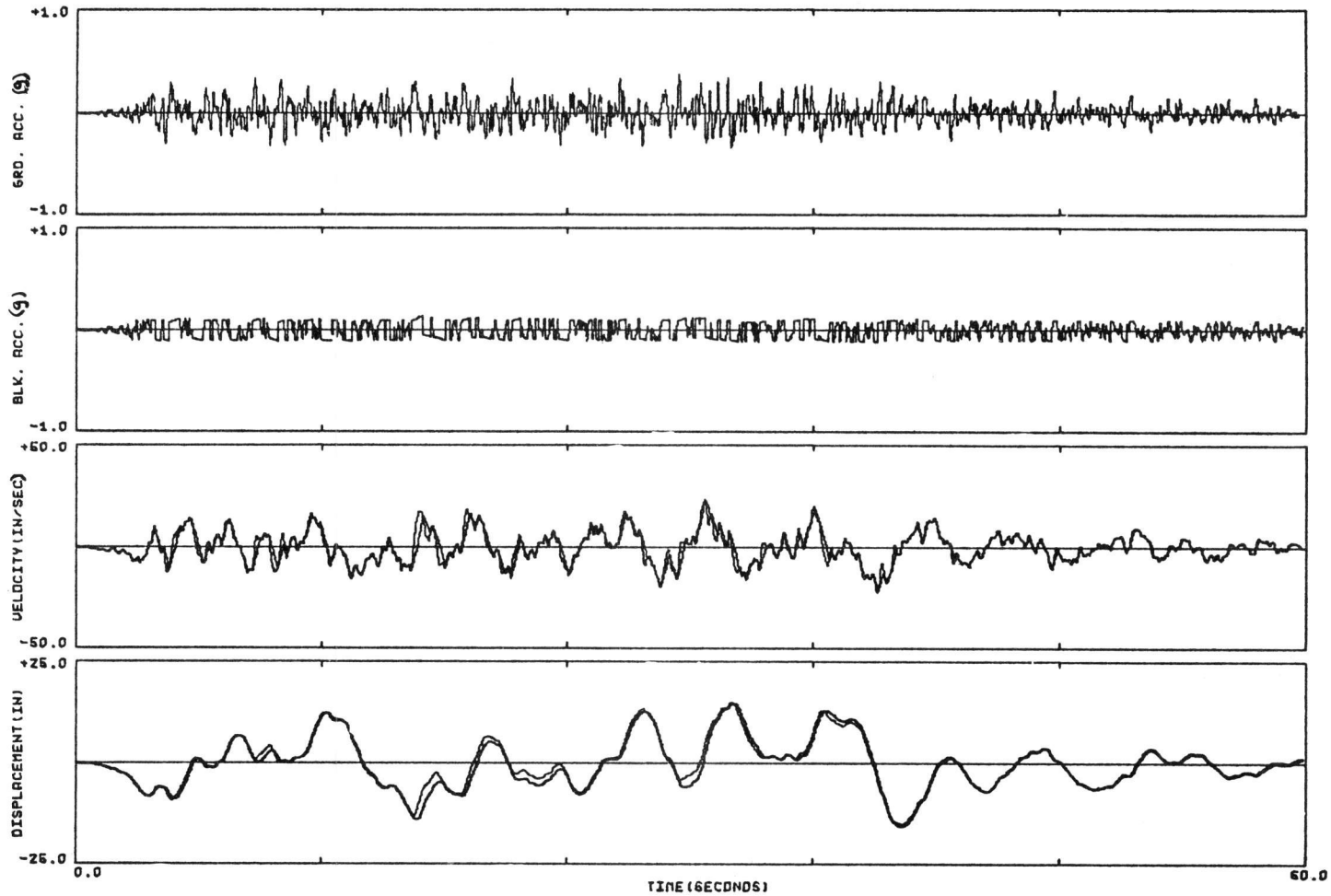

FIG. 4-34. MOTION OF A SHIELDING BLOCK SUBJECTED TO THE ARTIFICIAL EARTHQUAKE A-1, U=.10, K=.010W/IN

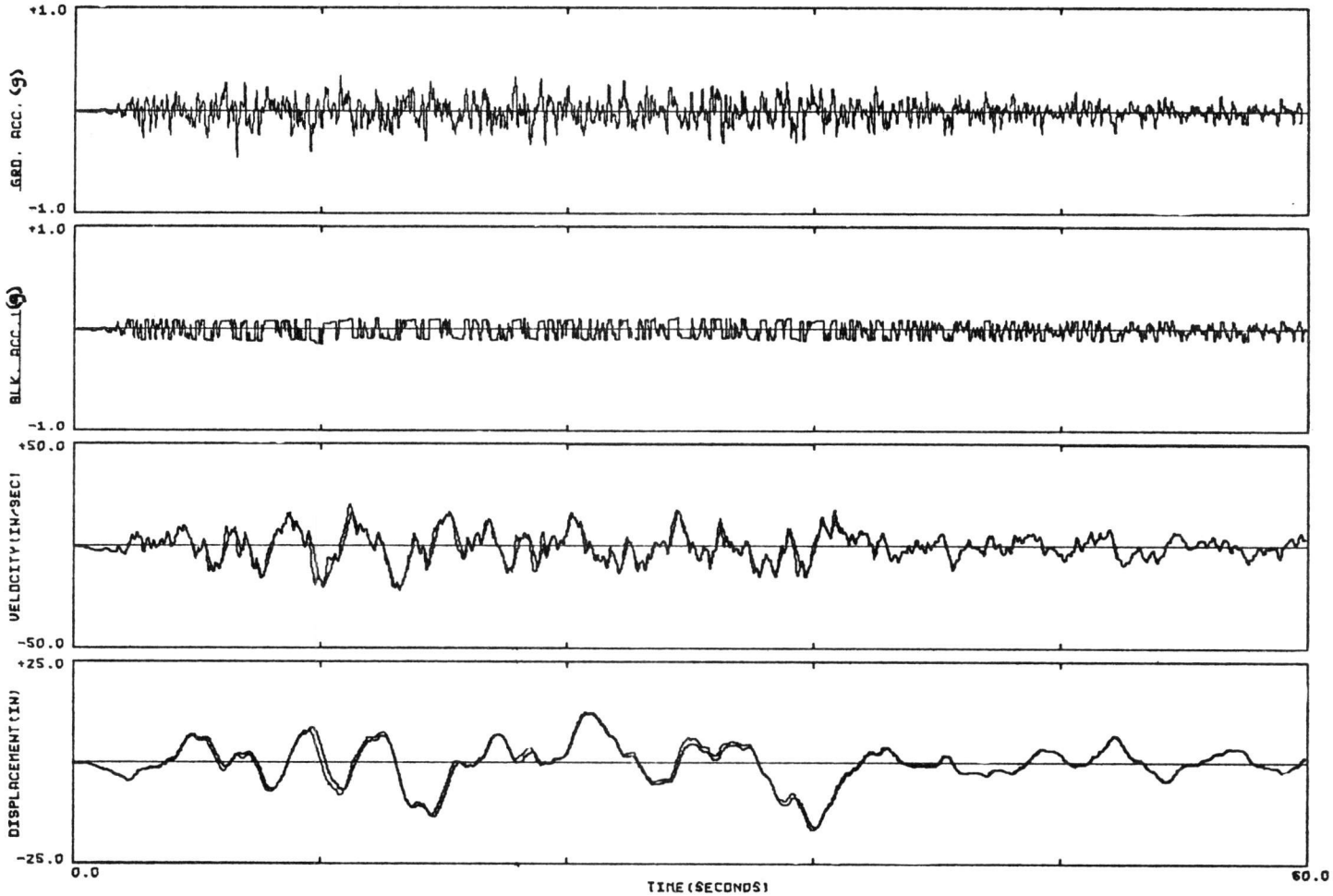

FIG. 4-35. MOTION OF A SHIELDING BLOCK SUBJECTED TO THE ARTIFICIAL EARTHQUAKE A-2, U=.10, K=.010W/IN

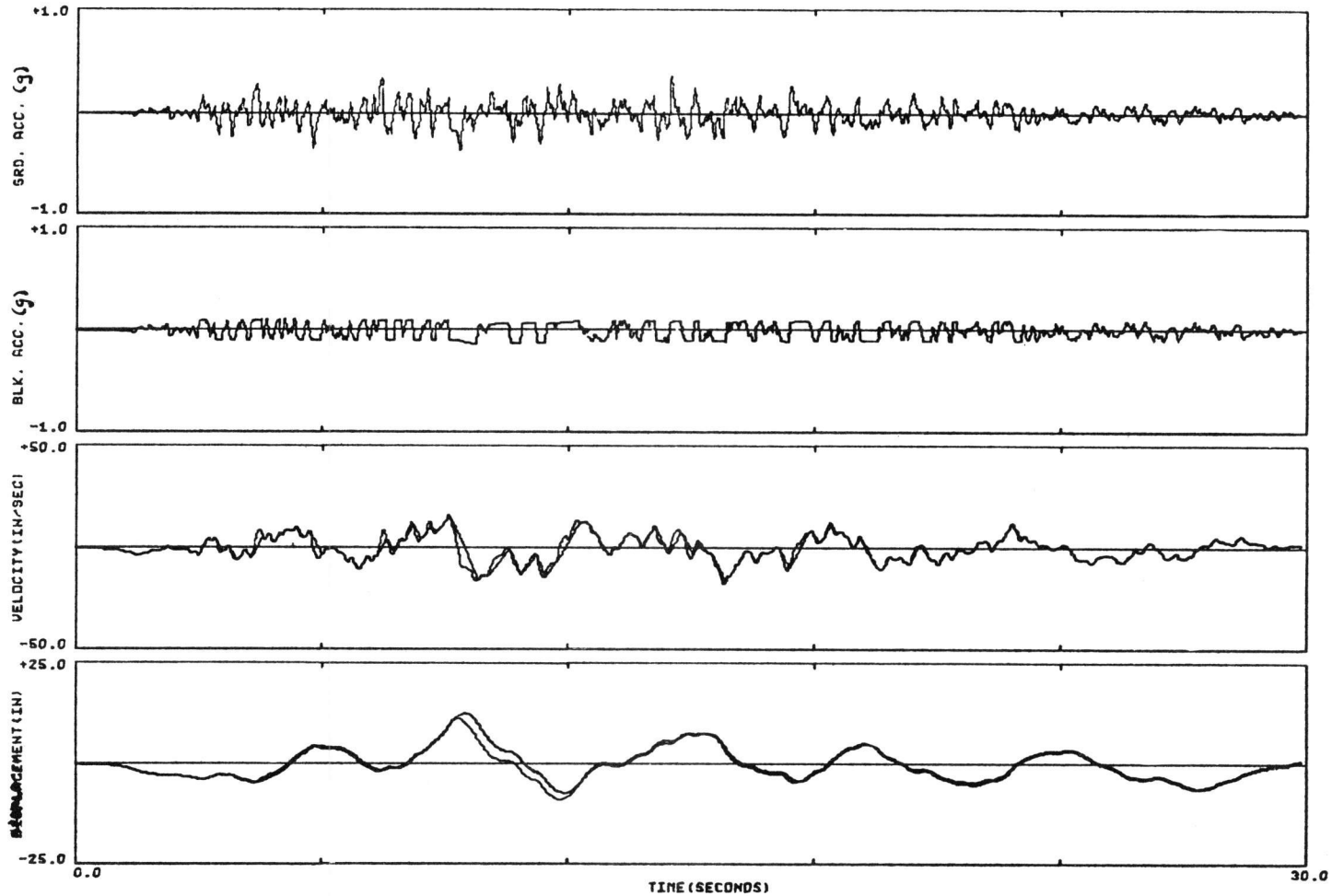

FIG. 4-36. MOTION OF A SHIELDING BLOCK SUBJECTED TO THE ARTIFICIAL EARTHQUAKE B-1, U=.10,K=.010W/IN

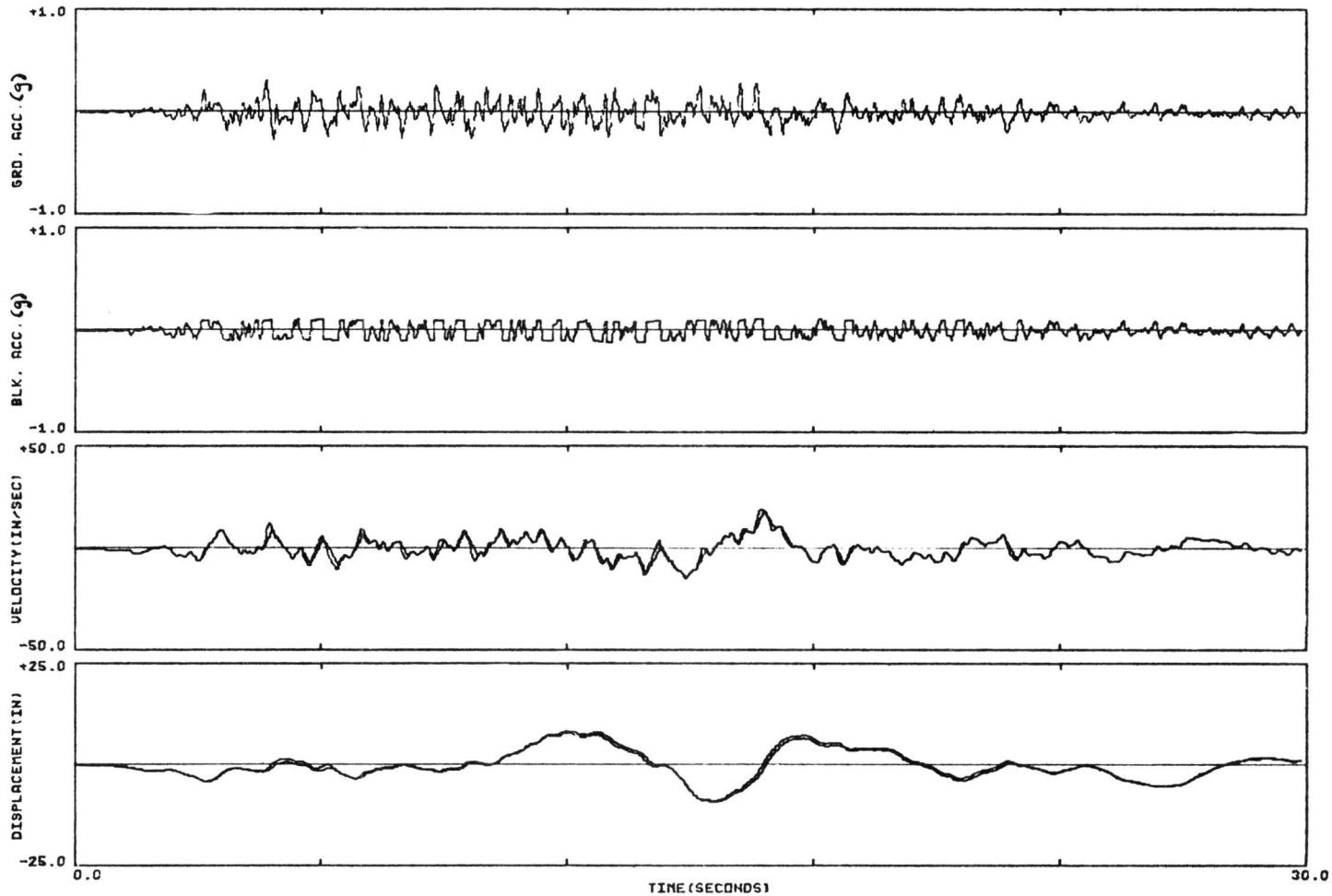

FIG. 4-37. MOTION OF A SHIELDING BLOCK SUBJECTED TO THE ARTIFICIAL EARTHQUAKE B-2, U=.10,K=.010W/IN

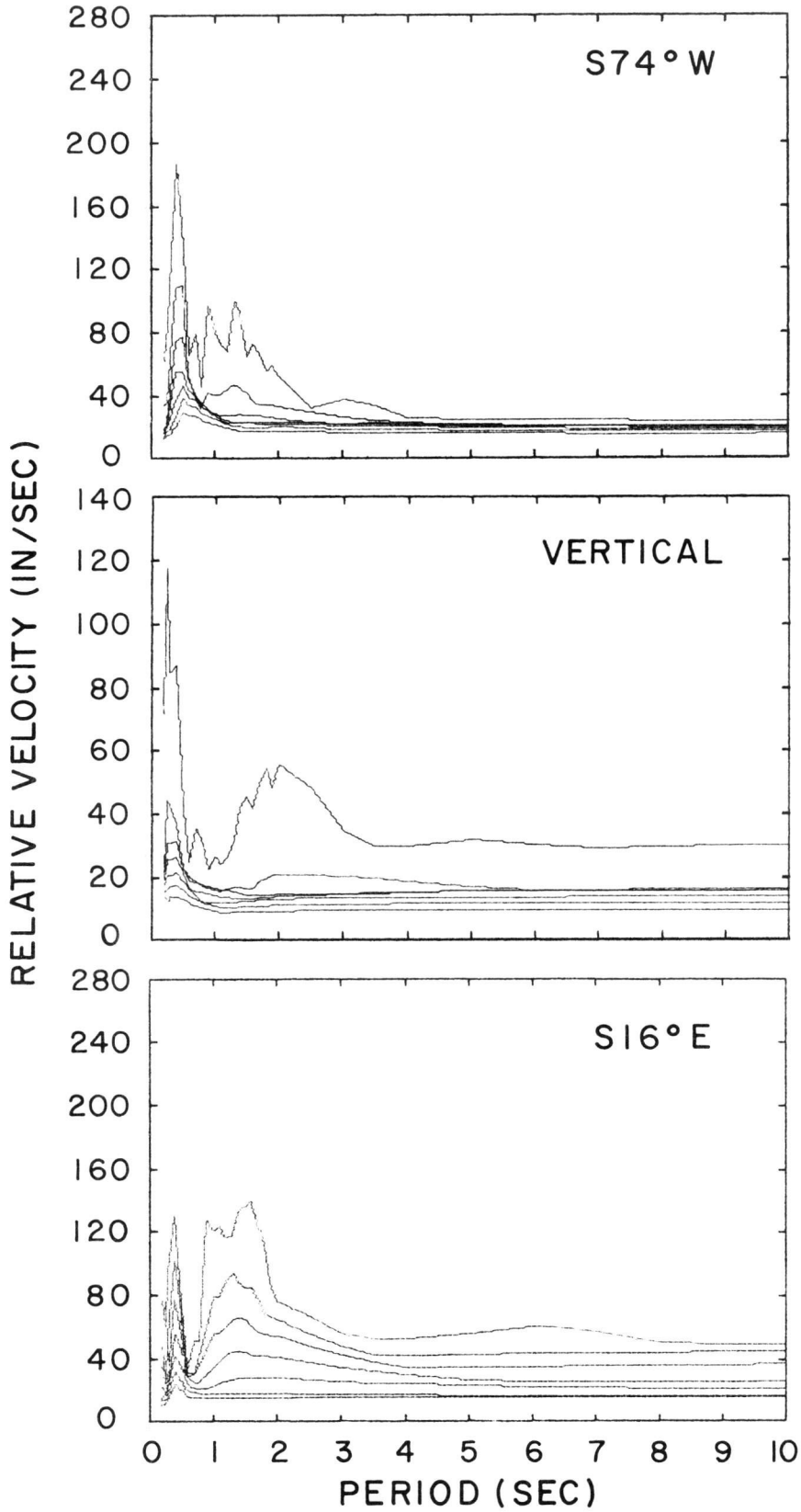

FIG. 4-38. RELATIVE VELOCITY RESPONSE SPECTRA FOR SAN FERNANDO EARTHQUAKE 1971(PACOIMA DAM). THE CURVES ARE FOR μ VALUES OF 0.0, 0.05, 0.10, 0.15, 0.20, 0.25, AND 0.30.

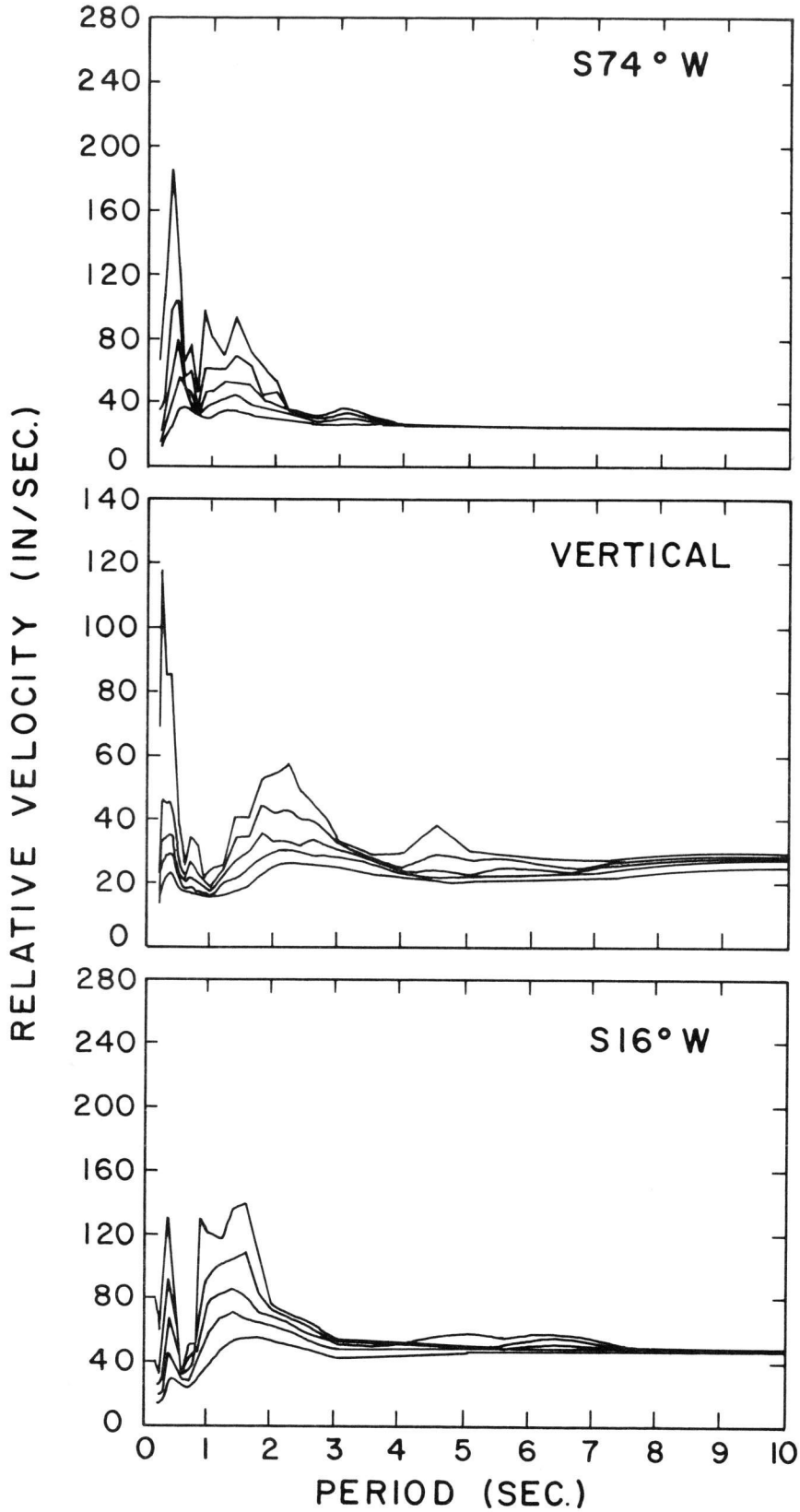

FIG. 4-39. RELATIVE VELOCITY RESPONSE SPECTRA FOR SAN FERNANDO EARTHQUAKE 1971 (PACOIMA DAM). THE CURVES ARE FOR 0, 2, 5, 10, AND 20 PERCENT VISCOUS DAMPING.

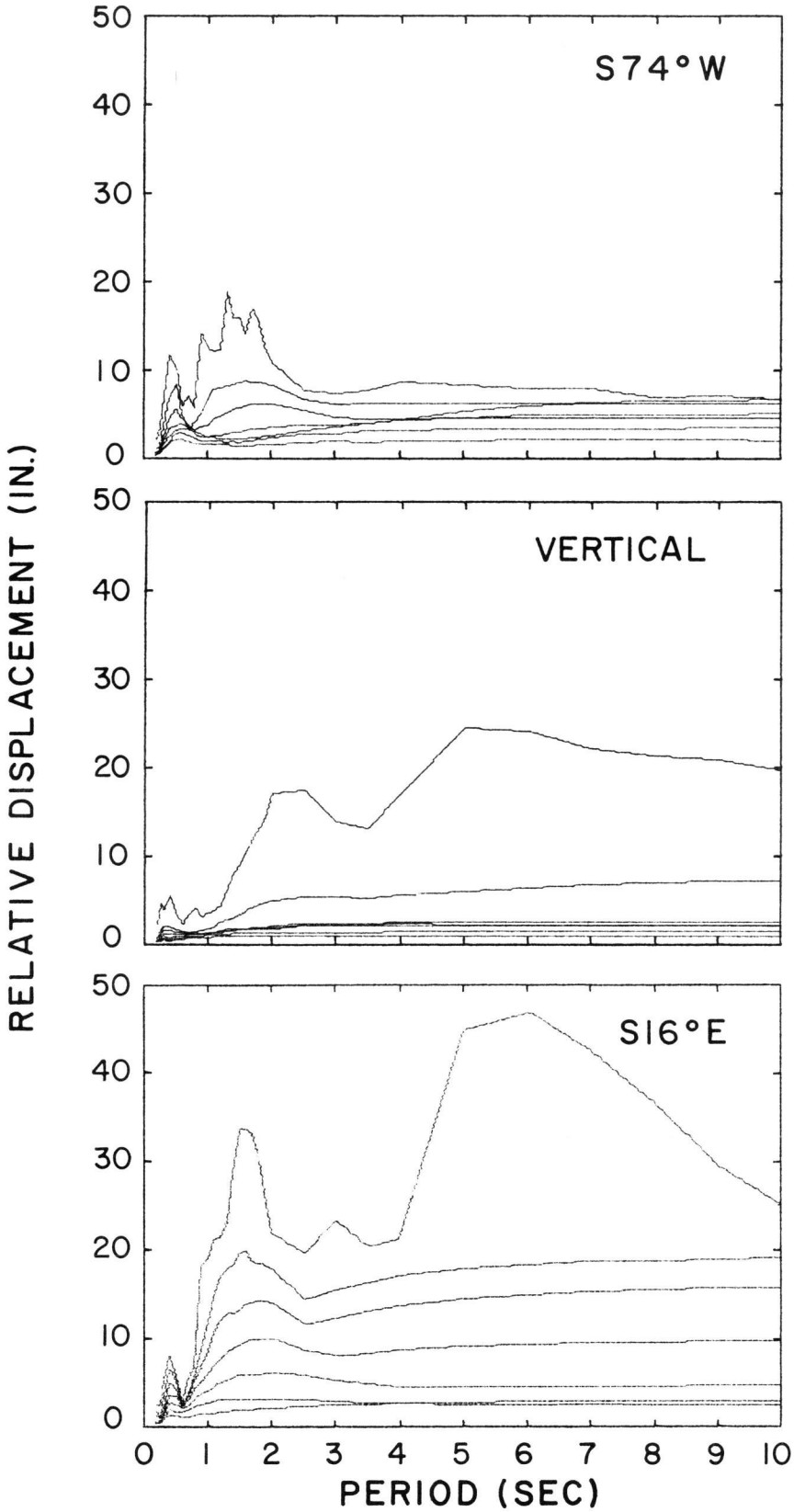

FIG. 4-40. RELATIVE DISPLACEMENT RESPONSE SPECTRA FOR SAN FERNANDO EARTHQUAKE 1971 (PACOIMA DAM). THE CURVES ARE FOR μ VALUES OF 0.0, 0.05, 0.10, 0.15, 0.20, 0.25, AND 0.30.

REFERENCES

1. Jennings, P. C., Housner, G. W., and Tsai, N.C., "Simulated Earthquake Motions," California Institute of Technology, Pasadena, Calif., April, 1968.

2. Jennings, P. C., "Engineering Features of the San Fernando Earthquake of February 9, 1971," California Institute of Technology, Pasadena, Calif., June, 1971.

ACKNOWLEDGEMENTS

This investigation was sponsored by the United States Energy Research and Development Administration. A portion of the funds was provided by the Lawrence Livermore Laboratory at Livermore, California.